Cretaceous (Hauterivian–Cenomanian) palaeoceanographic conditions in southeastern Tethys (Matruh Basin, Egypt): implications for the Cretaceous climate of northeastern Gondwana

Amr S. Deaf[1,*], Ian C. Harding[1], John E. A. Marshall[1]

[1]School of Ocean and Earth Science, University of Southampton, National Oceanography Centre, Southampton (NOCS), European Way, Southampton, SO14 3ZH, UK

*Current address: Geology Department, Faculty of Science, Assiut University, Assiut, 71516, Egypt

Corresponding author: Dr. Amr Deaf (amr.daif@science.au.edu.eg; asdeaf75@yahoo.com)

ORCID: Amr Deaf, http://orcid.org/0000-0002-5073-7911

Abstract

Quantitative palynological, sedimentological, and geophysical data analyses of the Cretaceous Abu Tunis 1X well from the Matruh Basin, northwestern Egypt indicate deposition of four major alternating regressive–transgressive successions. Sedimentation was largely affected by the Tethyan 2nd order sea level changes, with minor overprints by regional tectonics. The Lower Cretaceous part of the succession shows regressive sequences of deltafront to delta-top (upper Hauterivian–lowermost upper Barremian), delta channel (upper Aptian–middle Albian), and distal deltaic (upper Albian) settings that were interrupted by transgressive inner–proximal middle shelf deposits (uppermost Barremian–middle Aptian). These sediment packages correspond to Tethyan sea level fall from the late Hauterivian to late Barremian, and to the early–middle Aptian long-term sea level high stand. The Tethyan late Aptian–middle Albian long-term (2nd order) sea level rise was masked by regional late Aptian–Albian uplift, which affected deposition of the later regressive sequence. The Cenomanian shows a change in depositional setting from a proximal inner shelf (lower Cenomanian) to a middle shelf setting (middle–upper Cenomanian), corresponding to the Tethyan long-term latest early–late Cenomanian sea level rise.

We demonstrate that northeastern Gondwana (Egypt) experienced different climatic conditions from other parts of the Northern Gondwana Phytogeographic Province. The climate in Egypt shifted from less warm and more humid conditions of the Hauterivian–early Barremian to a warmer and drier climate during the late Barremian–middle Aptian, although never becoming as dry as western Northern Gondwana. Warmer and more humid conditions were reestablished during the late Aptian and became even more accentuated during the Albian–Cenomanian, in contrast to the warm and much drier climate of Northern Gondwana at that time. Turonian climatic conditions may have been less humid as a result of the breakup of the

Western Gondwanan supercontinent and the northeasterly drift of the African continent. The climatic conditions experienced in northeastern Gondwana developed through the early-mid Cretaceous as a result of changes in palaeolatitudinal position, variations in sea level, and shifts in the Intertropical Convergence Zone, which drove fluctuations between periods of warm humid and warm dry conditions.

Keywords: Quantitative; palynofacies; palaeoenvironment; palaeoclimate; Intertropical Convergence Zone, Cretaceous; Tethys; Northern Gondwana; Egypt.

1. Introduction

The use of the palynofacies concept in palaeoenvironmental interpretation has improved our understanding of the depositional settings of various Cretaceous sequences in northern Egypt (e.g., Mahmoud and Deaf, 2007; Tahoun and Deaf, 2016; Mahmoud et al., 2017; Deaf and Tahoun, 2018; Mahmoud et al., 2019; Gentzis et al., 2019). Previous research was based mainly on semi-quantitative abundances of palynomorphs and palynodebris, whereas here we present palaeoenvironmental interpretations of the Cretaceous of southeastern Tethys/northeastern Gondwana (i.e., Egypt) utilizing statistically defined, quantitative palynofacies analyses and dinoflagellate cyst (dinocyst) species diversity data. Similar dinoflagellate communities/events and sedimentation cycles were recorded from several areas of the northern (e.g., Davey and Verdier, 1974: SE France; Leereveld, 1997: SE Spain; Torricelli, 2000: Southern Alps of Italy) and southern Tethyan Realm (e.g., Thusu et al., 1988: NE Libya; Foucher et al., 1994; SE Algeria). Similar dinocyst communities/events of Tethyan affinity were also recorded from the Central South Atlantic Ocean (e.g., Arai et al., 2000: NE Brazil; Carvalho et al., 2016: NE Brazil; Garcia et al., 2018: NE Brazil). This similarity in the dinocyst communities/events between the Tethyan Realm and the Central South Atlantic Ocean probably resulted from the latest Jurassic–Cretaceous breakup of Western Gondwana and the Early Cretaceous (middle Aptian–middle Albian) connection of the Atlantic Ocean to the Neo-Tethyan Ocean (e.g., Koutsoukos and Bengston, 2007). Thus, this work aims to present a well-constrained foundation for future correlations of the Cretaceous oceanographic conditions and

dinocyst ecological events between the northern and southern Tethyan margins and the Central South Atlantic Ocean.

Although Cretaceous climatic conditions in the western part of the Northern Gondwana Phytogeographic Province have been investigated by several authors (e.g., Doyle et al., 1982; Herngreen et al., 1996; Doyle, 1999; Bettar and Méon, 2001, 2006), those of northeastern Gondwana (including Egypt) have received less attention. Palynological studies of the latter area have examined regional climate and/or ecologically-controlled regional bioevents (e.g., Abdel-Kireem et al., 1996; Schrank, 2001; Deaf et al., 2014, 2016; Deaf and Tahoun, 2018) but the picture is very much incomplete. To further our understanding we firstly link the sedimentary succession in the Abu Tunis 1X well from the coastal Matruh Basin in the northern part of Egypt's Western Desert to the Tethyan Cretaceous sea level curve. We then present the first quantitative analysis of the distribution of climate proxy sporomorphs from the Egyptian Cretaceous, and by comparing our results with other Gondwanan studies, we compare Cretaceous climatic conditions across Northern Gondwana.

2. Geological setting and lithostratigraphy

The Matruh Basin lies in the northern part of the Western Desert of Egypt and represents a part of the northeastern African Craton, which was tectonically active during much of the Paleozoic and Mesozoic (Guiraud and Bosworth, 1999; Guiraud et al., 2001). This part of northern Egypt was referred to by Said (1990) as the western part of the 'Unstable Shelf' (Fig. 1).

Figure 1 about here

During the Mesozoic, Egypt was affected by three main regional tectonic events. The first event, known as the late Cimmerian Orogeny, occurred during the Middle Jurassic, when the Apulian "Turkish" microplate separated from the Egyptian landmass and rifted northward. This event was related to the formation of the Neo-Tethyan Ocean and the closure of the Palaeo-Tethyan

Ocean. At the same time, the African Plate was also moving eastward with respect to the European Plate as the Atlantic Ocean opened (Kerdany and Cherif, 1990; Bumby and Guiraud, 2005). These regional tectonics resulted in the formation of several extensional intra-cratonic rift basins across the northern Western Desert, including the NNE–SSW trending Matruh Basin (e.g., Sultan and Halim, 1988; Meshref, 1996; Guiraud and Bosworth, 1999). The second event occurred during the Late Cretaceous–Early Palaeogene, when the northern African Plate migrated northwards towards Europe, the resulting compressional stresses produced a series of ENE–WSW trending folds (the so-called 'Syrian Arc System') and faults (Hantar, 1990; Guiraud and Bosworth, 1997; Bumby and Guiraud, 2005; Guiraud et al., 2005). Hantar (1990) and Kerdany and Cherif (1990) provide more details on the tectonic setting of the northern part of the Western Desert. Some studies of the regional tectonic and stratigraphic evolution of northern Egypt suggest that Cretaceous sedimentation in the northern part of the Western Desert was mainly affected by the global eustatic sea level and regional tectonics (Guiraud and Bosworth, 1999; Guiraud et al., 2001, 2005). In general, the Lower Cretaceous sedimentation represents largely a major regressive phase – except for the Aptian sequence –; a shallow sea covered the northern margin of Africa including the northern Western Desert of Egypt (Guiraud and Bosworth, 1999; Guiraud et al., 2001; Fig. 2A).

Figure 2 about here

This resulted in deposition of marginal marine sandstones and shales with rare carbonate streaks of the Alam El Bueib Formation of Hauterivian–Barremian age (Kerdany and Cherif, 1990; Said, 1990; Fig. 3). This formation was significantly affected by ENE–WSW folding (Kerdany and Cherif, 1990; Said, 1990). Aptian strata were then deposited during a transgressive episode, where a shallow sea covered most of northern Africa including western Egypt during a relative sea level rise (Guiraud and Bosworth, 1999; Guiraud et al., 2001; Fig. 2B). As a result, a carbonate unit (made up of light brown dolomite with a few thin shale

interbeds) representing the Alamein Formation was deposited in the north Western Desert (Fig. 3). Deltaic–shallow marine clastics of the Abu Ballas Formation were deposited as far as south of the Western Desert in the Dakhla Basin (Said, 1990; Schrank and Mahmoud, 1998; Guiraud et al., 2001). The coarse-grained sandstones of the Kharita Formation of the Albian age (Fig. 3) indicate another regressive phase, when a retreated shallow sea covered the entire Western Desert (Said, 1990). Sedimentation of the Upper Cretaceous rocks indicates a major transgressive phase (Said, 1990; Mahmoud et al., 2017). During the late Cenomanian, a regional subsidence related to Neo-Tethyan rifting took place across the northern African margin, and a marine transgression covered the entire North Africa (Guiraud and Bosworth, 1999; Guiraud et al., 2001, 2005; Fig. 2C). As a result, fluvio–marine deposits (mainly fine to medium-grained sandstones and siltstone with minor shale and calcareous deposits) of the Bahariya and shales with siltstones/fine sandstone and carbonate alternations of the lower Abu Roash formations accumulated conformably in much of the northern basins of the Western Desert, including the Matruh Basin (Hantar, 1990; Said, 1990; Fig. 3). A summary of the stratigraphy, description of the formation lithologies of the sedimentary sequences of the north Western Desert of Egypt and the depositional environment of the Cretaceous sequences is shown in Figure 4. Detailed age dating and recognition of the originally undifferentiated rock units, which were deemed as “No Information” by the drilling company WEPCO (1968), were handled by Deaf et al. (2014, 2016).

Figure 3 about here

A summary of the palynological biozonation, dating of the Abu Tunis 1X well Cretaceous succession and sample position is shown in Figure 4.

Figure 4 about here

3. Materials and methods

One hundred and thirty four ditch-cutting samples were collected from 10,150 ft to 2,950 ft (3094–899 m) in the Abu Tunis 1X well, drilled in the Matruh Basin by WEPCO in 1968 (lat. 31° 16′ 08″ N, long. 26° 50′ 41″ E; Fig. 1), covering most of the Cretaceous sequence in the northern Western Desert of Egypt. Samples were processed by standard palynological methods (see below), and palynological yield and palynomorph recovery (grains/gram of dry sediments) were recorded (online Supplementary Appendix 1).

Standard HCl/HF acid maceration palynological processing was employed (Phipps and Playford, 1984; Wood et al., 1996; Green, 2001). However, after the first HF decanting, each sample was spiked with one tablet of modern *Lycopodium* spores for absolute abundance analysis. The *Lycopodium* tablets used were from Batch no. 124961 (one tablet containing 12,542 spores, with V ± 3.3 %) made by the Department of Quaternary Geology, Lund University. Residues were boiled in 15 ml of 36% HCl for 1–2 minutes to remove neo-formed fluorides and sieved through 15 µm nylon meshes. Finally, two permanent slides were prepared for light microscope investigation by air-drying an aqueous strew mount of each residue onto a cover slip and cementing it to a glass microscope slide using Elvacite 2044. Organic residues were not subjected to ultrasonic treatment or oxidation to minimize bias of the organic matter composition for palynofacies analyses. Rock samples, organic residues, and palynological slides containing illustrated palynomorphs with museum accession number (MAN) are stored in the type and reference collections of the Geological Museum, Geology Department, Faculty of Science, Assiut University, Egypt.

3.1. Qualitative analysis

Qualitative palynological and palynofacies investigations were based on the light microscopic description of the different organic matter constituents (i.e., phytoclasts and palynomorphs) using an Olympus (BX41) transmitted-light microscope (serial no. 8B25715) equipped with an Infinity-1 digital camera for microphotography. Taxonomic identification of the miospores and dinoflagellate cysts was made with reference to the original descriptions and diagnoses of the species in their original published articles alongside Jansonius and Hills (1976,

and subsequent supplements). Furthermore, the Eisenack Catalog of Fossil Dinoflagellates (Fensome et al., 1995, 1996) and the updated electronic database DINOFLAJ3, Version 1 (Williams et al., 2017) were used as additional sources for identification and resolution of taxonomic problems.

As ditch-cutting samples were used for this study, it was necessary to minimize the effects of possible caving during the drilling process, or due to mixing with other lithologies during sample splitting, shipment and final storage. This was done by examining the downhole logs from the studied well and isolating specific lithologies from ditch cutting samples from specific depth intervals prior to palynological processing; in this way, it is possible to maximize the quality of information that ditch-cutting samples can provide. Further assessment of possible caving and/or lithological mixing was done by investigating the vertical distribution of the index palynomorph taxa. For details of the quantitative distribution of these palynomorphs, see Deaf et al. (2014, 2016).

3.2. Quantitative analyses

The integration of palynological data with sedimentary facies data is very valuable in interpreting depositional settings and palaeoceanographic conditions (Tyson, 1995; Koutsoukos, 2005; Deaf and Tahoun, 2018). Thus, a framework for the palaeoenvironmental interpretations in this paper was made by integrating quantitative palynological data with the sedimentological characters identified from geophysical data and the original lithological descriptions provided by the operating company.

3.2.1. Palynology and palynofacies analyses

Quantitative palynological analysis was achieved by spiking the samples with a known number of modern *Lycopodium* spores during processing. The absolute abundance (grains/gram of dry sediments) of each phytoclast and palynomorph type was obtained by using the absolute abundance formula of Stockmarr (1971):

208 $c = \frac{S_c \times L_t \times t}{L_c \times w}$

209 where

210 c = concentration = total number of specimens/gram of dried sediments
211 S_c = number of specimens counted
212 L_t = number of *Lycopodium* spores/tablet
213 t = number of tablets added to the sample
214 L_c = number of *Lycopodium* spores counted
215 w = weight of dried sediments (g)
216

217 Two hundred and fifty specimens were counted per sample, providing a total maximum error of
218 7% according to the Stockmarr (1971) curve. The palaeoenvironmental interpretations were
219 based on analyses of the quantitative data of different particulate organic matter (POM)
220 constituents in preference to relative abundance data to avoid problems with data closure. The
221 quantification of the terms of minimum, maximum, and average absolute abundances (grains/g)
222 of selected palynomorphs, phytoclasts, and amorphous organic matter (AOM) follow that of
223 Tyson (1995).
224

225 **3.2.2. Dinocyst diversity**

226 A second count of the absolute abundances of the dinocysts was made in order to
227 counter the dilution effect of the extremely abundant terrestrial POM, and to allow determination
228 of the species diversity of the dinocyst assemblages. Abundances of the three main cyst
229 morphotypes (proximate, cavate, and chorate) of the dinocyst assemblages were also
230 calculated. Gotelli and Colwell (2011) used a rarefaction curve to determine the adequate
231 number of specimens to be counted to provide an accurate representation of the species
232 present in a single sample and suggested at least 20 individuals should be counted. In case of
233 lean samples, the count of at least 30 individuals was suggested by Chang (1967) to be
234 sufficient to produce a reliable interpretation of palaeoecological conditions. To determine how
235 many specimens of dinocysts needed to be counted here to provide a representative indication

of species diversity, counts were made firstly of 50 and then of 100 specimens from a single sample. The count of 50 individuals was found to be both representative and practical, firstly as such numbers of individuals could be obtained from dinocyst-poor and from dinocyst-rich samples, and secondly this number of specimens was sufficient to register the vast majority of species present in these relatively low diversity samples. Samples that yielded <10 dinocyst specimens after scanning two microscope slides per sample were deemed effectively barren of this category of palynomorphs, and thus not included in further interpretations. Dinocyst species diversity was measured using the Simpson's diversity index (1-λ') as follows:

$$1-\lambda' = 1- \{\sum_i N_i(N_i-1)/N(N-1)\}$$

Where

1-λ' = Simpson's diversity index

N_i = number of individuals of species *i* in a sample

N = total number of individuals of all species in a sample

Simpson's diversity index (Simpson, 1949) was used because it takes into consideration both species richness and evenness, but moreover it is independent of the total count of the number of individuals, and thus, unlike other diversity measures, it can be compared between samples from which different numbers of individuals have been counted (Clarke and Warwick, 2001).

3.3. Cluster analysis

Absolute abundances of POM constituents, including pteridophyte spores, schizaeacean spores, sphaeroidal pollen grains, *Classopollis*, *Ephedripites*, dinocysts, microforaminiferal test linings (MFTLs), brown wood, black wood, cuticles, and membranous tissue were used in an agglomerative cluster analysis to group samples having palynofacies of similar composition and abundance (see online Supplementary Appendix 2). The Bray-Curtis similarity coefficient (Bray and Curtis, 1957) was chosen over other forms of correlation (e.g., Pearson's product momentum *r*, Spearman's rank r_s) to assess similarity between the samples, because it takes

into consideration changes in the abundances of the sample components (Etter, 1999), an important criterion in palaeoenvironmental interpretation. The Bray-Curtis similarity coefficient also has an advantage over other similarity coefficients, where it yields zero similarity when two samples have completely different POM constituents, something which most similarity coefficients cannot do (Clarke and Warwick, 2001).

Figure 5 about here

It should be borne in mind that the clustering of the studied samples provides here an approximation of the original similarity between the different samples. Taphonomic processes may have altered the original biological composition of the samples through the decay and transport of some of the organic matter (Bennington and Bambach, 1996), and the palynological assemblages will represent time-averaged accumulations, which conflate environmental conditions during the time period over which that sediment was deposited (Kidwell and Bosence, 1991).

A mild square root ($\sqrt{}$) transformation of the original absolute abundance data was made before clustering with the *PRIMER v6* software of Clarke and Gorley (2006) in order to down-weight the very abundant POM constituents and to allow the less common POM groups to contribute more meaningfully to the similarity analysis. The clustered data was used to define three palynofacies types at about 72–75 % similarity levels (Fig. 5) according to Tyson's (1995) definition of palynofacies, which is only based on the proportional distribution of the POM with no consideration of lithologies. In general, the palynofacies clusters follow lithological type, with vertical changes in the overall organic matter concentrations reflecting changes in the depositional environments in terms of regressive–transgressive regime. At higher levels of similarity (between 78–83 %), sub-facies (subzones) were also identified within two of the palynofacies types; these are again controlled by lithology.

3.4. Wireline geophysical data (self-potential log) analysis

Self-potential is the only geophysical data available to interpret the lithology of the Abu Tunis 1X successions (Fig. 6). Amongst other things, self-potential (SP) can be used to indicate facies permeability, shale volumes, and changes in rock types (Rider, 2002). Self-potential does not deal with absolute value, as its profile moves between a predefined zero line (also called shale base line) and is defined using a thick shale interval at which self-potential does not move. Maximum self-potential reading correlates with a permeable water-bearing formation with no shale, and thus detects changes in the sedimentary facies as it moves with changes in sand:shale volumes (Rider, 2002).

Figure 6 about here

4. Regional and intercontinental biozonal correlation and links to the Tethyan eustatic sea level curve

Many of the independently calibrated dinocyst bioevents of the Early Cretaceous European Tethys (Hardenbol et al., 1998) can be recognized in the southern Tethys. However, correlation of the Late Cretaceous bioevents is more problematic due to environmental exclusion, as has previously been observed in NE Libya (Thusu et al., 1988) and NW Egypt (Deaf et al., 2014). In the current study, late Barremian and Aptian dinocyst bioevents are closely comparable with their counterparts in northern Tethys (Fig. 7; Haq et al., 1988; Hardenbol et al., 1998). In addition, the foraminifera-calibrated dinocyst biozones of Abdel-Kireem et al. (1993) and foram- and nannoplankton-calibrated spore-pollen zones of Aboul Ela and Tahoun (2010), span most of the Cretaceous of northern Egypt and connect the Egyptian zones to the calibrated European Tethys dinocyst bioevents of Ogg and Hinnov (2012). These zonation schemes enable us to correlate the late Barremian and Aptian dinocysts in the Abu Tunis 1X well with those independently dated in Egypt (Aboul Ela and Tahoun, 2010; Fig. 7). Additionally, the Abu Tunis 1X well records other late Barremian–Aptian dinocysts bioevents namely, the first appearances of *Odontochitina operculata*, *Pseudoceratium anaphrissum, Pseudoceratium securigerum*, and *Palaeoperidinium cretaceum*. These species were previously

recorded from the Barremian and Aptian type sections, and from other ammonite and foram-dated upper Barremian–Aptian rocks in northern and southern Tethys (e.g., Davey and Verdier, 1974; Renéville and Raynaud, 1981; Thusu and van der Eem, 1985; Foucher et al., 1994; Hoedemaeker and Leereveld, 1995; Leereveld, 1997; Torricelli, 2000, 2006; see also Deaf et al., 2014).

Figure 7 about here

The Albian dinocysts found in this study are mainly facies-controlled, and the miospores therefore play an important role in correlation. This is because the Albian sequence in Egypt was deposited in regressive shallow marine settings, and thus is lacking in rich and diverse dinocyst assemblages and other micropalaeontological groups (i.e., foraminifera, nannoplankton). The late Albian miospore events in Abu Tunis 1X were thus correlated by Deaf et al. (2014, fig. 3) with similar micropalaeontologically calibrated miospore zones (e.g., Jardiné and Magloire, 1965) outside Egypt but within the Albian–Cenomanian Elaterates Phytogeographic Province of Hergreen et al. (1996). The Cenomanian miospore events in Abu Tunis 1X are almost identical to the foram-calibrated miospore events recorded by Abdel-Kireem et al. (1993) and Schrank and Ibrahim (1995) from Egypt (Fig. 7). Moreover, the Cenomanian miospore events in Abu Tunis were also correlated by Deaf et al. (2014, p. 63–67, fig. 3) with other similar micropalaeontologically calibrated miospores zones in the Albian–Cenomanian Phytogeographic Province. Finally, the first appearance datum of *Canningia senonica* in Abu Tunis has also previously been recorded in the foram-calibrated lower Santonian of Egypt (Schrank and Ibrahim, 1995). Consequently, we have been able to use the palynological bioevents in the Abu Tunis 1X well to correlate the succession with the Tethyan Cretaceous eustatic sea level curve of Haq (2014), and use the palynological assemblages and sedimentology to characterize regressive and transgressive depositional sequences.

5. Palynofacies and palaeoenvironmental interpretation

Combaz (1964) defined ‘palynofacies’ as the total complement of acid-resistant particulate organic matter recovered from sediments by palynological processing techniques, with Tyson (1995, p. 4) later defining palynofacies analysis as “*the palynological study of depositional environments and hydrocarbon source rock potential based upon the total assemblage of particulate organic matter*”. Both the composition and distribution of organic matter are controlled by ecological conditions and sedimentological processes in the depositional environment, while microbial, physical and biogeochemical processes in sediments (taphonomic effects) affect organic matter preservation and abundance (Tyson, 1995). These compositional changes in palynofacies can be used for producing palaeoenvironmental interpretations of sedimentary rocks, as such changes are the product of the interaction of several parameters (e.g., terrestrial *versus* marine palynomorph influx, source and rate of sediment influx, water salinity, depth and oxygen concentrations, etc.) within a given depositional environment (Tyson, 1995).

The palaeoenvironmental interpretations presented herein for each palynofacies (PF) type are based on quantitative analyses of selected palynomorph components, which are known to have palaeoenvironmental significance. These include terrestrially derived palynomorphs such as miospores (which comprise pteridophyte spores, spherical, circumpolles, gnetalean and elaterate gymnosperm pollen, and angiosperm pollen), and aquatic phytoplankton (e.g., dinocysts). In addition, there may be terrestrially derived phytoclasts, which can be represented by black wood (inertinite/charcoal), brown wood (e.g., tracheids), plant cuticles, and membranous tissues. Other minor constituents may include MFTLs and freshwater algae. The absolute abundances (grains/g) of different counted palynofacies constituents (sporomorphs, phytoclasts, and AOM) are shown in the online Supplementary Appendix 3. However, the absolute abundances (grains/g) of AOM were obtained from a separate count to counter the dilution effect of the phytoclasts to AOM (cf. Tyson, 1995; Deaf and Tahoun, 2018). In the current investigation, a local 2nd order sea level curve showing the main regressive–transgressive intervals has been constructed based on changes in the palynological data in terms of the terrestrial/marine palynomorphs ratio (*t/m*) according to Prauss (2001, 2006) and

Hermann et al. (2011). Changes in this local palynologically based curve are consistent with changes in lithology and reflect regressive and transgressive trends in sedimentation.

5.1. Palynofacies subzone (PF-1A)

Stratigraphic distribution and content: Samples clustered as subzone PF-1A (samples 1–14, spanning 10,150–9,500 ft / 2,914–2,716 m) represent the lower–middle Alam El Bueib Formation of late Hauterivian–earliest late Barremian age (Fig. 8) and show a strong terrestrial influence (Fig. 9A). This is reflected by very high concentrations of phytoclasts (17,570–123,031, avg. 59,485 particles/g) and sporomorphs (4,320–35,274, avg. 12,326 grains/g). Marine palynomorphs are represented by rare dinocysts (127–1,680, avg. 1,250 cysts/g), MFTLs (only in sample 1, 597 grains/g), and acritarchs (in sample 2, 25 grains/g). AOM shows very high concentrations (5,226–103,123, avg. 39,740 particles/g).

Figure 8 about here

The phytoclasts are dominated by large, lath-shaped black wood particles (10,981–96,155, avg. 39,177 particles/g) and tracheids (5,317–41,209, avg. 17,678 particles/g). Cuticle fragments (557–8,801, avg. 2,309 particles/g) and membranous tissues (116–1,194, avg. 499 particles/g) are of subordinate concentrations. The miospore assemblages are dominated by frequent pteridophyte spores (4,041–32,475, avg. 11,296 grains/g), whilst low concentrations (231–2,240, avg. 1,153 grains/g) of the xerophytic gymnosperm pollen *Classopollis* are the second most significant component of the sporomorphs. Gymnosperm pollen grains occur in very low concentrations (127–597, avg. 428 grains/g) and are represented by the araucariacean pollen (*Araucariacites* and *Balmeiopsis*) and *Exesipollenites* (Fig. 10). Another minor terrestrially derived palynomorph component in PF-1A (27 grains/g) is the freshwater algae *Ovoidites*. Dinocysts are rare, but of high diversity (avg. 0.78) and are represented by nearly equal proportions of cavate (279–1,181, avg. 556 cysts/g) and proximate forms (252–1,091, avg. 616 cysts/g), with very low (16–217, avg. 92 cysts/g) chorate cyst concentrations (Fig. 11). Cavate

cysts are mainly represented by *Subtilisphaera* and the low salinity genus *Muderongia*, while proximate cysts are mainly composed of *Cribroperidinium* and *Circulodinium*, with the genus *Oligosphaeridium* representing the chorate cyst community (Fig. 10).

Palynofacies association of PF-1A: black wood/spore-dominated (Fig. 8, Fig. 9A).

Sedimentary facies of PF-1A: The self-potential readings associated with sample of the PF-1A subzone indicate several small-scale coarsening upward sedimentary cycles (Rider, 2002; Fig. 6). By integrating the geophysical data, original log descriptions and cuttings interpretations, PF-1A assemblages are derived from light grey to green shales containing some black carbonaceous material and pyrite, intercalated with thin streaks of poorly sorted sandstones and a very few dolomite layers.

Figure 9 about here

Depositional environment of PF-1A: deltaic (delta-top to delta-front)

The low abundance but high diversity dinocyst assemblages found in PF-1A suggest deposition in marine settings of normal marine salinity (Mutterlose and Harding, 1987; Lister and Batten, 1988; Habib et al., 1992; Tahoun and Deaf, 2016; Deaf and Tahoun, 2018). However, the dominance of the inner shelf cavate peridinioids *Subtilisphaera* (Harding, 1986; Lister and Batten, 1988; Deaf and Tahoun, 2018) and proximate cysts (*Cribroperidinium* and *Circulodinium*), which are collectively characteristic of restricted (brackish–costal) marine conditions indicates restricted marine environments of below normal salinity (Harding, 1986; Lister and Batten, 1988; Prauss, 2001, 2006; Deaf and Tahoun, 2018). The chorate gonyaulacoid genus *Oligosphaeridium,* characteristic of open marine middle shelf conditions (e.g., Lister and Batten, 1988), is very rare. These restricted marine conditions are further supported by the presence of the low salinity indicator *Muderongia* (Piasecki, 1984; Harding, 1986; Lister and Batten, 1988), rare brackish water acritarchs (sample 2; Schrank, 1984; Tyson,

1995), and very low concentration of the freshwater algae *Ovoidites* (27 grains/g; Lister and Batten, 1988; Batten, 1999). This interpretation indicates that the rocks yielding PF-1A were deposited in nearshore shelf environments that were close to fluvio–deltaic systems, where mixing of continental freshwater with waters of normal marine salinities occurred.

The sporomorphs confirm this interpretation. Spore producing-plants are known to produce fewer propagules than gymnospermous pollen-producing plants, and pteridophyte spores also have relatively limited transport efficiency (Mutterlose and Harding, 1987; Prauss, 1989; Tyson, 1989). Thus, the dominance of pteridophyte spores over spherical gymnosperm pollen grains (*Araucariacites*, *Balmeiopsis* and *Exesipollenites*) in PF-1A also supports a setting close to fluvio–deltaic sources. Such a setting is also consistent with the hydrodynamic properties of the dominant terrestrial plant debris (wood tracheids) in PF-1A samples, as the distribution of woody phytoclasts in sediments is controlled by their particle size/shape. As woody tracheids are usually relatively large and dense fragments, they tend to concentrate in coarse silts and very fine sands that are commonly found in proximal fluvio–deltaic facies (e.g., Habib, 1983; Firth, 1993; Tyson, 1993, 1995).

Figure 10 about here

Figure 11 about here

High concentrations of black wood, also common in PF-1A, have previously been recorded from high energy, coarse-grained proximal facies of fluvial and delta-top systems (e.g., Nagy et al., 1984; Smyth et al., 1992; Williams, 1992), again controlled by particle size/shape (Tyson, 1995). Large, lath-shaped black wood particles are concentrated in the coarser sand lithologies (indicated by self-potential profile, Fig. 6), indicative of proximal, relatively high-energy silt and sand lithologies (Van der Zwan, 1990; Baird, 1992). We therefore suggest that the coarser sedimentary facies (sandstones) yielding PF-1A assemblages were deposited on partly submerged delta-tops, whilst the finer-grained deposits (fine sands and shales) were laid down

in continuously submerged delta-front settings. Furthermore, the alternating sandstone/shale beds and the development of several small-scale coarsening upward cycles as indicated by the self-potential profile suggest a prograding deltaic setting for PF-1A (Fig. 6; Rider, 2002). The presence of some black carbonaceous material in shales (e.g., 9,980, 9,740–9,650 ft / 2,862, 2,789–27,623 m) of PF-1A also suggests proximal deltaic settings, where Selley (1976) linked the occurrence of black carbonaceous matter in shale horizons in a coarsening upward sequence to proximal deltaic conditions. The coarse sandstone intervals of PF-1A have low concentrations of thin, membranous tissues, likely due to oxidative removal in the high-energy, highly oxygenated depositional setting, or due to winnowing and re-deposition of this material in the delta-front sediments. However, in contrasting fashion, the presence of pyrite in the shales (9,740–9,650 ft / 2,789–27,623 m) of PF-1A implies at least periodically low oxygen concentrations in bottom or pore-waters (Tyson, 1995; Deaf and Tahoun, 2018). The occurrence of very high concentrations of AOM in most of PF-1A samples indicates the prevalence of reducing conditions and/or rapid deposition (Tyson, 1995). Plotting the PF-1A constituents on the ternary kerogen diagram of Tyson (1995) indicates suboxic–anoxic conditions for this palynofacies (Fig. 12A).

Figure 12 about here

Palynological and sedimentological characteristics indicate deposition of the lower–middle Alam El Bueib Formation (upper Hauterivian–lowermost upper Barremian) represented by PF-1A took place during a regressive phase in a proximal deltaic environment (Fig. 12B), specifically in sub-aqueous delta-front to delta-top sub-environments (Fig. 13A), with periodic anoxic pore-water conditions in the delta-front sub-environment. This local sea level fall at Abu Tunis 1X well coincides with the Tethyan late Hauterivian–late Barremian long-term sea level fall (Haq, 2014; Fig. 7). Generally, reducing, suboxic–anoxic conditions were prevailing during deposition of the lower–middle Alam El Bueib Formation.

Figure 13 about here

A general decrease in the absolute abundances of pteridophyte spores, brown and black wood through samples of PF-1A from base to top (Fig. 8) suggests a relative rise in sea level (e.g., Tyson, 1993; Batten, 1999), as sporomorph absolute abundances decrease exponentially in an offshore trend (e.g., Habib, 1983; Habib and Drugg, 1987).

In the northern Tethyan margin in SE Spain, upper Hauterivian regressive and lower Barremian transgressive depositional sequences were recorded (Hoedemaeker and Leereveld, 1995), which correlate with the lower part of PF-1A of the Abu Tunis 1X well (Fig. 7).

5.2. Palynofacies subzone (PF-1B)

Stratigraphic distribution and content: Those samples clustered in subzone PF-1B (samples 15–42; 9,450–8,100 ft / 2,701–2,289 m) correspond to the upper Alam El Bueib (upper Barremian) and Alamein (lower–middle Aptian) formations. PF-1B demonstrates a strong decrease in concentrations of terrestrially derived organic matter (Fig. 9B) compared to PF-1A assemblages, with sporomorphs and phytoclasts dropping to 1,387–14,632 (avg. 4,718) grains/g and 2,679–61,038 (avg. 26,186) particles/g, respectively. There is a coeval increase in the dinocyst concentration (157–8,361, avg. 2,196 cysts/g), but MFTLs are still of very low concentrations (72–418, avg. 194 grains/g). AOM is of relatively lower concentration (4,013–125,420, avg. 31,752 particles/g) than in PF-1A.

The structured plant debris is still dominated by tracheids (1,558–48,496, avg. 17,025 particles/g). The mainly equant-shaped black wood (475–12,296, avg. 4,812 particles/g) is still the second most common component, whilst there is a reduction in the concentration of cuticle (361–6,271, avg. 2,625 particles/g) and an increase in membranous tissue (237–5,226, avg. 1,885 particles/g). Miospores are represented by rare pteridophyte grains (1,007–6,271, avg. 2,352 grains/g; including rare schizaeacean taxa), rare *Classopollis* (72–7,316, avg. 1,345 grains/g), and very rare spherical (mainly *Araucariacites* and *Balmeiopsis*) and monoporoid (*Exesipollenites*) gymnosperm pollen grains (131–975, avg. 459 grains/g). Dinocysts are of

517 slightly higher abundance than in PF-1A and are of high diversity (~ 0.77). The dinocyst
518 assemblage is dominated by proximate cysts (113–3,345, avg. 1,346 cysts/g), with subordinate
519 cavate (188–2,628, avg. 738 cysts/g) and chorate (46–1,003, avg. 335 cysts/g) concentrations.
520 The proximate cysts are represented by *Pseudoceratium* and *Circulodinium*, while the cavate
521 cysts are mainly *Subtilisphaera*, with *Oligosphaeridium* and *Florentinia* representing the chorate
522 cysts.
523
524 **Palynofacies association of PF-1B:** black wood/dinocyst-dominated (Fig. 8, Fig. 9B).
525
526 **Sedimentary facies of PF-1B:** Information gleaned from the geophysical log data, the original
527 well log description, and the visual interpretation of the ditch cutting samples indicate
528 alternations of shales and light yellow to brown dolostones. Basal shales contain traces of pyrite
529 and are overlain by 200 feet (61 m) of dolostone that is in turn overlain by a siltstone and shale
530 unit containing traces of glauconite at the basal shale and carbonaceous material at its
531 uppermost part (Fig. 8), which are intercalated with thin dolostone beds. In their turn, these are
532 overlain by a second 200 feet (61 m) thick sequence of pale brown dolostone. The self-potential
533 profile of PF-1B indicates the development of two major fining upward sequences (Fig. 7; Rider,
534 2002). The upper dolostone unit is identified as the Alamein Dolomite Formation, which has a
535 wide regional extent over the northern part of Egypt (Kerdany and Cherif, 1990; Said, 1990).
536 The Alamein Dolomite is secondary in origin. It was originally formed from accumulation of lime
537 mud in a low energy, relatively shallow neritic environment that was later subjected to various
538 diagenetic processes (e.g., dolomitization, silcification, and pyritization; Abou Khadrah et al.,
539 1978; Rifai, et al., 2006).
540
541 **Depositional environment of PF-1B:** prodelta–proximal inner shelf to proximal middle shelf
542 By comparison with PF-1A, the dinocyst concentration is increased except for the
543 lowermost (15–20) and uppermost (38–42) parts of PF-1B, but has a similar species diversity
544 (Fig. 8). This indicates the development of normal and deeper marine conditions for much of the

PF-1B samples following the underlying deposits yielding PF-1A assemblages, as higher dinocysts concentrations occur with increasing water depth from onshore to offshore (e.g., Tyler et al., 1982; Balch et al., 1983; De Vernal and Giroux, 1991). In addition, dinocyst species diversity in PF-1B assemblages is high (samples 21–37) like those in PF-1A, but is less variable than in PF-1A (Fig. 11), implying more stable normal marine conditions for this part of the PF-1B against the stressed conditions represented PF-1A. Normal marine conditions are also supported by the high species diversity and low dominance of open marine (middle shelf) dinocyst taxa such as *Oligosphaeridium* and *Florentinia* recorded in samples 21–37. Similar high diversity/low dominance assemblages have been found to increase in basinward shelfal settings of normal marine salinity (e.g., Mutterlose and Harding, 1987; Lister and Batten, 1988; Habib et al., 1992). The increase in the abundance of *Oligosphaeridium* and *Florentinia* may represent periodically slightly more offshore/deeper water conditions or the influence of onshore currents re-depositing more offshore taxa (Lister and Batten, 1988; Prauss, 2001, 2006; Carvalho et al., 2016; Deaf and Tahoun, 2018). Generally, the higher abundance of inner–middle shelf, proximate cysts *Pseudoceratium* and *Circulodinium* (Harding, 1986; Brinkhuis, 1994; Deaf and Tahoun, 2018) over the inner shelf cavate cysts *Subtilisphaera* (Harding, 1986; Lister and Batten, 1988; Deaf and Tahoun, 2018) and the open marine (middle–outer shelf) chorate cysts suggests a proximal middle shelf setting for samples 21–37. The increasing dinocyst abundance and coeval sharp declines in terrestrially derived organic matter in samples 21–37 is indicative of a relative rise in sea level (Tyson, 1993; Tyson, 1995; Batten, 1999) and is consistent with inferred deeper marine conditions. This local sea level rise corresponds to the Tethyan early Aptian, high sea level stand (Fig. 7). A more offshore setting would also be supported by the slight increase in concentrations of *Classopollis* and other spherical pollen grains, such as *Araucariacites* and *Balmeiopsis,* over those found in PF-1A, as they show nearshore to offshore increases in abundance due to their buoyancy (Habib, 1979; Tyson, 1995). Cuticles and membranous tissues are rare in the dolostones, and the overall strong decrease in the brown and black wood concentrations also support a more offshore setting for PF-1B than PF-1A. Meanwhile, the increase in the equant-shaped black wood at the upper

shale unit of PF-1B reinforces the development of a marine setting deeper than that of PF-1A (e.g., Tyson, 1995; Tahoun and Deaf, 2016; Deaf and Tahoun, 2018). Generally, deposition of the finer-grained marine shales and limestones in PF-1B also suggests the development of a deeper depositional setting in comparison to the marginal marine, coarser sandstones and shales of the underlying PF-1A. The upward change in lithofacies and the self-potential profile of PF-1B indicates two major fining upward sequences; a sedimentation pattern that is suggested by Rider (2002) to indicate a transgressive marine shelf setting. Combining all data mentioned above, samples 21–37 yielding PF-1B were deposited in a proximal inner shelf setting.

Nevertheless, traces of glauconite in the coarser clastic (siltstones) interval (samples 27–30, 8,850–8,700 ft / 2,518–2,472 m) indicate the development of a shallower marine setting in comparison to the rest of the palynofacies samples (Mahmoud et al., 2017). Glauconite is formed in marine waters at the sediment-water interface and in argillaceous clastic deposits is linked to very low rates of sedimentation and/or non-deposition (e.g., Einsele, 1992; Dooley, 2006; Khalifa and Catuneanu, 2008). The occurrence of the thick-walled, heavy spore *Murospora* (32–287, avg. 127 grains/g) in the silty samples (27–33) and *Balmeisporites* (15–33, avg. 22 grains/g) in samples 28–30 of PF-1B suggest a deltaic setting, as heavy spores are known to concentrate in high energy, nearshore sediments (e.g.; Mutterlose and Harding, 1987; Tyson, 1995). Similar records of these thick-walled spores were also documented from coarse clastic Aptian deposits (siltstones) of marginal to shallow inner shelf settings in Egypt (Mahmoud and Deaf, 2007). This shallower setting is probably linked to the regional latest Barremian–Aptian tectonic uplift, which affected some basins of the north Western Desert (Kerdany and Cherif, 1990). This local sea level fall can be correlated with the Tethyan early Aptian, short-term sea level fall (Haq, 2014; Fig. 7).

The lowermost (15–20) and uppermost (38–42) samples yielding PF-1B assemblages show lower cavate and proximate dinocyst concentrations than those recorded from the rest of the PF-1B samples and from the deltaic deposits of PF-1A (Fig. 11). This suggests that the lowermost and uppermost parts of PF-1B were deposited in a deltaic setting.

Dolomitization has probably biased the palynofacies extracted from the dolostone samples, and caused diminishing in the abundance of the dinocysts among other terrestrial and marine palynomorphs (Traverse, 2007; Rifai, et al., 2006, and references therein). Preservation of palynomorphs especially the dinocysts and the thin-walled pteridophyte spores in the abovementioned samples is poor; the majority of the grains are broken, abraded, and/or corroded. Deposition of the lowermost and uppermost dolostone units took place around the onset of regressive sedimentation phases as indicated by the association with coarser clastics (Fig. 8). Petrographic log of PF-1B probably indicates the middle dolomite unit as of a primary origin because it is finely crystalline and show poor porosity and rare vugs. While, the uppermost and lowermost units are coarsely crystalline (granular) and are partly vuggy (WEPCO, 1968). Based on the palynofacies, lithofacies, and petrographic data mentioned above, the lowermost samples yielding PF-1B assemblages came from alternating shales and dolostones, and the dominance of restricted shallow marine dinocysts suggest deposition of this part of PF-1B in a prodelta setting. However, the uppermost dolostone unit yielding PF-1B shows higher abundances of this group of dinocysts, and is relatively enriched in open marine chorate cysts and equant-shaped black wood. This suggests deposition of PF-1B assemblages in the uppermost dolostone in a distal deltaic (prodelta) to proximal inner shelf setting. Traces of carbonaceous material in the upper shale unit (sample 36, 8,400 ft / 2,381 m) also indicate a deltaic setting for the uppermost part of PF-1B. Membranous tissue (237–5,226, avg. 1,885 particles/g) is confined to the shale horizons of the lowermost and uppermost parts of the sequence yielding PF-1B, indicating these fragile, oxidation-prone tissues were deposited in slightly more distal, lower energy marine settings, but still nearshore, possibly prodelta, during brief low stands (e.g., Tyson, 1995). The ternary plot of the palynomorph contents of samples yielding PF-1B indicates a shift in deposition from distal deltaic to deeper (shallow marine) conditions and a return to the more nearshore setting through time (Fig. 12B). The presence of pyrite in one of the shale samples (sample 22: 9,100 ft / 2,594 m), diagenetic sphaeroidal pyrite inside some of the spores (Fig. 9B), and high concentrations of AOM, indicate periodically reducing (suboxic–anoxic) bottom water conditions (e.g., Tyson, 1995; Pittet and Gorin, 1997;

629 Tahoun and Deaf, 2016; Deaf and Tahoun, 2018). The upward increase in AOM indicates a
630 shift in reducing conditions from dysoxic–anoxic to suboxic–anoxic (Fig. 12A).

631 Thus, the lower–middle Alamein Formation (lower Aptian) yielding most of PF-1B
632 assemblages was deposited in open marine, proximal middle shelf conditions during a general
633 local sea level rise, which corresponds to the Tethyan early Aptian long-term high stand sea
634 level (Fig. 13B). However, the uppermost lower Alamein Formation (uppermost lower Aptian)
635 was deposited in a shallower marine deltaic setting that probably represents the effect of the
636 minor local Aptian uplift and the Tethyan early Aptian short-term sea level falls. The upper Alam
637 El Bueib (uppermost Barremian) and upper Alamein (middle Aptian) formations were deposited
638 in distal deltaic (prodelta) and prodelta–proximal inner shelf settings, respectively due to minor
639 sea level falls, which correlate with the Tethyan late Barremian and middle Aptian major short-
640 term sea level falls. Developing reducing, dysoxic–anoxic to suboxic–anoxic conditions occurred
641 in bottom water during deposition of the studied formations.

642 Similar regressive deltaic deposits alternating with relatively deeper marine, carbonate-
643 dominated ramp deposits have been recorded in North Sinai, in northeastern Egypt (Bachmann
644 et al., 2010). These deposits correspond to the Tethyan late Barremian minor long-term (2nd
645 order) and short-term (3rd order) sea level falls, and the Tethyan early Aptian high stand sea
646 level. On the Levant plate of NW Syria, the Aptian carbonate successions have relatively
647 deeper marine settings in comparison to the shallow carbonates recorded in the present study.
648 However, sea level oscillations resulted in the development of a lower Aptian 2nd order
649 transgressive-regressive sequence (Ghanem and Kuss, 2013), which correlates with the
650 Egyptian lower–middle Aptian 2nd order and 3rd order depositional sequences (evidenced by
651 samples yielding PF-1B). Through this time period, sedimentation in Egypt and Syria moves
652 from carbonate-dominated to clastic-dominated deposits (Fig. 7; Ghanem and Kuss, 2013, fig.
653 21). Likewise, on the eastern Arabian shelf, the upper Barremian–lower Aptian of Oman exhibits
654 the influence of the minor 3rd order late Barremian sea level fall and the early Aptian 2nd order
655 high stand, where clastic-starved, high-energy, bioturbated shallow lagoonal carbonates
656 alternated with relatively deeper open-water, lagoonal carbonates (Hillgartner et al., 2003).

Upper Barremian–lower Aptian successions in southeastern Tethys (Egypt and Oman) can therefore be shown to have been influenced by the Tethyan eustatic late Barremian sea level fall and the early Aptian high stand. The lower Aptian 3rd order transgressive–high stand depositional sequence identified in Tunisia by Hfaiedh et al. (2013) can also be equated to the relatively transgressive depositional sequence represented by PF-1B, and corresponds to the Tethyan early Aptian high stand sea level. The relatively minor middle Aptian regressive sequence (upper PF-1B) of the Abu Tunis 1X well can also be correlated with the regressive 3rd order sequence in North Sinai (Bachmann et al., 2010) and Tunisia (Ghanem and Kuss, 2013; Hfaiedh et al., 2013).

In the northern Tethyan successions of SE Spain, Hoedemaeker and Leereveld (1995) and Bernaus et al. (2003) recognized upper Barremian regressive depositional sequences and lower Aptian relatively transgressive depositional sequences. These sequences also equate to the lowermost parts of PF-1B (upper Barremian–lower Aptian) in the Abu Tunis 1X well (Fig. 7), and correspond respectively to the Tethyan late Barremian minor long-term (2nd order), major short-term (3rd order) sea level falls, and the Tethyan early Aptian high stand. Based on the data presented above, it is clear that Tethyan eustatic sea level changes exerted strong control on the upper Barremian and lower–middle Aptian sequences, which developed in the aforementioned regions of northern and southern Tethys (including Egypt).

5.3. Palynofacies subzone (PF-2A)

Stratigraphic distribution and content: samples 43–85 (8,050–5,950 ft / 2,274–1,634 m) from the Dahab (upper Aptian) and lower Kharita (lower Albian) formations yielded assemblages grouped as subzone PF-2A (Fig. 8). This palynofacies demonstrates a recurring terrestrial influence (Fig. 9C), which is stronger than that noted from PF-1A. This is reflected here in the extremely abundant phytoclasts (28,667–487,048, avg. 194,033 particles/g) and high concentrations of sporomorphs (1,194–108,697, avg. 18,205 grains/g). Dinocyst concentrations decrease by comparison to the underlying PF-1B (250–4,181, avg. 1,365 cysts/g) and there are only low MFTL concentrations (418–1,394, avg. 906 grains/g). Extremely high concentrations

(23,363–689,810, avg. 172,434 particles/g) of AOM are recorded here in comparison to those recorded from PF-1A and PF-1B (Fig. 8).

Tracheid abundances are also extremely high (28,548–487,048, avg. 185,128 particles/g) and dominate the phytoclast assemblages along with cuticle fragments (119–62,710, avg. 12,209 particles/g; Fig. 9C). However, membranous tissues (1,003–20,903, avg. 5,890 particles/g) and black wood (1,170–12,542, avg. 5,964 particles/g) show concentrations lower than those recorded from the underlying PF-1B assemblages. Sporomorph abundances in PF-2A are noticeably higher than in PF-1B, exemplified by higher concentrations of pteridophyte spores (836–94,065, avg. 13,194 grains/g), *Classopollis* (119–4,181, avg. 1,899 grains/g), and other spherical gymnosperm pollen (239–10,452, avg. 2,047 grains/g). A few freshwater algae, including representatives of *Ovoidites* (19–109, avg. 53 grains/g) and *Botryococcus* (12–76, avg. 44 grains/g), and the euglenoid freshwater form *Chomotriletes* (19–56, avg. 37 grains/g) occur, along with rare acritarchs (31 grains/g). Dinocysts show a decrease in abundance and diversity (~ 0.67), and are again dominated by cavate (182–2,323, avg. 880 cysts/g) and proximate (91–1,951, avg. 529 cysts/g) forms, with chorates showing the lowest concentrations (30–2,926, avg. 328 cysts/g). The cavate cysts are again mainly represented by the genera *Subtilisphaera* and *Senegalinium,* with subordinate *Palaeoperidinium*. The proximate cyst assemblage is composed of *Pseudoceratium* and *Cribroperidinium* species, while *Oligosphaeridium* and *Florentinia* are the only genera in the chorate cyst community.

Palynofacies association of PF-2A: AOM/brown wood/spore-dominated (figs. 8, 9C).

Sedimentary facies of PF-2A: downhole log responses for samples yielding PF-2A indicate the development of several fining upward sequences, which are reflected in increases in the self-potential profile as it crosses the sand:shale line (Fig. 7). This part of the succession is a thick, fine to medium-grained sandstone with a silicic to carbonate matrix, which contains various traces of pyrite and anhydrite. These beds are intercalated with thin, light grey to green fissile shale horizons, which contain macroscopic carbonaceous material (Fig. 8).

Depositional environment: deltaic (delta channel)

By comparison with the underlying part of the succession (PF-1A and PF-1B), PF-2A shows a general decrease in dinocyst abundance/species diversity and a dominance of restricted, lower salinity species (e.g., *Subtilisphaera* and *Pseudoceratium*). This data suggests that whilst PF-2A shows a marine signal, the deposits from which this assemblage comes were deposited during a regressive phase (e.g., Batten, 1983; Leckie and Singh, 1991; Tyson, 1993; 1995), similar to that suggested for PF-1A. However, deposition probably took place in a more stressed marine situation (e.g., Mutterlose and Harding, 1987; Lister and Batten, 1988; Tahoun and Deaf, 2016; Deaf and Tahoun, 2018). The very high abundances of terrestrially derived organic matter and the decline in dinocyst abundance and diversity confirm the more marginal marine (brackish–coastal) conditions. The work of Degens and Mopper (1976) also suggests that high influxes of terrestrially derived phytoclasts can be indicative of sedimentation in estuarine and very nearshore areas during a regressive event, and the same has been reported for spores in delta-top channel-fill sand and silt deposits (Batten, 1982; Tyson, 1995). Most of the samples from which this palynofacies come are indeed comprised of a coarser clastic facies (mainly sandstones) than samples of the lower part of the succession, and they would thus have been deposited in a shallower setting and/or under relatively higher energy conditions than PF-1B. The high concentrations of tracheids are confirmation of deposition in proximal transitional environments that were close to the parent plants, and specifically in fluvio–deltaic systems (e.g., Pocklington and Leonard, 1979). This is also the case for the high concentration of cuticles, characteristic of delta-top, distributary channels, delta-front, and prodelta settings (e.g., Batten, 1973; Parry et al., 1981; Nagy et al., 1984). The coarser sandstone lithology of PF-2A-bearing samples excludes a prodelta interpretation, because the latter is characterised by finer-grained facies (e.g., mainly shale; Einsele, 1992; Boggs, 2006).

Although delta-front or delta channel settings are characterised by strong influxes of black wood (Tyson, 1995), the relatively low PF-2A concentrations of that maceral, coupled with extremely high brown wood concentrations, may be explained by the humid costal conditions

741 inferred for the Albian (Deaf, 2009; Deaf et al., 2014). This could have resulted in very high
742 runoff, enhancing supply of fresh brown wood (Tyson, 1995) that was coupled with high rates of
743 deposition in the continuously subaqueous depositional setting, diluting the black wood
744 concentrations (Lamberson et al., 1991). Thus, a delta channel setting is suggested as the
745 depositional environment for the samples yielding PF-2A assemblages. Furthermore, the
746 presence of freshwater algae and acritarchs also suggest deposition in very near shore
747 brackish, deltaic environments (Al-Ameri and Batten, 1997; Sarjeant and Taylor, 1999;
748 Courtinat, 2000). The SP profile identifies several fining upward sequences in the main
749 sandstone succession, which also suggests a deltaic distributary channel setting under
750 regressive conditions (Fig. 6; Rider, 2002), also indicated by the ternary plot of PF-2A
751 constituents (Fig. 12C). This local regressive event is coincident with the late Aptian–Albian
752 regional uplift, which affected most of northern Egypt (Meshref, 1990), and was recognized by
753 Darwish (1994, p. 278) in the Matruh Basin during the early Albian.

754 Local anoxic conditions are reflected in the widespread occurrences of AOM and pyrite
755 in the sandstones and shales (e.g., 7,930 ft / 2,237.5 m, 7,620 ft / 2,143, 7,480–7,340 / 2,100–
756 2,057 m, 7,140–7,120 ft / 1,997–1,991 m, 6,300–6,280 ft / 1,741–1,735 m) of PF-2A (Tyson,
757 1995; Deaf and Tahoun, 2018). The extremely high concentrations of AOM in most PF-2A
758 samples indicate the development of significant reducing conditions. These reducing conditions
759 represent suboxic to anoxic conditions given the ternary kerogen plot of PF-2A samples (Fig.
760 12A). Membranous tissues are typically found in higher concentrations in non-marine and
761 proximal deltaic facies, and become much rarer in a basinward direction (e.g., Tyson, 1995).
762 These tissues cannot tolerate oxidising conditions, and degrade three times faster than lignified
763 wood (e.g., Stout et al., 1981). Therefore, as Tyson (1995) has suggested, high concentrations
764 of such tissues may be taken to indicate short-lived, high sedimentation rates for samples
765 yielding these membranous tissues, where rapid burial must have prevented the removal of
766 these fragile tissues by the oxic conditions at the sediment-water interface.

767 Combining all of these characteristics, and given the predominance of PF-2A
768 assemblages in sandstone lithologies, the Dahab (upper Aptian) and lower Kharita (lower

Albian) formations were deposited in a delta channel system during a regressive phase, which may have incised into or prograded out over the underlying prodelta–proximal inner shelf sequence of the Alamein Formation (Fig. 13C). This regressive phase probably reflects the strong effect of the local tectonics, which masked the late Aptian–middle Albian minor long-term (2nd order) Tethyan sea level rise. Stronger reducing, suboxic–anoxic conditions than those of the underlying Alamein Formation prevailed.

An analogous trend of an upward change in sedimentation from marginal clastic to shallow marine carbonate deposits was recorded in the north Eastern Desert of Egypt by Abd-Elshafy and Abd El-Azeam (2010). In North Sinai, a similar broadly deltaic system with high siliciclastic influx evolved northward into a relatively deeper marine carbonate-dominated ramp (Bachmann et al., 2010). These two sequences can thus also be shown to correspond to the late Aptian–middle Albian minor long-term and short-term Tethyan eustatic sea level rises. In NW Syria, the upper Aptian regressive sequences similarly exhibiting a change in sedimentation from carbonate through to clastic deposits, were related by Ghanem and Kuss (2013) to the late Aptian eustatic lowstand. In a similar fashion, in Oman, situated on the eastern margin of the Arabian shelf, the upper Aptian–lower Albian succession of carbonate rocks was also effected by late Aptian–early Albian regional uplift and regression (Hillgartner et al., 2003).

5.4. Palynofacies subzone (PF-2B)

Stratigraphic distribution and content: the palynofacies constituents of samples 86–100 (5,900–4,800 ft / 1,798–1,463 m) are derived from the middle–upper Kharita (middle–upper Albian) and lower–middle Bahariya (lower Cenomanian) formations. Samples of the subzone PF-2B show a relatively weaker terrestrial signal in comparison to the underlying PF-2A (Fig.13A); although phytoclasts still dominate the POM assemblages (9,007–253,976, avg. 101,423 grains/g). Sporomorph concentrations diminish to (114–66,293, avg. 12,539 grains/g), but dinocyst concentrations increase considerably (139–4,181, avg. 1,744 cysts/g), while MFTL concentrations are lower than in PF-2A (597–1,045, avg. 826 grains/g). AOM (37,858–564,390, avg. 222,969 particles/g) still shows high concentrations similar to that of PF-2A.

The phytoclasts are still dominated by tracheids (6,727–227,846, avg. 94,391 particles/g) and cuticle (1,672–34,839, avg. 10,283 particles/g). Membranous tissues show concentrations similar to those of PF-2A: 418–27,871, avg. 5,575 particles/g. Black wood occurs only at the base of the succession containing PF-2B, with a concentration of 10,452 particles/g.

Figure 14 about here

Miospore concentrations continue the decrease seen through PF-2A, but pteridophyte spores still dominate (557–60,321, avg. 8,570 grains/g) the palynomorph assemblage, with subordinate schizaeacean spores (1,394–1,792, avg. 1,593 grains/g), spherical pollen grains (418–1,792, avg. 909 grains/g), and *Classopollis* (418–1,347, avg. 674 grains/g). Dinocyst abundance and dominance increases and this coincides with a decrease in diversity (~ 0.55). The cavate *Senegalinium* dominates dinocyst assemblages (196–4,738, avg. 1,507 cysts/g), while proximate (e.g., *Trichodinium*) and chorate (e.g., *Oligosphaeridium, Coronifera*, and *Florentinia*) taxa are minor constituents (61–1,394, avg. 379 cysts/g and 33–836, avg. 362 cysts/g respectively).

Palynofacies association of PF-2B: AOM/brown wood/dinocyst-dominated (Fig. 8, Fig. 14A).

Sedimentary facies of PF-2B: SP profile indicates a fining upward sequence for the clastic part of the succession yielding this palynofacies. The original well log and cutting sample descriptions evidence a lower sequence of alternating shale and limestone beds, which is overlain by a pale brown dolostone unit. The upper sequence of samples yielding PF-2B come from a thick clastic unit of very fine to medium-grained sandstone beds with dolomitic cement and traces of glauconite. Light grey shale streaks containing traces of pyrite in the silty-shale horizons of lower and upper parts of the palynofacies occur as thin alternations in the main sandstone unit.

Depositional environment: deltaic to inner shelf

The dinocysts in PF-2B differ from those of PF-2A, with the general upward increase in the dinocyst abundance indicating the development of a more offshore setting than that of PF-2A, possible evidence of relative sea level rise (e.g., Davey, 1970), compatible with declines in the terrestrially derived organic matter (e.g., Tyson, 1993, 1995; Batten, 1999). Such a relative rise could be related to the Tethyan late Albian–early Cenomanian sea level rise (Haq, 2014; Fig. 7).

Samples 86–90 at the base of the PF-2B succession consist of alternating shale/dolostone facies containing traces of glauconite (5,780 ft / 1,582 m) and contain similar pteridophyte spores and membranous tissues to those recorded in the prodelta facies of the lower PF-1B-bearing samples (Fig. 8). However, samples of lower PF-2B are relatively enriched in the inner–middle shelf cavate dinocyst *Senegalinium* (Brinkhuis and Zachariasse, 1988; Slimani et al., 2010; Deaf and Tahoun, 2018). Lower PF-2B samples also contain subordinate concentrations of the middle shelf chorate cysts *Coronifera* and *Spiniferites* (Marshall and Batten, 1988; Brinkhuis, 1994) and the inner–middle shelf proximate cyst *Trichodinium castanea* (Ibrahim et al., 2009; Peyrot et al., 2011; Deaf and Tahoun, 2018). The relatively higher tracheid and cuticle concentrations in the lower PF-2B in comparison to those recorded from the lower PF-1B indicate a stronger terrestrial influence, which could be explained in the context of the coastal and regionally humid Albian–Cenomanian climate in contrast to the drier late Barremian–Aptian (Abdel-Kireem et al., 1996; Deaf, 2009; Deaf et al., 2014). The shales and carbonates producing PF-2B overlie the coarser delta channel sequence of PF-2A, and indicate a relative sea level rise, which is probably linked to the Tethyan late Albian eustatic sea level rise (Fig. 7).

However, the subsequent upward increase in siltstone and sandstone lithologies and the occurrence of some glauconite traces (5780 ft, 1,582 m and 5,530 ft / 1,506 m) and pyrite (5,500 ft / 1,497 m) in the clastic unit of PF-2B (middle Kharita) indicate a minor regressive phase. By analogy with the sedimentary facies of PF-2A and its associated SP profile, the

853 coarse clastic unit of PF-2B (samples 91–96) was also deposited in a regressive delta channel
854 setting. This local marine regression corresponds to the Tethyan middle Albian short-term sea
855 level fall (Figs. 6, 7; Haq, 2014).

856 Above this, the slight increase in dinocyst concentrations dominated by *Senegalinium*,
857 subordinate proximate (*Trichodinium*) and chorate dinocyst concentrations, and the decrease in
858 tracheids and cuticles at the uppermost samples (97–100) of PF-2B – the upper Kharita–middle
859 Bahariya formations – indicate the onset of the latest Albian–earliest Cenomanian marine
860 transgression. The dinocyst assemblages and the sandstone/siltstone alternating with shales
861 containing traces of glauconite (4,850 ft / 1,299 m), suggest delta-front to proximal inner shelf
862 settings for this interval. The persistently high concentrations of AOM indicate the same bottom-
863 water suboxic–anoxic conditions that produced the underlying PF-2A (Fig. 12A).

864 Thus, we suggest the major clastic unit of the middle–lowermost upper Kharita (middle–
865 lowermost upper Albian) was deposited in a location that evolved from a delta channel
866 environment to prodelta–proximal inner shelf settings under suboxic–anoxic conditions.
867 Deposition of the uppermost Kharita (uppermost Albian) and lower–middle Bahariya (lower
868 Cenomanian) was influenced by the Tethyan latest Albian–earliest Cenomanian long-term sea
869 level rise, in prodelta–proximal inner shelf and deltafront–proximal inner shelf settings,
870 respectively.

871 This is a very similar interpretation to that made for the clastic deposits at the type
872 locality of the Bahariya Formation (Bahariya Oasis), which show strong terrestrial influx. At the
873 type locality, the formation was deposited in a fully fluviatile setting, but pronounced lateral
874 facies variations resulting in a change from fining upward fluvio–deltaic channel sandy facies in
875 the south to coarsening upward costal–shallow marine clastic facies at the northern margin of
876 the basin were recorded (Khalifa and Catuneanu, 2008). This deltaic–shallow marine facies
877 exhibits a general long-term (2nd order) relative sea level rise (Catuneanu et al., 2006). A
878 similar change is seen in the north Eastern Desert of Egypt, where marginal, shallow marine
879 clastics are overlain by alternations of shallow marine clastics and carbonates and then by deep
880 marine carbonates were recorded by Abd-Elshafy and Abd El-Azeam (2010). In NW Syria, two

major Albian 2nd order regressive–transgressive sequences correlate with the two Egyptian Albian 2nd order regressive–transgressive depositional sequences (upper PF-2A and PF-2B; Ghanem and Kuss, 2013). Elsewhere in the southern Tethyan Realm, this late Albian long-term sea level rise was also expressed by deposition of an upper Albian 2nd order transgressive carbonate sequence in NW Algeria (Nagm and Boualem, 2019).

5.5. Palynofacies zone (PF-3)

Stratigraphic distribution and content: Samples 100–121 (4,750–3,750 ft / 1,447.8–1,143 m) represent the upper Bahariya (lower–? middle Cenomanian) and Abu Roash (middle–upper Cenomanian) formations. The organic matter content of this PF-3 is more impoverished, but provides evidence for a return to more marine conditions, as it is almost entirely composed of marine palynomorphs. All terrestrially derived macerals are rare (132 cuticles/g, 113 tracheids/g, 75 membranous tissues/g, 9–55, avg. 25 pteridophyte spores/g; Fig. 8, Fig. 14B). Whilst also uncommon, the palynofacies is dominated by marine palynomorphs (25–4051, avg. 936 dinocysts/g and 166–1,991, avg. 967 MFLTs/g). Indeed, dinocyst diversity is lower (~ 0.35) than that recorded in all the underlying palynofacies, but cavates continue to dominate the assemblage (287–3,428, avg. 1,760 cysts/g), represented by the genus *Senegalinium.* There are subordinate concentrations of chorate cyst genera *Spiniferites* and *Florentinia,* along with *Xiphophoridium alatum* (10–1,359, avg. 299 cysts/g) and the proximate genus *Trichodinium* (31–523, avg. 142 cysts/g).

Palynofacies association of PF-3: AOM/dinocyst/MFTL-dominated (Fig. 8, Fig. 14B).

Sedimentary facies of PF-3: the sequence yielding PF-3 assemblages is interpreted from cutting samples as comprising a lower carbonate unit made of white to pale grey microcrystalline limestone with rare silt/shale intercalations, overlain by a second carbonate unit of light brown dolomitic limestones. A third carbonate unit lies above this, comprising a chalk and a second thin dolostone bed containing traces of pyrite .

Depositional environment: middle shelf

PF-3 contains a dinocyst assemblage similar to that of the upper PF-2B samples, dominated by the inner–middle shelf cavate *Senegalinium*. However, PF-3 shows higher concentrations of the middle–outer shelf chorate cysts *Spiniferites*, *Florentinia*, and *Xiphophoridium alatum* (e.g., Dale, 1983; Lister and Batten, 1988, Tahoun and Deaf, 2016), with lower concentrations of the inner–middle shelf *Trichodinium*. This suggests that PF-3 was deposited during a relative sea level rise in a deeper open marine middle shelf environment by comparison to that of PF-2B. The high dominance of *Senegalinium* here has previously been suggested by Slimani et al. (2010) to indicate open marine transgressive phases, and was recently recorded by Deaf and Tahoun (2018) from the transgressive systems tract (TST) sequence no. 3 (SQ. 3) of Abu Tunis. Deaf and Tahoun (2018) recorded a marine palynomorph assemblage from the BED 2-4 well in the southern Abu Gharadig Basin in the north Western Desert of Egypt, where MFTLs of the probably benthic foraminifera *Thomasinella punica*, *Thomasinella fragmentari*, and *Daxia cenomana* occur with the dinocyst genus *Senegalinium.* Despite the occurrence of a few dinocysts more typical of outer shelf settings, this assemblage was interpreted as representing an inner shelf situation based on the accompanying benthic foraminifera. The aforementioned foram taxa occur in inner shelf water depths (10–30 m), flourish in the inner middle shelf (depths 30–50 m), but are not present in outer middle shelf settings deeper than 50 m (El Ashwah and El Deeb, 2000; Gräfe, 2005; Shahin and Elbaz, 2013). Both palynofacies types of BED 2-4 showed the lowest frequencies of the terrestrially derived organic matter (pteridophyte spores, brown and black wood) except for the climatically/hydrodynamically controlled acme of the spherical pollen grains of *Classopollis*, which are typically abundant in the middle shelf settings of the intracratonic graben basins of the north Western Egypt (Deaf and Tahoun, 2018). In the current work, the lower (samples 102–107) and upper (samples 114–119) parts of the PF-3 zone show a decreased dinocyst assemblage, common MFTLs and lower *Senegalinium* cyst concentrations. In contrast, the

936 middle part (samples 108–112) of the PF-3 zone shows dominance of *Senegalinium* at the
937 expense of MFTLs.

938 In addition, the lower concentrations of terrestrially derived organic matter in PF-3 in
939 comparison to that of the underlying PF-2B also indicate the deposits yielding PF-3 were
940 deposited away from active fluvio–deltaic systems and represent relatively deeper/more
941 offshore marine conditions. The weak terrestrial influxes likely reached the open marine settings
942 only during periods of excessive rainfall and strong terrestrial input (Tyson, 1984, 1995; Deaf
943 and Tahoun, 2018). This is exemplified here by the occurrences of the terrestrial palynomorphs
944 in the clastic shale horizons within the otherwise carbonate-dominated succession of PF-3. The
945 regionally humid middle–late Cenomanian climate (Abdel-Kireem et al., 1996, Deaf, 2009; Deaf
946 et al., 2014), would argue against reduced terrestrial runoff being the reason for the diminishing
947 of terrestrially derived organic matter in PF-3.

948 Based on the aforementioned parameters, the lower and upper parts of the succession
949 yielding PF-3 are interpreted as having been deposited in a proximal middle shelf setting that
950 corresponds to the minor latest early and earliest late Cenomanian Tethyan short-term sea level
951 falls. The shallow proximal middle shelf setting of lower and upper PF-3 deposits is
952 characterised by frequent clastic (shale) intercalations containing terrestrial palynomorphs. The
953 middle part of the PF-3-bearing succession was deposited in a more distal (outer) middle shelf
954 setting, represented by deposition of pure carbonates containing only marine palynomorphs
955 (Fig. 8). This change in deposition from a proximal to a distal middle shelf setting supports the
956 interpreted local sea level rise, which corresponds generally to the Tethyan middle–late
957 Cenomanian long-term sea level rise (Fig. 7; Haq, 2014).

958 The younger samples yielding PF-3 (samples 114–119) have lower dinocyst and much
959 higher MFTLs concentrations, which may be the result of a bias resulting from the process of
960 dolomitisation. Whilst the low dinocyst abundance/diversity hinders interpretation of the
961 depositional environment of the upper PF-3 samples, the MFTLs would point to a proximal
962 middle shelf setting. This interpretation is consistent with the sedimentological/palaeontological
963 and the palynological/foraminiferal interpretations of the inner to middle shelf origin of the upper

964 Bahariya and Abu Roash formations in the north Western Desert of Egypt (Kerdany and Cherif,
965 1990; Said, 1990; Abdel-Kireem et al., 1996). These formations were deposited in a slightly
966 deeper (middle shelf) setting in the costal Matruh Basin compared with the shallower (inner
967 shelf) setting seen in the southern Abu Gharadig Basin (Mahmoud et al., 2017; Deaf and
968 Tahoun, 2018). This is shown by the occurrence of the early–middle Cenomanian bloom of
969 *Senegalinium* of the middle shelf setting in Abu Tunis 1X well in the Matruh Basin (Deaf and
970 Tahoun, 2018) that is replaced southward in AG-13 well in the Abu Gharadig Basin by the
971 early–middle Cenomanian bloom of *Subtilisphaera* of the inner shelf (Ibrahim et al., 2009). The
972 ternary palynomorph plot confirms deposition of PF-3 in proximal to distal offshore settings in
973 comparison to the underlying palynofacies types (Fig. 12C). The dominance of AOM and traces
974 of pyrite around 3770 ft / 969.5 m indicate suboxic–anoxic conditions (Fig. 12A).

975 By combining all data discussed above, it is suggested that samples of PF-3 were
976 deposited during transgressive phase under suboxic–anoxic conditions. The upper Bahariya
977 (lower–? middle Cenomanian) and upper Abu Roash (upper Cenomanian) formations were
978 deposited in proximal middle shelf settings (Fig. 13D), whilst the lower Abu Roash Formation
979 (middle Cenomanian) was deposited in a relatively more distal middle shelf setting. This general
980 relative sea level rise matches well with the Tethyan middle–late Cenomanian long-term sea
981 level rise.

982 In NW Egypt, sequence stratigraphic analysis of a transect of middle-upper Cenomanian
983 successions including the upper Cenomanian of the Abu Tunis 1X well showed the
984 development of a middle Cenomanian 3rd order transgressive depositional sequence overlain
985 by an upper Cenomanian 3rd order regressive sequence (Deaf and Tahoun, 2018). A
986 transgressive sequence of deep marine carbonates similar to those of the Abu Tunis 1X in the
987 Matruh Basin is also found in the upper Cenomanian of the north Eastern Desert of Egypt (Abd-
988 Elshafy and Abd El-Azeam, 2010), representing a continuation of the late Cenomanian Tethyan
989 long-term sea level rise. The Cenomanian long-term (2nd order) sea level rise is also expressed
990 in NW Algeria with deposition of mixed clastic–carbonate, evaporite–clastic, and inner–outer
991 ramp carbonate deposits (Benyoucef et al., 2017).

The northern Tethyan margin of SW France records a lower Cenomanian 3rd order depositional regressive sequence (C_2) and a middle Cenomanian 3rd order transgressive depositional sequence (C_3; Andrieu et al., 2015). These sequences bear a striking similarity to the lower Cenomanian 2nd order regressive sequence (lower PF-3) and the middle Cenomanian 3rd order transgressive sequence (middle PF-3) in the present study.

6. Implications for Cretaceous climate across northeastern Gondwana

Previous interpretations of the Cretaceous climate on micro- and macro-palaeontological and lithologic evidences have been published by various authors (e.g., Doyle et al., 1982; Parrish et al., 1982; Herngreen et al., 1996; Doyle, 1999; Mejia-Velasquez et al., 2018), with other studies using general circulation models (e.g., Sellwood and Valdes, 2006; Fluteau et al., 2007). Here, we provide some inferences about the equatorial climate that prevailed over Egypt (i.e., northeastern Gondwana) during the Cretaceous from a palynofloristic point of view. Certain sporomorphs of known botanical affinities are indicators of specific ecological parameters and thus allow not only reconstruction of the vegetation growing on the source areas but also permit a robust interpretation of palaeoclimatic conditions. A summary table of some of the known botanical affinities of certain spore and pollen grains found in the Abu Tunis 1X samples (Table 1) provides an indication of known ecological preferences.

Table 1 about here

The data in Table 1 are based on the ecological/palaeoenvironmental interpretations of spore and pollen taxa of Mesozoic, and specifically Cretaceous and Jurassic age from published literature (e.g., Balme, 1995; Schrank and Mahmoud, 1998; Doyle, 1999; Schrank, 2001; Abbink et al., 2004; Deaf et al., 2016). The most conspicuous climate indicators are the xerophytic *Classopollis* and *Ephedripites* pollen grains. The gymnospermous pollen *Classopollis* is known to have been produced by thermophilous, drought-resistant cheirolepidiacean conifers and thus provides a valuable proxy indicator for palaeoclimatic conditions (e.g., Doyle, 1999).

As high abundances of *Classopollis* were found to be associated with evaporites, salts, and red bed deposits, and also with xeromorphic wood and leaf macrofossils of cheirolepidiacean affinity. These associations indicate that this pollen genus was produced by parent plants adapted to hot and dry conditions (e.g., Watson, 1988; Doyle, 1999).

The fossil gymnospermous gnetalean pollen genus *Ephedripites* shows a great similarity to pollen produced by the modern xerophytic gnetalean plants *Ephedra* and *Welwitschia* (Trevisan, 1980). Furthermore, the gnetalean macrofossils *Drewira* and *Eoanthus* revealed close relation between plants that produced these macrofossils and modern gnetalean plants of well-known xeromorphic nature (Crane, 1988). High abundances of *Ephedripites* pollen have thus been taken to indicate hot and dry conditions (e.g., Doyle et al., 1982; Doyle, 1999). Trevisan (1972) suggested a cheirolepidiacean conifer affinity for *Dicheiropollis etruscus,* a pollen grain similar to the thermophilous *Classopollis*, and it was therefore suggested that the parent plant of the former was adapted to warm arid conditions (Deaf et al., 2016). In this context, fluctuations in the abundances of these xerophytic genera can be used to infer temperature changes in the Early Cretaceous. Pteridophytes are known humidity indicators, as they thrive in warm, humid lowlands, such as riversides and coastal areas (e.g., Pelzer et al., 1992; Abbink et al., 2004). Therefore, high relative abundances of fossil pteridophyte spore taxa such as *Deltoidospora, Concavissimisporites,* and *Impardecispora* are regularly used as a proxy for humid conditions (e.g., Abbink et al., 2004; Bornemann et al., 2005).

We present quantitative palynomorph data along with percentage occurrence data for some selected palaeoclimate-indicator palynomorphs, to permit comparison with previous northern Gondwana Province palynological studies, which provide percentage frequency data. Quantitative data is taken from Deaf (2009, p. 313–314) and Deaf et al. (2014, 2016) and is tabulated in the online Supplementary Appendix 4. The semi-quantitative (percentage) data calculated herein derive from the total palynomorph assemblage counts of our wider palynofacies counts to permit a wider comparison with previous studies.

A succession of authors have examined the distribution of Cretaceous micro- and macro-floral fossil assemblages across Africa and South America and have defined a

succession of Gondwanan phytogeographic provinces, including the work of Brenner (1976), who defined the Northern Gondwana Province, and Herngreen and Chlonova (1981) who described the West African–South American (WASA) Province. Later work by Herngreen et al. (1996) included northern and eastern Africa and defined a pre-Albian Early Cretaceous equatorial palynoprovince that they named the *Dicheiropollis etruscus*/*Afropollis* Province (Fig. 15A). In the later middle Cretaceous (Albian–Cenomanian) Africa and South America fell within the African–South American (ASA) Province of Herngreen (1974), the equivalent of Brenner's (1976) Northern Gondwana Province. The work of Herngreen et al. (1996) later redefined the ASA Province, renaming it the Albian–Cenomanian Elaterates Province (Fig. 15B). These phytogeographic provinces have approximately latitudinal boundaries, which adjacent provinces that largely reflect the effect of palaeoclimate on the distribution of miospore-producing land plants (e.g., Herngreen et al., 1996), and thus they have been used successfully in the reconstruction of the regional Cretaceous climate (e.g. Doyle, 1999).

The spores and pollen grains from the Abu Tunis 1X well, belong to the pre-Albian *Dicheiropollis etruscus*/*Afropollis* and the Albian–Cenomanian Elaterates phytogeographic provinces. Whereas most of the pre-Albian (late Hauterivian–Aptian) palynofloras from the Abu Tunis well contain taxa characteristic of the *Dicheiropollis etruscus*/*Afropollis* province, the abundances of some of the diagnostic taxa differ (Deaf et al., 2016), discussed briefly below (see also Deaf et al., 2014, 2016). Herngreen et al. (1996) believed the early angiosperm pollen taxa *Stellatopollis* spp. and *Retimonocolpites* spp. were characteristic only of the late Barremian of Brazil. However, previous palynological work in North Africa (e.g., Gübeli et al., 1984: Morocco; Thusu and van der Eem, 1985; Thusu et al., 1988: northeast Libya; Penny, 1991; Schrank, 1992: Egypt and north Sudan) and West Africa (e.g., Doyle et al., 1977: Gabon) clearly indicates *Stellatopollis* and *Retimonocolpites* as important elements in the eastern Northern Gondwana Province.

Figure 15 about here

1076 The identification of several new species of *Stellatopollis* and *Retimonocolpites* and a
1077 new species of *Tucanopollis* from the Lower Cretaceous of Egypt (e.g., Penny, 1988a, b, 1991;
1078 Schrank and Mahmoud, 1998, Ibrahim, 2002) confirmed that these angiosperm genera were not
1079 limited to the Cretaceous of northern South America (NE Brazil). However, they were also
1080 characteristic of the whole Northern Gondwana Province (Fig. 15A). The high number of
1081 angiosperm pollen taxa (22 genera and 39 species) in the Abu Tunis 1X well (Deaf, 2009; Deaf
1082 et al., 2014, 2016), further emphasizes the importance of Egypt in the proliferation of early
1083 angiosperms in the northeastern Gondwana Province (Doyle, 1999; Schrank and Mahmoud,
1084 2002, and references therein).

1085 Regional correlation of the Cretaceous palynofloras of Abu Tunis 1X with those recorded
1086 from the Siqeifa 1X well on the eastern margin of the Matruh Basin and those of Sanhur-1 well
1087 in the neighbouring costal Dahab–Mireir (= Alamein) Basin (Fig. 1) show palynofloras similar in
1088 nature and composition. Palynofloras of the latter two wells were also deposited in marginal and
1089 shallow marine settings similar to those interpreted for the Abu Tunis 1X well (Mahmoud and
1090 Moawad, 2002; Mahmoud and Deaf, 2007). The Hauterivian–lower Barremian of Siqeifa 1X
1091 shows minor occurrences of *Classopollis* (0.5–4%) similar to the very rare *Classopollis* (45–
1092 1,120, avg. 361 grains/g; 0.4–4.4%, avg. 3.12%) and *Ephedripites* (21 grains/g; 0.4%) in the
1093 Abu Tunis 1X well (Mahmoud and Deaf, 2007; Fig. 8, online Supplementary Appendices 3 and
1094 4). However, increased abundances of *Classopollis* (1–6%) and *Ephedripites* (0.5–5.5%) are
1095 seen from the upper Barremian–Aptian of Siqeifa 1X (Mahmoud and Deaf, 2007) and the Aptian
1096 (>5%; 1– >5%) of Sanhur-1 wells (Mahmoud and Moawad, 2002). Similar increases in diversity
1097 and frequency of *Ephedripites* (25–608, avg. 163 grains/g; 0.4–5.2%, avg. 2.4%) and frequency
1098 of *Classopollis* (19–4,457, avg. 668 grains/g; 0.8–38.4%, avg. 9.4%) are also recorded from the
1099 upper Barremian–Aptian of the Abu Tunis 1X well. The Albian–lower Cenomanian of Siqeifa 1X
1100 and Sanhur-1 exhibits lower occurrences of *Classopollis* (0.5–3.5%; 1–5%) and *Ephedripites*
1101 (0.5–4%; 0.5–5%) by comparison to those recorded from the upper Barremian–Aptian of those
1102 wells. The xerophytic pollen in Abu Tunis 1X also shows a similar upward decrease in

abundance of *Ephedripites* (8–470, avg. 172 grains/g; 0.4–5.2%, avg. 2.6%) and *Classopollis* (5–1,394, avg. 261 grains/g; 0.4–5.6%, avg. 2%).

To determine whether xerophytic pollen abundances in the marine-influenced Abu Tunis 1X well deposits can be taken as reliable palaeoclimatic indicators, we examined the distribution of these taxa in other continental/shallow marine sequences in the same area and of similar age. Terrestrial palynofloras from continental successions should provide the most reliable representation of the land flora as they are less affected by dilution by marine palynomorphs, and should therefore indicate regional Cretaceous climatic conditions over much of Egypt and hence northeastern Gondwana. Palynofloras recovered from the continental (Hauterivian–lower Barremian and Albian–lower Cenomanian) and continental to restricted shallow marine (upper Barremian–Aptian) strata from six water wells in the Dakhla Basin show similar low occurrences of *Classopollis* and *Ephedripites* (1– >5.5%; 0.5–5%) in the Hauterivian–lower Barremian (Schrank and Mahmoud, 1998) as we find in Abu Tunis 1X. The upper Barremian–Aptian of the Dakhla Basin shows relatively higher occurrences (1.5– >5.5%) of *Ephedripites* in comparison to the preceding interval, while *Classopollis* shows a diminishing frequency (0.5–5%). The latter is related to the development of an inner shelf setting that is known to be characterised by low occurrences of *Classopollis* (e.g., Deaf and Tahoun, 2018) and partly due to high dilution of terrestrially derived palynomorphs (13% of the palynomorphs) by a short-lived dinocyst (87%) incursion in this Aptian interval (Schrank and Mahmoud, 1998, p. 179). *Classopollis* and *Ephedripites* again show nil to a very low occurrence (0 %; 0.5%) in the Albian–lower Cenomanian, probably the result of an eastward shift of the depocentre from the Dakhla Basin towards the Kharga Basin from the Albian onwards (Schrank and Mahmoud, 1998, p. 181). These regional data indicate that coastal and inland basins show very similar distribution trends of the climate indicator sporomorphs with time. Thus, the xerophyte pollen grains of Abu Tunis 1X will be used as an indicator of the regional climatic conditions over northeastern Gondwana.

Herngreen et al. (1996) suggested a regionally warm humid climate for the Hauterivian of the pre-Albian *Dicheiropollis etruscus*/*Afropollis* of Northern Gondwana based on palynofloras recovered from the West African (Gabon) and north South American (Brazil) regions. The warm

conditions were inferred from the very high frequencies of *Classopollis* (~ 80%) and *Ephedripites* (50–70%) recorded from Berriasian-Aptian successions (Herngreen et al., 1996), whereas inferences of high humidity were based on the common occurrence of pteridophytes and bisaccate pollen grains, an indicator of more temperate conditions.

However, by comparison, a less warm late Hauterivian-early Barremian climate is inferred from the lower occurrences of *Classopollis* (45–1,120, avg. 361 grains/g; 0.8–8%, avg. 3.42%) and *Ephedripites* (21 grains/g; 0.4%) pollen grains in the Abu Tunis 1X well (Doyle et al., 1982; Doyle, 1999). Regionally, less warm conditions are also supported by the low occurrences of *Dicheiropollis* (23–110, avg. 65 grains/g; 0.4–1.2%, avg. 0.8%; Deaf et al., 2016, p. 32, fig. 5). Furthermore, the high occurrences of pteridophyte spores (3,164–20,493, avg. 7,534 grains/g; 62.4–82.8%, avg. 74%, mainly *Deltoidospora*) in the upper Hauterivian–lower Barremian section of Abu Tunis 1X implies more humid conditions, especially in the uppermost Hauterivian–lowermost Barremian part. High absolute and relative abundances in the uppermost Hauterivian–lowermost Barremian correlate here with the minor latest Hauterivian–earliest Barremian marine transgressive period (Figs. 7 and 8). Several studies of the Cretaceous climate have shown that increases in the relative sea level and inundation of inland basins promoted a regional humid climate, whereas decreases in relative sea level promoted a regional arid climate over these inland areas. These sea level changes resulted in latitudinal shifts in the Cretaceous equatorial humid belt – known as the Intertropical Convergence Zone (ITCZ) – over Northern Gondwana (e.g., Parrish et al., 1982; Föllmi, 2012; Carvalho et al., 2019). Therefore, high abundances of the humidity indicators pteridophyte spores suggest that the ITCZ was positioned over northeastern Gondwana (i.e. Egypt) during the late Hauterivian–early Barremian (Fig. 16A).

Figure 16 about here

These more humid conditions are also supported by the occurrences of lignitic coal and coaly carbonaceous material in the upper Hauterivian–lower Barremian succession of the Abu

Tunis 1X well (Fig. 8), the formation of coal at low-latitudes being associated with the ITCZ (Ziegler et al., 2003; Hasegawa et al., 2012). This is supported by greater frequencies and diversities of pteridophyte spores recorded from other Egyptian localities and from Morocco (Herngreen et al., 1996, and references therein), which indicate that the ITCZ was probably situated to the north of the late Hauterivian–early Barremian palaeoequator. The ocean-driven wetter climate prevailed over these areas (Fig. 16A) because of the proximity of the Neo-Tethyan Ocean (Fluteau et al., 2007). Seasonal extremes are reduced in areas bordered by epicontinental seas, and as such this area of northeastern Gonwana likely experienced milder winters and less warm summers (e.g., Fluteau et al., 2007). A mild seasonality in rainfall levels is indeed inferred from the very low occurrence of the arid indicators *Dicheiropollis* and *Classopollis*.

Conversely, the lower abundances of pteridophyte spores and higher occurrences of *Classopollis* and *Ephedripites* in West Africa (Gabon) and northern South America (Brazil) suggest that the western part of northern Gondwana was warmer and drier than the eastern, and probably situated away from the ITCZ. It is important to note that before the breakup of the Gondwana supercontinent, the Afro-Brazilian (Gabon-Brazil) part of the western Northern Gondwana Province comprised a large shallow continental basin, where ponds and shallow lakes were developed in some parts of the basin (Da Rosa and Garcia, 2000). This basin experienced humid winters because of convective winds and local topographic highs, where shade rainfall was developed over some parts of the basin, and as a result, conifer forests thrived on the wet hinterlands (Da Rosa and Garcia, 2000). Thus, the few fern spores recorded in this region (Herngreen et al., 1996, and references therein) were probably thriving in the local lacustrine environments, while the temperate plants producing bisaccate pollen grains were thriving over the cooler hinterlands. Prior to being flooded by the opening Atlantic Ocean, the low-latitude Afro-Brazilian continental interior basin likely experienced very cold winters and very warm summers due to the local tectonic configuration of the basin and developments of palaeotopographic highs (Da Rosa and Garcia, 2000). Thus, arid vegetation (represented by *Classopollis* and *Ephedripites*) must have flourished during the very warm summers.

The late Barremian–middle Aptian of Egypt probably experienced a warm but relatively drier climate, but less dry than that suggested by Herngreen et al. (1996) for the western part (Gabon and Brazil) of Northern Gondwana. Drier conditions of the upper Barremian-middle Aptian in the Abu Tunis 1X well are based on the lower occurrences of pteridophyte spores (512–11,326, avg. 3,003 grains/g; 18.4–75.2%, avg. 49.1%) by comparison to that of the upper Hauterivian-lower Barremian. This is also supported by slight increases in diversity (12 species) and frequency of *Ephedripites* (25–608, avg. 157 grains/g; 0.4–5.2%, avg. 2.6%) and an increase in frequency of *Classopollis* (19–4,457, avg. 746 grains/g; 0.4–58%, avg. 10.7%) in Abu Tunis 1X over the preceding interval. However, these Egyptian frequencies contrast with the very high frequencies of *Classopollis* (~ 80%) and *Ephedripites* (50–70%) recorded in the pre-Albian *Dicheiropollis etruscus*/*Afropollis* Province (Herngreen et al., 1996). The worldwide latitudinal distribution of *Classopollis* shows that this taxon was most abundant during Barremian–Aptian times in the hot and relatively dry palaeosubtropical latitudes (15–30° N and S of the palaeoequator), while it was present in lower abundances in the warm, but slightly wetter palaeotropical region (Doyle, 1999). Doyle et al. (1982), Schrank (1990), and Brenner (1996) all suggested relatively wetter palaeoclimates for the African palaeotropics (e.g., Egypt and Sudan), based on the high occurrences of pteridophytic humidity indicators (fern spores) and lower occurrences of *Classopollis* than that seen in the palaeosubtropics. A less dry palaeoclimate is further corroborated by the low occurrence (21–136, avg. 56 grains/g; 0.4–5.2%, avg. 1.9%) of the drought indicator pollen *Exesipollenites* (Doyle et al., 1982) in Abu Tunis 1X. In addition, the constant occurrences (26–1,520, avg. 263 grains/g; 0.8–8%, avg. 3.8%) of the more temperate indicator pollen *Araucariacites* (e.g., Doyle et al., 1982; Brenner, 1996) in Abu Tunis 1X also support less dry regional conditions than that suggested for the whole Northern Gondwanan region.

The upper Aptian palynoflora of the Abu Tunis 1X well continues to provide evidence for a warm but relatively wetter climate. This is expressed by the upward increases in abundances of *Araucariacites* (186–509, avg. 366 grains/g; 1.6–6.4%, avg. 4.6%) and pteridophyte spores (2,897–12,928, avg. 6,968 grains/g; 59.6–80.4%, avg. 68%) and decreases in *Classopollis*

(125–418, avg. 249 grains/g; 0.8–6%, avg. 2.9%). The relatively more humid conditions are again supported by lignitic coal and bulk coaly carbonaceous material in the upper Aptian deposits of the Abu Tunis 1X well (Fig. 8). Modelling of the Aptian climate over the Northern Gondwana Province indicates the ITCZ was located between 20 N° and S° of the palaeoequator (Chaboureau et al., 2012; Fig. 16B). Through this period, northeastern Gondwana (including Egypt) was characterised by seasonality in rainfall, with wet humid summers and dry winters because of the latitudinal shift of the ITCZ (Chaboureau et al., 2012; Carvalho et al., 2019). The significant increase in pteridophyte spores in the upper Aptian support the location of the ITCZ over northeastern Gondwana during this period (Carvalho et al., 2017, 2019). In Tunisia, Godet et al. (2014) interpreted arid conditions near the early late Aptian boundary based on the clay minerals; similarly, Hfaiedh et al. (2013) postulated an arid earliest late Aptian time based on gypsum deposition and a humid late Aptian based on resumed deposition of clastic deposits. According to Chaboureau et al. (2012), Tunisia was probably situated near the Aptian ITCZ, which was characterised by strong seasonality in rainfall. Thus, the suggested arid conditions near the early late Aptian boundary probably correspond to a latitudinal shift in ITCZ and the development of dry summers. Recent intra-continental data from the western part of Northern Gondwana (NE Brazil), also suggested the development of a late Aptian humid climate in that region due to the movement of the ITCZ and the late Aptian relative sea level rise (Carvalho et al., 2017, 2019). This interpretation was also based on an decreasing trend in xerophytic taxa during the late Aptian, expressed by a progressive replacement of the xerophytic flora (*Classopollis* and *Equisetosporites*) by humidity loving highland gymnosperm pollen grains (*Araucariacites*) and lowland pteridophyte spores (e.g., *Cicatricosisporites* and *Cyathidites*). Likewise, palynofloristic data from the upper Aptian of central Columbia (Mejia-Velasquez et al., 2012) shows high dominance of the fern spores over the dry indicators gymnosperm pollen grains. The link between the relative sea level rise and the development of more humid conditions is further supported in the upper Aptian palynofloras of the Abu Tunis 1X well by the upward increase in the frequency of *Afropollis* pollen grains (14–2,584, avg. 335 grains/g; 0.4–14%, avg. 4%; Fig. 17, online Supplementary Appendix 4).

Dino et al. (1999) and Schrank (2001) suggested that the parent plant of *Afropollis* thrived in humid coastal plains, and high abundances of the pollen taxon were therefore suggested by Deaf et al. (2016) as a proxy indicator for warm, humid coastal conditions. Based on the current data, the highest abundance of *Afropollis* corresponds to the tectonically induced upper Aptian regressive sequence and the ocean-driven regional late Aptian humid climate (Fig. 17). In the upper Albian–lower Cenomanian succession of Abu Tunis 1X, the highest relative and absolute abundances of the *Afropollis* pollen grains corroborate a more humid Albian–early Cenomanian climate, and are mainly confined to the late transgressive middle Albian, regressive upper Albian, and the lower Cenomanian initial transgressive sequences (Fig. 17). Thus, the high relative and absolute abundances of *Afropollis* pollen grains can be used to mark the Cretaceous relative sea level falls and the initial relative sea level rises. The stratigraphic distribution of the *Afropollis* pollen grains may therefore have a potential to identify depositional sequences (i.e., highstand systems tracts HST, lowstand systems LST, and early transgressive systems tracts eTST) in humid tropical areas. However, further investigation of its application in sequence stratigraphic analysis is necessary.

Figure 17 about here

The Albian–Cenomanian palynofloras of the Abu Tunis 1X well display characteristics similar to that of the Albian–Cenomanian Elaterates Phytogeographic Province. However, there are differences, for example, there are lower frequencies of xerophtyic pollen grains *Ephedripites* and *Classopollis* (Deaf et al., 2014) by comparison to the common/very common frequencies of these taxa described for the Elaterates Province (Herngreen et al., 1996). This province is characterised by several important miospores, with *Afropollis jardinus*, *Crybelosporites*, *Elaterosporites*, and *Cretacaeiporites* all being recorded in the Abu Tunis 1X well (Fig. 15B). During the Albian–Cenomanian, a regionally warm but notably wetter palaeoclimate than that prevailed during the late Barremian–Aptian is thought to have developed in the Abu Tunis area. This contrasts the general warm and dry (arid to semi-arid)

climate suggested by Herngreen et al. (1996) for the Albian–Cenomanian Elaterate Phytogeographic Province/Northern Gondwana Province. Our interpretation is based on the slight upward decrease in abundances of *Ephedripites* (8–470, avg. 172 grains/g; 0.4–5.2%, avg. 2.6%) and *Classopollis* (4–1,394, avg. 261 grains/g; 0.4–5.6%, avg. 2%). Although the frequency of *Classopollis* pollen grains being known to increase in a basinward direction (Tyson, 1995); however, the distribution of this taxon was recently proved by Deaf and Tahoun (2018) to be principally controlled by ecological/climatic factors rather than lithology. Thus, the development of a more humid regional climate together with more humid costal conditions near the site of the Abu Tunis 1X well were unfavourable for the proliferation of the dry indicator *Classopollis*-producing plants. This suggestion is corroborated by the high abundances of *Afropollis jardinus* (4–7,003, avg. 1,385 grains/g; 0.4–53.6%, avg. 15%) in the middle Albian–lower Cenomanian samples from the Abu Tunis 1X well (Fig. 17; online Supplementary Appendix 4). Humid coastal conditions are further supported by the occurrence of *Elaterosporites* pollen grains (25–581, avg. 156 grains/g; 0.4–7.6%, avg. 2.6%) in the middle Albian–lower Cenomanian at Abu Tunis, as elaterate pollen-producing plants are also known to have thrived in humid costal settings (Schrank, 2001). The consistent and relatively higher occurrences of pteridophyte spores in the Albian–Cenomanian (8–49,959, avg. 5,664 grains/g; 0.8–86.8%, avg. 41%) also suggest more humid regional conditions, as again does the coaly material in the upper Albian strata of the Abu Tunis 1X well (Fig. 8). These data again suggest that the Albian ITCZ was located over this region, supported by the examination of climate-indicating sediments/minerals and palynofloras by Chumakov et al. (1995, 2004), which also suggested the development of an equatorial humid belt (i.e. ITCZ) over Northern Gondwana during the Albian and Cenomanian (Fig. 16C; Hay and Floegel, 2012). A more humid Albian–Cenomanian climate for the northeastern Gondwana is also supported by data from central and northern Sudan, where pteridophyte spores outnumber the xerophytic pollen grains (Awad, 1994, Schrank, 1994). Elsewhere in northern Gondwana, there is evidence to indicate humidity in the Albian–Cenomanian climate of Morocco, although this region was also influenced by the Boreal *Cerebropollenites* Province of Herngreen et al. (1996) to the north (Bettar and Méon,

2001, 2006). The western part of Northern Gondwana also seems to have experienced a more humid climate, as evidenced by pteridophyte spores (e.g., *Cyathidites*) overwhelming the xerophytic flora (e.g., *Classopollis* and *Equisetosporites*) in central Columbia (Mejia-Velasquez et al., 2012) and Peru (Mejia-Velasquez et al., 2018).

The Turonian–Coniacian of Abu Tunis is palynologically barren and the early Santonian palynofloras are represented by marine dinocysts only, which hampers interpretation of the palaeoclimatic conditions of this time span.

Nevertheless, the palaeolatitudinal position of Egypt is probably helpful in this regard. Egypt had been located at the palaeotropical zone during the Hauterivian, where northern Egypt was located around 10° N, and the palaeoequator roughly cut through central Egypt (Fig. 16A). As described above, at this time, Egypt experienced warm but wetter conditions than those prevailing in the relatively dry palaeosubtropical regions such as Brazil and Gabon (e.g., Doyle, 1999; Hay and Floegel, 2012). By the Albian-middle Cenomanian, the marine inundation of northern Africa by broad Tethyan epicontinental seas began to influence climatic conditions, such that northern/northeastern and western Africa experienced different climates. This promoted wetter summers in northern Africa in contrast to the West African continental area (including Senegal), which stood high above sea level and received lower rainfalls (Parrish et al., 1982; Fluteau et al., 2007; Föllmi, 2012). This is exemplified by Albian-middle Cenomanian palynofloras from Senegal, which have higher abundances of *Classopollis* (30–80 %) by comparison to those recorded from Egypt, despite being located at the same palaeotropical latitude (Fig. 16C; Jardiné and Magloire, 1965). The African Plate moved northward towards Laurasia (Fig. 16C) and by the end of the Turonian, Egypt was situated more northward (Fig. 16D) in a relatively palaeosubtropical position with the palaeoequator nearly bordering its southern limit (Scotese, 2014). As a result, a continuous warm but less humid (semi-humid) palaeoclimate was probably developed in the Turonian, an interpretation supported by the notable decline in pteridophyte spores and the common occurrences of the *Ephedripites* recorded from elsewhere in the north Western Desert of Egypt (El Beialy et al., 2010; El-Soughier et al., 2014). A non-marine Turonian sequence in north Sudan also indicates a dry

Turonian climate based on the occurrence of the dry indicator proteacean pollen grain (*Triorites africaensis*) and low abundances of pteridophyte spores (Schrank, 1994). However, by contrast, in other north and central basinal areas of the Western Desert, the dominance of the freshwater algae and the common occurrences of the humid indicator spores (e.g., *Ariadnaesporites*) have been used to suggest warm humid Turonian climates (Schrank and Ibrahim, 1995; Ibrahim, 1996; Ibrahim and Abdel-Kireem 1997, Ibrahim et al., 2009). This may suggest that the proximity of marine waters may have produced sufficient moisture for the Egyptian landmass to support pteridophytic vegetation, and again lends support to the idea that the Tethyan Ocean played an important role in the development of the Cretaceous palaeoclimate over the Northern Gondwana Province. Further investigations of more Egyptian Turonian successions are thus necessary to determine the regional Turonian climate over the northeastern Gondwana.

7. Conclusion

Clustered analysis of quantitative palynofacies data integrated with information derived lithological analysis and wireline logs have produced an interpretation of Cretaceous palaeoceanographic conditions in northwestern Egypt, located to the southeast of the Tethyan Ocean. We idenfity four major regressive and transgressisve sequences, where sedimentation was largely affected by Tethyan long-term (2nd order) and short-term (3rd order) sea level changes. However, a regional tectonic imprint is probably superimposed on sedimentaion of the upper Lower Cretcaeous sequence.

In the Matruh Basin, the clastic (shales and sandstones) unit of the lower Alam El Buieb (upper Hauterivian–lowermost upper Barremian) and the major sandstone unit of the Dahab (upper Aptian) and Kharita (Albian) formations represent the regressive sequences. These were deposited in deltafront to delta-top, delta channel, and distal detlaic settings, where the first regressive sequence corresponds to the Tethyan late Hauterivian–late Barremian long-term (2nd order) and short-term (3rd order) sea level falls. The second regressive sequence corresponds to the regional late Aptian–Albian uplift, which masked the Tethyan late Aptian–middle Albian minor long-term (2nd order) sea level rise. Shale and dolostones of the upper

Alam El Bueib (uppermost Barremian) and Alamein (lower–middle Aptian) formations represent the first major tansgressive sequence that was mostly deposited in proximal settings of the inner and middle shelf and correspond to the Tethyan early Aptian high sea level stand. The second transgressive sequence is represented by a fine clastic (sandstones and siltstones with few shale horizons) unit of the lower–middle Bahariya (lower Cenomanian) and a carbonate (limestone and dolostone) unit with some minor shale horizons of the upper Bahariya (lower–?middle Cenomanian) and Abu Roash (middle–upper Cenomanian) formations. This sequence accumulated in proximal inner shelf and middle shelf settings, respectively, and generally corresponds to the Tethyan latest early–late Cenomanian long-term sea level rise.

Palaeogeographically, the northeastern Gondwana Phytogeographic Province represented by the Egyptian landmass was situated during much of the Cretaceous in a palaeolatitudinal position different from that of western Northern Gondwana (e.g., West Africa - Gabon, Congo, Senegal, and northern South America - Brazil), and as such experienced different regional palaeoclimatic conditions. The succession in the Abu Tunis 1X well records a shift from a less warm and more humid climate during the Hauterivian–early Barremian to a warm and relatively drier climate during the late Barremian–middle Aptian, but never becoming as dry as the conditions experienced in western Northern Gondwana at that time. A warm but relatively more humid climate developed during the late Aptian and more accentuated during the Albian–Cenomanian by contrast to the general warm and arid to semi-arid climate that prevailed in western Northern Gondwana. Conditions in northeastern Gondwana may have become relatively less humid (semi-humid) in the Turonian as a response to the continental breakup of the Western Gondwanan supercontinent and the northeast drift of the African continent. The analyses presented here demonstrate that complex interactions between sea level, the northward migration of the African continent, and the changing position of the Intertropical Convergence Zone (ITCZ) all played a role in climatic fluctuations between periods of warm humid and warm dry conditions experienced in northeastern Gondwana during the early-mid Cretaceous.

Disclosure of interest

To the best of our knowledge, no financial conflict of interest, or other, exists.

Acknowledgements

The authors wish to thank the Egyptian General Petroleum Corporation for providing well logs and samples from the Abu Tunis 1X well. Thanks are also due to the Editor-in-Chief Dr. Eduardo Koutsoukos, Associate Editor Dr. Elena Yazykova, and the two anonymous reviewers for their critical review and constructive comments, which improved the quality of the manuscript.

Supplementary data

Supplementary data to this article can be found at: http://

ORCID

Amr Deaf, http://orcid.org/0000-0002-5073-7911

Ian C. Harding, http://orcid.org/0000-0003-4281-0581

John Marshall http://orcid.org/0000-0002-9242-3646

References

Abbink, O.A., Van Konijnenburg-van Cittert, J.H.A., Visscher, H., 2004. A sporomorph ecogroup model for the Northwest European Jurassic–Cretaceous: concepts and framework. Netherlands Journal of Geosciences – Geologie En Mijnbouw 83, 17–38.

Abd-Elshafy, E., Abd El-Azeam, S., 2010. Paleogeographic relation of the Egyptian Northern Galala with the Tethys during the Cretaceous Period. Cretaceous Research 31, 291–303.

Abrams, M.A., Greb, M.D., Collister, J.W., Thompson, M., 2016. Egypt far Western Desert basins petroleum charge system as defined by oil chemistry and unmixing analysis. Marine and Petroleum Geology 77, 54–74.

Abubakar, M.B., Obaje, N.G., Luterbacher, H.P., Dike, E.F.C., Ashraf, A.R., 2006. A report on the occurrence of Albian–Cenomanian elater-bearing pollen in Nasara-1 well, Upper Benue

Trough, Nigeria: Biostratigraphic and palaeoclimatological implications. Journal of African Earth Sciences 45, 347–354.

Abdel-Kireem, M.R., Samir, A.M., Ibrahim, M.I.A., Schrank, E., 1993. Cretaceous palaeoecology, palaeoclimatology and palaeogeography of the northern Western Desert of Egypt. In: Thorweihe, U., Schandelmeier, H. (Eds.), Geoscientific Research in Northeast Africa. Balkema, Rotterdam, Brookfield, 375–380.

Abdel-Kireem, M.R., Schrank, E., Samir, A.M., Ibrahim, M.I.A., 1996. Cretaceous palaeoecology, palaeogeography and palaeoclimatology of the northern Western Desert, Egypt. Journal of African Earth Sciences 22, 93–112.

Abou Khadrah, A.M., SANA, A., Khaled, K.A., 1978. Origin and diagenesis of the Aptian Alamein Dolomite in Razzak oil field, northern Western Desert, Egypt. Chemie der Erde 37, 154–164.

Aboul Ela, N.M., Tahoun, S.S., 2010. Dinoflagellate cyst stratigraphy of the subsurface middle–upper Jurassic/lower Cretaceous sequence in north Sinai, Egypt. Fifth International Conference on the Geology of the Tethys Realm, South Valley University, January 2010, 85–115.

Andrieu, S., Brigaud, B., Rabourg, T., Noret, A., 2015. The Mid-Cenomanian Event in shallow marine environments: Influence on carbonate producers and depositional sequences (northern Aquitaine Basin, France). Cretaceous Research 56, 587–607.

Arai, M., Botelho Neto, J., Lana, C.C., Pedrão, E., 2000. Cretaceous dinoflagellate provincialism in Brazilian marginal basins. Cretaceous Research 21, 351–366.

Atta-Peters, D., Salami, M.B., 2006. Aptian–Maastrichtian palynomorphs from the offshore Tano Basin, western Ghana. Journal of African Earth Sciences 46, 379–394.

Awad, M.Z., 1994. Stratigraphic, palynological and palaeoecological studies in the east–central Sudan (Khartoum and Kosti Basins), late Jurassic to mid–Tertiary. Berliner Geowissenschaftliche Abhandlungen, Reihe A, 161, 1–163.

Bachmann, M., Kuss, J., 1998. The Middle Cretaceous carbonate ramp of the northern Sinai: sequence stratigraphy and facies distribution. In: Wright, V.P., Burchette, T.P. (Eds), Carbonate Ramps. Geological Society, London, Special Publications 149, 253–280.

Bachmann, M., Kuss, J., Lehmann, J., 2010. Controls and evolution of facies patterns in the Upper Barremian–Albian Levant Platform in North Sinai and North Israel. In: Homberg, C., Bachmann, M. (Eds), Evolution of the Levant Margin and Western Arabia Platform since the Mesozoic. Geological Society, London, Special Publications 341, 99–131.

Baird, J.G., 1992. Palynofacies of the eastern margin of Gippsland Basin. Energy, Economics, and Enviroment (EEE), the Gippsland Basin Symposium, Melbourne. Australian Institute of Mining and Metallurgy, 25–42.

Balch, W.M., Reid, P.C., Surrey-Gent, S.C., 1983. Spatial and temporal variability of dinoflagellate cyst abundance in a tidal estuary. Canadian Journal of Fisheries and Aquatic Sciences, Supplement 40, 244–261.

Balme, B.E., 1995. Fossils in situ spores and pollen grains: an annotated catalogues. Review of Palaeobotany and Palynology 87, 81–323.

Batten, D.J., 1973. Use of palynological assemblage-types in Wealden correlation. Palaeontology 16, 1–40.

Batten, D.J., 1982. Palynofacies, palaeoenvironments, and petroleum. Journal of Micropalaeontology 1, 107–114.

Batten, D.J., 1983. Identification of amorphous sedimentary organic matter by transmitted light. In: Brooks, J. (Ed.), Petroleum Geochemistry and Exploration of Europe. Geological Society of London Special Publication, 275–287.

Batten, D.J., 1999. Palynofacies analysis. In: Jones, N.P., Rowe, N.P. (Eds.), Fossil Plants and Spores: Modern Techniques. Geological Society of London, 194–198.

Bennington, J.B., Bambach, R.K., 1996. Statistical testing for paleocommunity recurrence: Are similar fossil assemblages ever the same? Palaeogeography Palaeoclimatology Palaeoecology 127, 107–133.

Benyoucef, M., Mebarki, K., Ferré, B., Adaci, M., Bulot, L.G., Desmares, D., Villier, L., Bensalah, M., Frau, C., Ifrim, C., Malti, F.-Z., 2017. Litho- and biostratigraphy, facies patterns and

depositional sequences of the Cenomanian-Turonian deposits in the Ksour Mountains (Saharan Atlas, Algeria). Cretaceous Research 78, 34–55.

Bernaus, J.M., Arnaud-Vanneau, A., Caus, E., 2003. Carbonate platform sequence stratigraphy in a rapidly subsiding area: the Late Barremian–Early Aptian of the Organyá basin, Spanish Pyrenees. Sedimentary Geology 159, 177–201.

Bettar, I., Courtinat, B., 1987. Palynologie de la série grésocarbonatée d`Imi n`Tanout (Cretacé inférieur, zone synclinale d`Essaouira, Maroc). Bulletin de l' Institut scientifique – Rabat 11, 103–108.

Bettar, I., Méon, H., 2001. Palynological study of the middle/upper Albian transition in the Tarfaya Basin (southwest of Morocco) and some new data about the African–South American Province. Revue de Micropaléontologie 44, 107–123.

Bettar, I., Méon, H., 2006. La palynoflore continentale de l'Albien du Bassin d'Agadir–Essaouira (Maroc). Revue de Paléobiologie 25, 593–631.

Boggs, S., 2006. Principles of Sedimentology and Stratigraphy. Pearson Prentice Hall, New Jersey.

Bornemann, A., Pross, J., Reichelt, K., JO., H., Hemleben, C., Mutterlose, J., 2005. Reconstruction of short-term palaeoceanographic changes during the formation of the Late Albian "Niveau Breistroffer" black shale (Oceanic Anoxic Event 1d, SE France). Journal of Geological Society 162, 623–639.

Bray, J.R., Curtis, J.T., 1957. An ordination of the upland forest communities of Southern Wisconsin. Ecological Monographs 27, 325–349.

Brenner, G.J., 1968. Middle Cretaceous spores and from north–eastern Peru. Pollen et Spores 10, 341–382.

Brenner, G.J., 1976. Middle Cretaceous floral provinces and early migrations of angiosperms. In: Beck, C.B. (Ed.), Origin and Early Evolution of Angiosperms. Colombia University Press, New York, 23–47.

Brenner, G.J., 1996. Evidence for the earliest stage of angiosperm pollen evolution: a paleoequarorial section from Israel. In: Taylor, D.W., Hickey, L.J. (Eds.), Flowering Plant Origin, Evolution and Phylogeny. Chapman and Hall, New York, 91–115.

Brinkhuis, H., 1994. Late Eocene to Early Oligocene dinoflagellate cysts from the Priabonian type-area (Northeast Italy): biostratigraphy and paleoenvironmental interpretation. Palaeogeography, Palaeoclimatology, Palaeoecology 107, 121–163.

Brinkhuis, H., Zachariasse, W.J., 1988. Dinoflagellate cysts, sea level changes and planktonic foraminifera across the Cretaceous–Tertiary boundary at El Haria, northwest Tunisia. Marine Micropaleontology 192, 153–191.

Bumby, A.J., Guiraud, R., 2005. The geodynamic setting of the Phanerozoic basins of Africa. Journal of African Earth Sciences 43, 1–12.

Carvalho, M.A., Bengtson, P., Lana, C. C., 2016. Late Aptian (Cretaceous) paleoceanography of the South Atlantic Ocean inferred from dinocyst communities of the Sergipe Basin, Brazil. Paleoceanography 31, 2–26.

Carvalho, M.A., Lana, C.C., Bengtson, P., Sá, N.P., 2017. Late Aptian (Cretaceous) climate changes in northeastern Brazil: A reconstruction based on indicator species analysis (IndVal). Palaeogeography, Palaeoclimatology, Palaeoecology 485, 543–560.

Carvalho, M.A., Bengtson, P. Lana, C.C., Sá, N.P, Santiago, G., Giannerini, M.C.S., 2019. Late Aptian (Early Cretaceous) dryewet cycles and their effects on vegetation in the South Atlantic: Palynological evidence. Cretaceous Research 100, 172–183.

Catuneanu, O., Khalifa, M.A., Wanas, H.A., 2006. Sequence stratigraphy of the Lower Cenomanian Bahariya Formation, Bahariya Oasis, Western Desert, Egypt. Sedimentary Geology 190, 121‑137.

Chaboureau, A.C., Donnadieu, Y., Sepulchre, P., Robin, C., Guillocheau, F., Rohais, S., 2012. In: The Aptian evaporites of the South Atlantic: a climatic paradox? Climate of the Past 8, 1047–1058.

Chumakov, N.M., 2004. Climatic zones and climate of the Cretaceous period. In: Semikhatov, M.A., Chumakov, N.M. (Eds.), Climate in the epochs of major biospheric transformations. Transactions of the Geological Institute of the Russian Academy of Sciences (550), 105‑123 (Moscow, Nauka [in Russian]).

Chumakov, N.M., Zharkov, M.A., Herman, A.B., Doludenko, M.P., Kalandadze, N.N., Lebedev, E.A., Ponomarenko, A.G., Rautian, A.S., 1995. Climate belts of the mid-Cretaceous time. Stratigraphy and Geological Correlation 3, 241–260.

Chang, Y.M., 1967. Accuracy of fossil percentage estimation. Journal of Paleontology 4, 500–502.

Clarke, K.R., Gorley, M.A., 2006. PRIMER, 6. PRIMER–E Limited, Plymouth.

Clarke, K.R., Warwick, R.M., 2001. Changes in Marine Communities: An Approach to Statistical Anallysis and Interpretation, 2nd ed. Primer–E Ltd, Plymouth.

Combaz, A., 1964. Les palynofaciès. Revue de Micropaléontologie 7, 205–218.

Crane, P.R., 1988. Major clades and relationships in the "higher" gymnosperms. In: Beck, C.B. (Ed.), Origin and Evolution of Gymnosperms. Columbia University, New York, 218–272.

Dale, B., 1983. Dinoflagellate resting cysts: “benthic plankton”. In: Fryxell, G.A. (Ed.), Survival Strategies of the Algae. Cambridge University Press, Cambridge, 69–136.

Da Rosa, A.A.S., Garcia, A.J.V., 2000. Palaeobiogeographic aspects of northeast Brazilian basins during the Berriasian before the break up of Gondwana. Cretaceous Research 21, 221–239.

Darwish, M., 1994. Cenomanian–Turonian sequence stratigraphy, basin evolution and hydrocarbon potentialities of northern Egypt. Second International Conference on the Geology of Arab World, Cairo University, 261–303.

Davey, R.J., 1970. Non-calcareous miroplankton from the Cenomnain of England, northern France, and North America, Part II. Bulletins of the British Museum (Natural History), Geology 18, 333–397.

Davey, R.J., Verdier, J.P., 1974. Dinoflagellate cysts from the Aptian type sections at Gargas and la Bédoule, France. Palaeontology 17, 623–653.

De Vernal, A., Giroux, L., 1991. Distribution of organic-walled microfossils in Recent sedimentsfrom the Estuary anf Gulf of St. Lawrence: some aspects of the organic matter fluxes. Canadian Journal of Fisheries and Aquatic Sciences, Special Publication 113, 189–199.

Deaf, A.S., 2009. Palynology, palynofacies and hydrocarbon potential ofthe Cretaceous rocks of northern Egypt (Published PhD thesis). University of Southampton, 348 pp. Available online at: https://www.eprints.soton.ac.uk/168943/).

Deaf, A.S., Harding, I.C., Marshall, J.E.A., 2014. Cretaceous (Albian–? early Santonian) palynology and stratigraphy of the Abu Tunis 1X borehole, northern western Desert, Egypt. Palynology 38, 51–77.

Deaf, A.S., Harding, I.C., Marshall, J.E.A., 2016. Early Cretaceous palynostratigraphy of the Abu Tunis 1X borehole, northern Western Desert, Egypt, with emphasis on the possible palaeoclimatic effect upon the range of *Dicheiropollis etruscus* in North Africa. Palynology 40, 25–53.

Deaf, A.S., Tahoun, S.S., 2018. Integrated palynological, organic geochemical, and sequence stratigraphic analyses of the middle to upper Cenomanian hydrocarbon reservoir/source Abu Roash “G” Member: a depositional model in northwestern Egypt. Marine and Petroleum Geology 92, 372–402.

Degens, E.T., Mopper, K., 1976. Factors controlling the distribution and early diagenesis of organiv material in marine sediments. In: Riley, J.P., Chester, R. (Eds.), Chemical Oceanography. Academic Press, London, 59–113.

Dooley, J.H., 2006. Glauconite. In: Kogel, J.E., Trivedi, N.C., Barker, J.M.,Krukowski, S.T. (Eds.), Industrial Minerals and Rocks, 7th ed. Society of Mining and Metal Exploration, Littleton, 495–506.

Doyle, J.A., 1999. The rise of angiosperms as seen in the African Cretaceous pollen record. Third Conference on African Palynology, Johannesburg 14–19 September, 1997. Balkema, Rotterdam, 3–29.

Doyle, J.A., Biens, P., Doerenkamp, A., Jardiné, S., 1977. Angiosperm pollen from the pre-Albian lower Cretaceous of equatorial Africa. Bulletin des Centres de Recherches Exploration–Production Elf-Aquitaine 1, 451–473.

Doyle, J.A., Jardiné, S., Doerenkamp, A., 1982. *Afropollis*, a new genus of early angiosperm pollen, with notes on the Cretaceous palynostratigraphy and paleoenvironments of northern Gondwana. Bulletin des Centres de Recherches Exploration–Production Elf Aquitaine 6, 39–117.

Duringer, P., Doubinger, J., 1985. La palynologie: un outil de characterisation des facies marines et continentaux a la limite Muschelkalk Supérieur– Lettenkohle. Science Géologie Bulletin, Strasbourg 38, 19–34.

Einsele, G., 1992. Sedimentary Basins: Evolution, Facies, and Sediment Budget. Springer–Verlag, Berlin.

El Ashwah, A., El Deeb, W., 2000. Late Cretaceous foraminiferal paleobathymetric study of Wadi El Natrun Well no. 1 succession, northeastern part of the Western Desert, Egypt. Egyptian Journal of Geology 44, 1–12.

El Beialy, S.Y., El Atfy, H.S., Zavada, M.S., El Khoriby, E.M., Abu-Zied, R.H., 2010. Palynological, palynofacies, paleoenvironmental and organic geochemical studies on the Upper Cretaceous succession of the GPTSW-7 well, North Western Desert. Egypt. Marine and Petroleum Geology 27, 370–385.

El-Soughier, M.I., Deaf, A.S., Mahmoud, M.S., 2014. Palynostratigraphy and palaeoenvironmental significance of the Cretaceous palynomorphs in the Qattara Rim-1X well, north Western Desert. Egypt. Arabian Journal of Geosciences 7, 3051–3068.

Erba, E., Channell, J.E.T, Claps, M., Jones, C., Larson, R., Opdyke, B., Premoli Silva, I., Riva, A., Salvini, G., Torricelli, S. 1999. Integrated stratigraphy of the Cismon Apticore (Southern Alps, Italy): a “reference” section for the Barremian–Aptian interval at low latitudes. Journal of Foraminiferal Research 29, 371–391.

Etter, W., 1999. Community analysis. In: Harper, D.A.T. (Ed.), Numerical Palaeobiology: Computer-based Modelling and Analysis of Fossils and their Distributions. John Wiley and Sons Ltd, Chichester, 285–360.

Federova, V.A., 1977. The significance of the combined use of microphytoplankton, spores, and pollen for differentiation of multi-facies sediments. In: Samoilovich, S.R., Timoshina, N.A. (Eds.), Questions of Phytostratigraphy. Leningrad, Trudy Neftyanoi nauchno-issledovatelskii geologorazvedochnyi Institute (VNIGRI), 70–88.

Fensome, R.A., Gocht, H., Williams, G.L., 1995. The Eisenack Catalog of Fossil Dinoflagellates. E. Schweizerbart'sche Verlagsbuchhandlung, Stuttgart, Germany.

Fensome, R.A., Gocht, H., Williams, G.L., 1996. The Eisenack Catalog of Fossil Dinoflagellates. E. Schweizerbart'sche Verlagsbuchhandlung, Stuttgart, Germany.

Firth, J.V., 1993. Palynofacies and thermal maturation analysis of sediments from the Nankai Trough. Proceedings of the Ocean Drilling Project, Scientific Results 131, 57–69.

Fluteau, F., Ramstein, G., Besse, J., Guiraud, R., Masse, J.P., 2007. Impacts of palaeogeography and sea level changes on Mid–Cretaceous climate. Palaeogeography, Palaeoclimatology, Palaeoecology 247, 357–381.

Föllmi, K.B., 2012. Early Cretaceous life, climate and anoxia. Cretaceous Research 35, 230–257.

Foucher, J.-C., Pons, D., Mami, L., Bellier, J.-P., 1994. Premier inventaire de la microflore crétacée (dinokystes, spores et pollen) du Sud–Est constantinois (Algérie): conséquences biostratigraphiques. Compte rendu hebdomadaire des seances de l'Academie des Sciences Paris 318, 1563–1570.

Ghanem, H., Kuss, J., 2013. Stratigraphic control of the Aptian–Early Turonian sequences of the Levant Platform, Coastal Range, northwest Syria. GeoArabia 18, 85–132.

Garcia, G.G., Garcia, A.J.V., Henriques, M.H.P., 2018. Palynology of the Morro do Chaves Formation (Lower Cretaceous), Sergipe Alagoas Basin, NE Brazil: Paleoenvironmental implications for the early history of the South Atlantic. Cretaceous Research 90, 7–20.

Gentzis, T., Carvajal, H., Tahoun, S.S, Deaf, A.S., Ocubalidet, S., 2019. Organic facies and hydrocarbon potential of the early–middle Albian Kharita Formation in the Abu Gharadig Basin,

Egypt as demonstrated by palynology, organic petrology, and geochemistry. International Journal of Coal Geology 209, 27–39.

Godet, A., Hfaiedh, R., Arnaud-Vanneau, A., Zghal, I., Arnaud, H., Ouali, J., 2014. Aptian palaeoclimates and identification of an OAE1a equivalent in shallow marine environments of the southern Tethyan margin: Evidence from Southern Tunisia (Bir Oum Ali section, Northern Chott Chain). Cretaceous Research 48, 110–129.

Gotelli, N.J., Colwell, R.K., 2011. Estimating species richness. In: Magurran, A.E., McGill, B.J. (Eds.), Frontiers in Measuring Biodiversity. Oxford University Press, New York, 39–54.

Gradstein, F.M., Ogg, J.G., 2012. In: Schmitz, M.D., Ogg, G.M. (Eds.), The Geological Time Scale 2012. Elsevier, Amsterdam, p. 1176.

Gräfe, K.U., 2005. Late Cretaceous benthic foraminifers from the Basque–Cantabrian Basin, Northern Spain. Journal of Iberian Geology 31, 277–298.

Green, O.R., 2001. A Manual of Practical Laboratory and Field Techniques in Palaeobiology. Kluwer Academic Publishers, Dordrecht.

Gübeli, A.A., Hochuli, P.A., Wildi, W., 1984. Lower Cretaceous turbiditic sediments from the Rif Chain (northern Morocco): palynology, stratigraphy and paleogeographic settings. Geologische Rundschau 73, 1018–1114.

Guiraud, R., Bosworth, W., 1997. Senonian basin inversion and rejuvenation of rifting in Africa and Arabia: synthesis and implications to plate–scale tectonics. Tectonophysics 282, 39–82.

Guiraud, R., Bosworth, W., 1999. Phanerozoic geodynamic evolution of north–eastern Africa and the north–western Arabian platform. Tectonophysics 315, 73–108.

Guiraud, R., Bosworth, W., Thierry, J., Delplanque, A., 2005. Phanerozoic geological evolution of Northern and Central Africa: an overview. Journal of African Earth Sciences 43, 83–143.

Guiraud, R., Issawi, B., Bosworth, W., 2001. Phanerozoic history of Egypt and surrounding areas. In: Ziegler, P.A., Cavazza, W., Robertson, A.H.F., Crasquin-Soleau, S. (Eds.), Peri-

Tethys Memoir 6: Peri-Tethyan Rift/Wrench Basins and Passive Margins. Mémoires du Muséum National d'Histoire Naturelle, Paris, 469–509.

Habib, D., 1979. Sedimentology of palynomorphs and palynodebris in Cretaceous carbonaceous facies south of Vigo Seamount. Initial Reports of the Deep Sea Drilling Project 47, 451–467.

Habib, D., 1982. Sedimentary supply origin of Cretaceous black shales. In: Schlanger, S.O., Cita, M.B. (Eds.), Nature and Origin of Cretaceous Carbon-Rich Facies. Academic Press, London, 113–127.

Habib, D., 1983. Sedimentation-Rate-Dependent Distribution of Organic-Matter in the North–Atlantic Jurassic–Cretaceous. Initial Reports of the Deep Sea Drilling Project 76, 781–794.

Habib, D., Drugg, W.S., 1987. Palynology of Site-603 and Site-605, Leg-93, Deep Sea Drilling Project. Initial Reports of the Deep Sea Drilling Project 93, 751–775.

Habib, D., Moshkovitz, S., Kramer, C., 1992. Dinoflagellate and calcareous nannofossils response to sea level change in Cretaecous–Tertiary boundary section. Geology 20, 165–168.

Hantar, G., 1990. North Western Desert. In: Said, R. (Ed.), The Geology of Egypt. Balkema, Rotterdam, 293–319.

Haq, B.U., 2014. Cretaceous eustasy revisited. Global and Planetary Change 113, 44–58.

Haq, B.U., Hardenbol, J., Vail, P.R., 1988. Mesozoic and Cenozoic chronostratigraphy and cycles of sea-level change. Society of Economic Paleontologists and Mineralogists 42, 71–108.

Hardenbol, J., Thierry, J., Farley, M.B., et al., 1998. Mesozoic and Cenozoic sequence chronostratigraphic framework of European Basins. In: de Graciansky, P.-C., et al. (Eds.), Mesozoic and Cenozoic Sequence Stratigraphy of European Basins. SEPM Special Publication, 60, 3–13 (Chart 5, "Cretaceous Chronostratigraphy").

Harding, I.C., 1986. An Early Cretaceous dinocyst assemblage from the Wealden of southern England. Palaeontology Special Paper 35, 95–109.

Hasegawa, H., Tada, R., Jiang, X., Suganuma, Y., Imsamut, S., Charusiri, P., Ichinnorov, N., Khand, Y., 2012. Drastic shrinking of the Hadley circulation during the mid-Cretaceous Supergreenhouse. Climate of the Past 8, 1323–1337.

Hay, W.W., Deconto, R., Wold, C.N., Wilson, K.M., Voigt, S., Schulz, M., Wold-Rossby, A., Dullo, W.-C., Ronov, A.B., Balukhovsky, A.N., Soeding, E., 1999. Alternative global Cretaceous paleogeography. In: Barrera, E., Johnson, C. (Eds.), The Evolution of Cretaceous Ocean/Climate Systems. Geological Society of America Special Paper, 1–47.

Hay, W.W., Floegel, S., 2012. New thoughts about the Cretaceous climate and oceans. Earth-Science Reviews 115, 262–272.

Herngreen, G.F.W., 1974. Middle Cretaceous palynomorphs from north–eastern Brazil. Sciences Géologiques Bulletin 27, 101–116.

Herngreen, G.F.W., Chlonova, A.F., 1981. Cretaceous microfloral provinces. Pollen et Spores 23, 441–555.

Herngreen, G.F.W., Jimenez, H.D., 1990. Dating of the Cretaceous Une Formation, Colombia and the relationship with the Albian–Cenomanian African–South American microfloral province. Review of Palaeobotany and Palynology 66, 345–359.

Herngreen, G.F.W., Kedves, M., Rovnina, L.V., Smirnova, S.B., 1996. Cretaceous palynofloral provinces: a review. In: Jansonius, J., McGregor, D.C. (Eds.), Palynology: Principles and Applications., American Association of Stratigraphic Palynologists Foundation 3, Texas, 1157–1188.

Hermann, E., Hochuli, P. A., Méhay, S., Bucher. H., Brühwiler, T., Ware, D., Hautmann, M., Roohi, G., ur-Rehman, K., Yaseen, A., 2011. Organic matter and palaeoenvironmental signals during the Early Triassic biotic recovery*:* The Salt Range and Surghar Range records. Sedimentary Geology 234, 19–41.

Hfaiedh, R., Vanneau, A.A., Godet, A., Arnaud, H., Zghal, I., Ouali, J., Latil, J.-L., Jallali, H., 2013. Biostratigraphy, palaeoenvironments and sequence stratigraphy of the Aptian sedimentary succession at Jebel Bir Oum Ali (Northern Chain of Chotts, South Tunisia): Comparison with contemporaneous Tethyan Series. Cretaceous Research 46, 177–207.

Hillgärtner, Heiko, Buchem, F.V., Gaumet, F., Razin, P., Pittet, B., Grötsch, J., Droste, H., 2003. The Barremian–Aptian evolution of the eastern Arabian carbonate platform margin (northern Oman). Journal of Sedimentary Research 73, 756–773.

Hochuli, P. A., 1981. North Gondwanan floral elements in lower to middle Cretaceous sediments of the southern Alps (southern Switzerland, northern Italy). Review of Palaeobotany and Palynology 35, 337–358.

Hoedemaeker, P.J., Leereveld, H., 1995. Biostratigraphy and sequence stratigraphy of the Berriasian–lowest Aptian (Lower Cretaceous) of the Rio Argos succession, Caravaca, SE Spain. Cretaceous Research 16, 195–230.

Ibrahim, M.I.A., 1996. Aptian–Turonian palynology of the Ghazalat-1 well (GTX-1), Qattara Depression, Egypt. Review of Palaeobotany and Palynology 94, 137–168.

Ibrahim, M.I.A., 2002. New angiosperm pollen from the upper Barremian–Aptian of the Western Desert, Egypt. Palynology 26, 107–133.

Ibrahim, M.I. A., Abdel-Kireem, M.R., 1997. Late Cretaceous palynofloras and foraminifera from Ain El-Wadi area, Farafra Oasis, Egypt. Cretaceous Research 18, 633–660.

Ibrahim, M.I.A., Al-Hitmi, H.H., Kholeif, S.E., 2000. Albian–Cenomanian palynology, paleoecology and organic thermal maturity of well DK-B in the Dukhan oil field of western Qatar. GeoArabia 5, 483–508.

Ibrahim, M.I.A., Dilcher, D., Kholeif, S.E., 2009. Palynomorph succession and paleoenvironment in the upper Cretaceous Abu Gahardig Oil Field, Northwestern Desert, Egypt. Micropaleontology 55, 225–558.

Jansonius, J., Hills, L.V., 1976. Genera File of Fossil Spores, Special Publication ed. Geology Department, University of Calgary, Canada, Calgary.

Jardiné, S., Biens, P., Doerenkamp, A., 1974. *Dicheiropollis etruscus*, un pollen caractéristique du Crétacé inférieur Afro-Sudamericain. Conséquences pour l`évaluation des unités climatiques et implication dans la dérive des continents. Sciences Géologiques Bulletin 27, 87–100.

Jardiné, S., Magloire, L., 1965. Palynologie et stratigraphie du Crétacé, des bassins de Sénégal et d` Côte De`Ivoire. Mémoire Bureau Recherche Géologie et Minéralogie 32, 187–245.

Kerdany, M.T., Cherif, O.H., 1990. Mesozoic. In: Said, R. (Ed.), The Geology of Egypt. Balkema, Rotterdam, 407–437.

Khalifa, M.A., Catuneanu, O., 2008. Sedimentology of the fluvial and fluvio-marine facies of the Bahariya Formation (Early Cenomanian), Bahariya Oasis, Western Desert, Egypt. Journal of African Earth Sciences 51, 89‑103.

Kidwell, S.M., Bosence, D.W.J., 1991. Taphonomy and time-averaging of marine shelly faunas. In: Allison, P.A., Briggs, D.E.G. (Eds.), Taphonomy: Releasing the Data Locked in the Fossil Record. Plenum Press, New York, 115–209.

Koutsoukos, E.A.M., 2005. Stratigraphy: Evolution of a Concept. In: Koutsoukos, E.A.M. (Ed.), Applied Stratigraphy. Springer, Dordrecht, 3‑19.

Koutsoukos, E.A.M., Bengtson, P., 2007. Evaluating the evidence on the opening of the Equatorial Atlantic Gateway and its global impact. Geological Society of America Annual Meeting, Abstract Program, 39, 445.

Lawal, O., Moullade, M., 1986. Palynological biostratigraphy of Cretaceous sediments in the Upper Benue Basin, NE Nigeria. Revue de Micropaléontologie 29, 61–83.

Leckie, D.A., Singh, C., 1991. Estuarine deposits of the Albian Paddy Member (Peace River Formation) and lowermost Shaftesbury Formation, Alberta, Canada. Journal of Sedimentary Petrology 61, 825–849.

Leereveld, H. 1997. Hauterivian–Barremian (lower Cretaceous) dinoflagellate cyst stratigraphy of the western Mediterranean. Cretaceous Research 18, 421–456.

Lister, J.K., Batten, D.J., 1988. Stratigraphic and paleoenvironmental distribution of early Cretaceous dinoflagellate cysts in the Hurlands Farm Borehole, West Sussex, England. Palaeontographica Abteilung B 210, 8–89.

Mahmoud, M.S., Deaf, A.S., 2007. Cretaceous palynology (spores, pollen and dinoflagellate cysts) of the Siqeifa 1-X borehole, northern Egypt. Rivista Italiana di Paleontologia e Stratigrafia 113, 203–221.

Mahmoud, M.S., Moawad, A.M.M., 2002. Cretaceous palynology of the Sanhur-1X borehole, northern western Egypt. Revista Española de Micropaleontologia 34, 129–143.

Mahmoud, M.S., Deaf, A.S., Tamam, M.A., Khalaf, M.M., 2017. Palynofacies analysis and palaeoenvironmental reconstruction of the Upper Cretaceous sequence drilled by the Salam-60 well, Shushan Basin: Implications on the regional depositional environments and hydrocarbon exploration potential of north–western Egypt. Revue de Micropaléontologie, 60, 449–467.

Mahmoud, M.S., Deaf, A.S., Tamam, M.A., Khalaf, M.M., 2019. Revised (miospores-based) stratigraphy of the Lower Cretaceous succession of the Minqar-IX well, Shushan Basin, north Western Desert, Egypt: Biozonation and correlation approach. Journal of African Earth Sciences 151, 18–35.

Marshall, K.L., Batten, D.J., 1988. Dinoflagellate cyst association in Cenomanian–Turonian "Black Shale" sequence of northern Europe. Review of Palaeobotany and Palynology 54, 85–103.

Mejia-Velasquez, P.J., Dilcher, D.L., Jaramillo, C.A., Fortini, L.B., Manchester, S.R., 2012. Palynological composition of a Lower Cretaceous South American tropical sequence: climatic implications and diversity comparisons with other latitudes. American Journal of Botany 99, 1819–1827.

Mejia-Velasquez, P.J., Manchester, S.R., Jaramillo, C.A., Quiroz, L., Fortini, L., 2018. Floristic and climatic reconstructions of two Lower Cretaceous successions from Peru. Palynology 42, 420–433.

Meshref, W.M., 1990. Tectonic Framework. In: Said, R. (Ed.), The Geology of Egypt. Balkema, Rotterdam, 113–156.

Meshref, W.M., 1996. Createcous tectonics and its impact on oil exploration in northern Egypt. Geological Society of Egypt, Special Publication No. 2, 199–214.

Mutterlose, J., Harding, I., 1987. Phytoplankton from the anoxic sediments of the Barremian (lower Cretaceous) of north–west Germany. Abhandlungen der Geologischen Bundesanstalt (Vienna) 39, 177–215.

Nagm, E., Boualem, N., 2019. First documentation of the late Albian transgression in northwest Algeria: Bivalve stratigraphy and Palaeobiogeography. Cretaceous Research 93, 197–210.

Nagy, J., Dypvik, H., Bjaerke, T., 1984. Sedimentological and paleontological analyses of Jurassic North Sea deposits from deltaic environments. Journal of Petroleum Geology 7, 169–188.

Ogg, J.G., Hinnov, L.A., 2012. Cretaceous. In: Gradstein, F.M., Ogg, J.G., Schmitz, M.D., Ogg, G.M. (Eds.), The Geological Time Scale. Elsevier, Amsterdam, 793–853.

Parrish, J.T., Ziegler, A.M., Scotese, C.R., 1982. Rainfall patterns and the distribution of coals and evaporites in the Mesozoic and Cenozoic. Palaeogeography, Palaeoclimatology, Palaeoecology 40, 67–101.

Parry, C.C., Whitley, P.K.J., Simpson, R.D.H., 1981. Integration of palynological and sedimentological methods in facies analysis of the Brent Formation. In: Illing, L.V., Hobson, G.D. (Eds.), Petroleum Geology of the Continental Shef of North West Europe. Heyden, London, 205–215.

Pelzer, G., Riegel, W., Wilde, V., 1992. Depositional control on the lower Cretaceous Wealden coals of Northwest Germany. Geological Society of America, Special Paper 267, 227–243.

Penny, J.H.J., 1988a. Early Cretaceous acolumellate semitectate pollen from Egypt. Palaeontology 31, 373–418.

Penny, J.H.J., 1988b. Early Cretaceous striate tricolpate pollen from the Borehole Mersa Matruh 1, North West Desert, Egypt. Journal of Micropalaeontology 7, 201–215.

Penny, J.H.J., 1991. Early Cretaceous angiosperm pollen from the borehole Mersa Matruh-1, north West Desert, Egypt. Palaeontographica Abteilung B, 222, 31–88.

Phipps, D., Playford, G., 1984. Laboratory techniques for extraction of palynomorphs from sediments. Papers, Deptartment of Geology, University of Queensland 11, 1–23.

Peyrot, D., Barroso-Barcenilla, F., Barrón, E., Comas-Rengifo, M.J., 2011. Palaeoenvironmental analysis of Cenomanian–Turonian dinocyst assemblages from the Castilian Platform (Northern–Central Spain). Cretaceous Research 32, 504–526.

Piasecki, S., 1984. Dinoflagellate cysts stratigraphy of the Lower Cretaceous Jydegard Formation, Bornholm, Denmark. Bulletin of the Geological Society of Denmark 32, 145–161.

Pittet, B., Gorin, E., 1997. Distribution of sedimentary organic matter in a mixed carbonate–siliciclastic platform environment: Oxfordian of the Swiss Jura Mountains. Sedimentology 44, 915–937.

Pocklington, R., Leonard, J.D., 1979. Terrigenous organic mattter in sediments of the St. Lawrence Estuary and the Saguenay Fjord. Journal of the Fisheries Research Board of Canada 36, 1250–1255.

Prauss, M., 1989. Dinozysten-stratigraphie und palynofazies im oberen Lias und Dogger von NW–Deutschland. Palaeontographica Abteilung B 214, 1–124.

Prauss, M., 2001. Sea-level changes and organic-walled phytoplankton response in a Late Albian epicontinental setting, Lower Saxony basin, NW Germany. Palaeogeography, Palaeoclimatology, Palaeoecology 174, 221–249.

Prauss, L. M., 2006. The Cenomanian/Turonian Boundary Event (CTBE) at Wunstorf, north–west Germany, as reflected by marine palynology. Cretaceous Research 27, 872–886.

Regali, M.S.P., Uesugui, N., Santos, A.S., 1974. Palinologia dos sedimentos Meso–Cenozoicos do Brasil (I and II). Boletim Tecnico da PETROBRAS 17, 177–191, 263–301.

Regali, M.S.P., Viana, C.F., 1989. Late Jurassic–early Cretaceous in Brazilian sedimentary basins: correlation with the international standard scale. Report. PETROBRAS, Rio de Janeiro, 90.

Renéville. P., Raynaud, J.-F., 1981. Palynologie du stratotypedu Barrémien. Bulletin des Centres de Recherches Exploration-Production Elf-Aquitaine 5, 1–29.

Rider, M.H., 2002. The Geological Interpretation of Well Logs. Rider-Frensh Counsulting Ltd., Scotland.

Rifai, R.I., Kolkas, M.M., Holail, H.M., Khaled, K.A., 2006. Diagenesis and geochemistry of the Aptian Dolomite (Cretaceous) in the Razzak Oil Field, Western Desert, Egypt. Carbonates and Evaporites 21, 176–187.

Said, R., 1990. Cretaceous paleogeographic maps. In: Said, R. (Ed.), The Geology of Egypt. Balkema, Rotterdam, 439–449.

Schrank, E., 1984. Oragic-geochemical and palynological studies of a Dakhla Shale profile (Late Cretyaceous) in southeast Egypt. Berliner Geowissenschaftliche Abhandlungen, Reihe A 50, 177–187.

Schrank, E., 1990. Palynology of the clastic Cretaceous sediments between Dongola and Wadi Muqaddam, northern Sudan. Berliner Geowissenschaftliche Abhandlungen – Reihe A 120, 149–168.

Schrank, E., 1992. Nonmarine Cretaceous correlations in Egypt and northern Sudan; palynological and palaeobotanical evidence. Cretaceous Research 13, 351–368.

Schrank, E., 1994. Non-marine Cretaceous palynology of northern Kordofan, Sudan, with notes on fossil Salviniales (water ferns). Geologische Rundschau 83, 773–786.

Schrank, E., 2001. Paleoecological aspects pf *Afropollis*/elaterate peaks (Albian–Cenomanian pollen) in the Cretaceous of Northern Sudan and Egypt. In: Goodman, D.K., Clarke, R.T. (Eds.), Proceeding of the IX International Palynological Congress, Houston, Texas, 1996. American Association of Stratigraphic Palynologists Foundation, 201–210.

Schrank, E., Ibrahim, M.I.A., 1995. Cretaceous (Aptian–Maastrichtian) palynology of foraminifera-dated wells (KRM-1, AG-18) in north–western, Egypt. Berliner Geowissenschaftliche Abhandlungen, Reihe A 177, 1–44.m

Schrank, E., Mahmoud, M.S., 1998. Palynology (pollen, spores and dinoflagellates) and Cretaceous stratigraphy of the Dakhla Oasis, central Egypt. Journal of African Earth Sciences 26, 167–193.

Schrank, E., Mahmoud, M.S., 2002. Barremian angiosperm pollen and associated palynomorphs from the Dakhla Oasis area, Egypt. Palaeontology 45, 33–56.

Scotese, C.R., 2014. Atlas of Early and Late Cretaceous Paleogeographic Maps, PALEOMAP Atlas for ArcGIS, 2. The Cretaceous, Maps 16–22 and 23–31, Mollweide Projection, PALEOMAP Project, Evanston, IL.

Shalaby, M.R., Hakimi, M.H., Abdullah, W.H., 2012. Organic geochemicalcharacteristics and interpreted depositional environment of the Khatatba Formation, northern Western Desert, Egypt. American Association of Petroleum Geologists Bulletin 96, 2019–2036.

Selley, R.C., 1976. Subsurface Environmental Analysis of North Sea Sediments. American Association of Petroleum Geologists Bulletin 60, 184–195.

Sellwood, B.W., Valdes, P.J., 2006. Mesozoic Climates: General Circulation Models and the Rock Record. Sedimentary Geology 190, 269–287.

Simpson, E.H., 1949. Measurement of diversity. Nature 163, 688.

Shahin, A., Elbaz, E., 2013. Cenomanian–Early Turonian Ostracoda of the shallow marine carbonate platform sequence at west central Sinai: biostratigraphy, paleobathymetry and paleobiogeography. Revue de Micropaléontologie 56, 103–126.

Slimani, H., Louwye, S., Toufiq, A., 2010. Dinoflagellate cysts from the Cretaceous–Paleogene boundary at Ouled Haddou, southeastern Rif, Morocco: biostratigraphy, paleoenvironments and paleobiogeography. Palynology 34, 90–124.

Smyth, M., Jian, F.X., Ward, C.R., 1992. Potential petroleum source rocks in Triassic lacustrine–delta sediments of the Gunnedah Basin, Eastern Australia. Journal of Petroleum Geology 15, 435–450.

Stockmarr, J., 1971. Tablets with spores used in absolute pollen analysis. Pollen et Spores 13, 616–621.

Stout, J.D., Goh, K.M., Rafter, T.A., 1981. Chemistry and turnover of naturally occuring resistant organic compounds in soil. Soil Biochemistry 5, 1–73.

Sultan, N., Halim, A., 1988. Tectonic Framework of northern Western Desert, Egypt and its effect on hydrocarbon accumulations. Proceedings of the EGPC Ninth Exploration Conference, Cairo, Egypt, 2, 1–22.

Tahoun, S.S., Deaf, A.S., 2016. Could the conventionally known Abu Roash “G” reservoir (upper Cenomanian) be a promising active hydrocarbon source in the extreme northwestern part of Egypt? Palynofacies, palaeoenvironmental, and organic geochemical answers. Marine and Petroleum Geology 76, 231–245.

Thusu, B., Van Der Eem, J.G.L.A., 1985. Early Cretaceous (Neocomian–Cenomanian) palynomorphs. Journal of Micropalaeontology 4, 131–150.

Thusu, B., Van Der Eem, J.G.L.A., El-Mehdawi, A., Bu-Argoub, F., 1988. Jurassic–early Cretaceous palynostratigraphy in north–east Libya. In: El-Aranuti, A., Owens, B., Thusu, B. (Eds.), Subsurface Palynostratigraphy of NE Libya. Benghazi, Garyounis University Publications, 171–213.

Torricelli, S., 2000. Lower Cretaceous dinoflagellate cyst and acritarch stratigraphy of the Cismon APTICORE (Southern Alps, Italy). Review of Palaeobotany and Palynology 108, 213–266.

Trevisan, L., 1972. *Dicheiropollis*, a pollen type from lower Cretaceous sediments of Southern Tuscany (Italy). Pollen et Spores 22, 85–132.

Trevisan, L., 1980. Ultrastructure notes and considerations on *Ephedripites, Eucommiidites* and *Monosulcites* pollen grains from Lower Cretaceous sediments of southern Tuscany (Italy). Pollen et Spores 22, 85–132.

Tyler, M.A., Coats, D.W., Anderson, D.M., 1982. Encystment in a dynamic environment: deposition of dinofalgellate cysts by a frontal convergence. Marine Ecology Progress Series 7, 163–178.

Tyson, R.V., 1984. Palynofacies investigation of Callovian (Middle Jurassic) sediments from DSDP Site 534, Black–Bahama Basin, Western Central Atlantic. Marine and Petroleum Geology 1, 3–13.

Tyson, R.V., 1989. Late Jurassic palynofacies trends, Piper and Kimmeridge Clay Formations, UK onshore and offshore. In: Batter, D.J., Keen, M.C. (Eds.), Northwest European Microplaeontology and Palynology. British Micropalaeontological Society Series, Ellis Horwood, Chichester, 135–172.

Tyson, R.V., 1993. Palynofacies analysis. In: Jenkins, D.G. (Ed.), Applied Micropaleontology. Kluwer, Dordrecht, 13–191.

Tyson, R.V., 1995. Sedimentary Organic Matter: Organic Facies and Palynofacies. Chapman and Hall, London.

Van der Zwan, C.J., 1990. Palynostratigraphy and palynofacies reconstruction of the Upper Jurassic to lowermost Cretaceous of the Draugen Field, offshore mid Norway. Review of Palaeobotany and Palynology 62, 157–186.

Watson, J., 1988. The Cheirolepidiaceae. In: Beck, C.B. (Ed.), Origin and Evolution of Gymnosperms. Columbia University Press, New York, 382–447.

WEPCO (1968) Final report and composite log of the Abu Tunis 1X borehole. *Report.* Cairo, Western Desert Operating Petroleum Company.

Williams, G.L., 1992. Palynology as a palaeoenvironmental indicator in the Brent Group, northern North Sea. In: Morton, A.C., Haszeldine, R.S., Giles, M.R., Brown, S. (Eds.), Geology of the Brent Group. Geolological Society of London Special Publication, London, 203–212.

Williams, G.L., Fensome, R.A., MacRae, R.A., 2017. DINOFLAJ3. American Association of Stratigraphic Palynologists, Data Series no. 2. http://dinoflaj.smu.ca/dinoflaj3.

Wood, G.D., Gabriel, A.M., Lawson, J.C., 1996. Palynological techniques, processing and microscopy. In: Jansonius, J., McGregor, D.C. (Eds.), Palynology: Principles and Applications. American Association of Stratigraphic Palynologists Foundation, Tulsa, 29–50.

Ziegler, A.M., Eshel, G., Rees, P.M., Rothfus, T.A., Rowley, D.B., Sunderlin, D., 2003. Tracing the tropics across land and sea: Permian to present. Lethaia 36, 227–254.

Figure captions

Figure 1. Map showing location of the Abu Tunis 1X well and Cretaceous basins in the north Western Desert of Egypt (Modified after Shalaby et al., 2012).

Figure 2. Cretaceous palaeogeographic maps of Egypt showing the main regional tectonic settings, depositional environments, and main lithological facies (after Guiraud et al., 2001). (a) Early Hauterivian (~ 130–132 Ma). (b) Mid Aptian (~ 115 Ma). (c) Late Cenomanian (~ 94 Ma). (d) Early Campanian (~ 81 Ma). M. Matruh Basin; 1. deep basin; 2. carbonate platform; 3. mixed platform (carbonate and siliciclastic facies); 4. fluviatile–lacustrine environment; 5. fluvio–deltaic environment; 6. exposed land; 7. uplifted arch (axes of anticlines); 8. active normal fault; 9. other faults.

Figure 3. Summary of the stratigraphy, description of the lithologies of the sedimentary sequences of the north Western Desert of Egypt and the depositional environment of the Cretaceous sequences (modified after Abrams et al., 2016).

Figure 4. The Abu Tunis 1X stratigraphy, formation lithologies, sample positions, palynological biozonation, and age dating of the studied sequence. N.B.: depths in meters here and elsewhere in the manuscript are calculated from the total depth in feet – elevation of the Kelly Bush (589 ft) * 0.3048.

Figure 5. Dendrogram of the hierarchical cluster analysis of the palynological samples of the Abu Tunis 1X and the isolated palynofacies types.

Figure 6. Lithological column, spontaneous potential, resistivity data (after WEPCO, 1968) and the interpreted sedimentary cycles of the Abu Tunis 1X well as deduced from the SP log.

Figure 7. Regional and intercontinental biozonal correlation of Abu Tunis 1X bioevents and the links to the global eustatic sea level curves of Haq (2014). For consistency of correlation, the numerical ages of the Cretaceous stages used here are those suggested by Gradstein et al. (2012) and used by Haq (2014). In addition, boundaries of the palynofacies identified in the Abu Tunis 1X well are placed according to the position of the recorded dinocyst/sporomorph bioevents in each palynofacies.

Figure 8. Absolute abundances (grains/g) of selected palynomorphs and particulate organic matter in the Abu Tunis 1X well, northern Western Desert, Egypt.

Figure 9. Representative palynofacies. (a) PF-1A dominated by terrestrially derived organic matter (sporomorphs and phytoclasts), Sample 11b/MAN-56 (9,650 ft / 2,762 m) at x250 magnification indicating the upper Hauterivian–lower Barremian regressive cycle, the Abu Tunis 1X well, northern Western Desert, Egypt. (b) PF-1B with a reduced abundance of terrestrially derived organic matter and increased dinocyst concentrations indicating the first marine transgressive cycle, Sample 32a/MAN-69 (8,600 ft / 2,442 m) at x250 magnification. (c) PF-2A showing terrestrial palynomorph and phytoclast dominance in the upper Aptian regressive cycle, Sample 46a/MAN-73 (7,900 ft / 2,228 m) at x250 magnification.

Figure 10. Examples of terrestrial and marine palynomorphs from the Abu Tunis 1X well. The sample/slide number and depth with museum accession number (MAN), England Finder coordinates, and position of taxa (numbers in parentheses) on the quantitative range chart

(online Supplementary Appendix 4) are indicated for all specimens. Scale bar represents 20 µm.

Spore and pollen grains: (a) *Dictyophyllidites harrisii* Couper, 1958, slide AT-1A/MAN-51, 10,150 ft (2,914 m), O28/1, (28). (b) *Deltoidospora toralis* (Leschik) Lund, 1977, slide AT-1A/MAN-51, 1,0150 ft (2,914 m), K34/3, (16). (c) *Concavisporites* sp., slide AT-6A/MAN-54, 9,900 ft (2,838 m), Q32/2, (19). (d) *Auritulinasporites scanicus* Nilsson, 1958, silde AT-7A/MAN-55, 9,850 ft (2,823 m), O11/2, (53). (e) *Auritulinasporites intrastriatus* Nilsson, 1958, slide AT-7A/MAN-55, 9,850 ft (2,823 m), R25, (55). (f) *Deltoidospora australis* (Couper) Pocock, 1970, slide AT-12A/MAN-57, 9,600 ft (2,747 m), E33, (38). (g) *Cicatricosisporites* sp., slide AT-30A/MAN-68, 8700 ft (2472 m), T49/2, (7). (h) *Impardecispora uralensis* (Bolkhovitina) Venkatachala et al., 1969, slide AT-3A/MAN-52, 10,050 ft (2,884 m), Q30, (60). (i) *Balmeiopsis limbatus* (Balme) Archangelsky, 1979, slide AT-1A/MAN-51, 10,150 ft (2,914 m), L17/4, (63). (j) *Ephedripites* sp., slide AT-28A/MAN-66, 8,800 ft (2,503 m), W24, (65). (k) *Ephedripites* sp., slide AT-19B/MAN-60, 9,250 ft (2,640 m), Q46/3, (65). (n) *Classopollis classoides* Pflug, 1953, slide AT-6A/MAN-54, 9,900 ft (2,838 m), R30, (13). (p) *Elaterosporites protensus* (Stover) Jardiné, 1967, slide AT-90A/MAN-77, 5,650 ft (1,543 m), U16, (74). (q) *Galeacornea causea* Stover, 1963, slide AT-84A/MAN-74, 6,000 ft (1,649 m), K46, (76). (r) *Sofrepites legouxiae* Jardiné, 1967, 21, slide AT-95A/MAN-78, 5,100 ft (1,375 m), H17/3, (71). (s) *Elaterosporites klaszii* (Jardiné and Magloire) Jardiné, 1967, slide AT-97A/MAN-80, 4,950 ft (1,329 m), G13/4, (66). (t), (u) *Afropollis jardinus* Doyle et al., 1982, slide AT-89B/MAN-76, Q22; slide AT-89A/MAN-75, 5,750 ft (1,573 m), R13 (92). **Freshwater algae and euglenoid freshwater forms:** (l) *Chomotriletes minor* (Kedves) Pocock, 1970, slide AT-18A/MAN-59, 9,300 ft (2,655 m), E34/2, (148). (m) *Ovoidites parvus* (Cookson and Dettmann) Nakoman, 1966, slide AT-16A/MAN-58, 9,400 ft (2,686 m), H37/2, (145). (o) *Botryococcus* sp., slide AT-99B/MAN-81, 4,850 ft (1,299 m), R42/4, (147). **Dinoflagellate cysts:** (v) *Pseudoceratium securigerum* (Davey and Verdier) Bint, 1986, slide AT-20A/MAN-61, 9,200 ft (2,625 m), T40/3, (185). (w) *Cribroperidinium edwardsii* (Cookson and Eisenack) Davey, 1969, slide AT-27A/MAN-65, 8,850 ft (2,518 m), H42/3, (181). (x) *Subtilisphaera scabrata* Jain and Millepied, 1973, slide AT-29A/MAN-67, 8,750 ft (2487 m), U46, (192). (y) *Palaeoperidinium cretaceum* (Pocock) Lentin and Williams, 1976, slide AT-36A/MAN-71, 8,400 ft (2,381 m), R12, (187). (z) *Cyclonephelium vannophorum* Davey, 1969, slide AT-12A/MAN-57, 9,600 ft (2,747 m), K28/4, (212). (aa) *Pseudoceratium retusum* Brideaux, 1977, slide AT-25A/MAN-64, 8,950 ft (2,548 m), L48/4, (190). (ad) *Aptea polymorpha* Eisenack, 1958a, slide AT-24A/MAN-63, 9,000 ft (2,564 m), N30/3, (193). (ae) *Florentinia mantellii* (Davey and Williams) Davey and Verdier, 1973, slide AT-22A/MAN-62, 9,100 ft (2,594 m), Q51, (172). (af) *Oligosphaeridium complex* (White) Davey and Williams, 1966, slide AT-25A/MAN-64, 8,950 ft (2,548 m), L43, (179). (ag) *Muderongia pariata* Duxbury, 1983, slide AT-4A/MAN-53, 10,000 ft (2,868 m), M15/3, (198). **Acritarchs:** (ab) *Veryhachium collectum* Wall, 1965, slide AT-33A/MAN-70, 8,550 ft (2,427 m), X39/4, (221). (ac) *Veryhachium metum* Davey, 1970, slide AT-42A/MAN-72, 8,100 ft (2,289 m), T31/3, (222).

Figure 11. Dinocyst absolute abundances (grains/g), species diversity, and different cyst morphotypes in the Abu Tunis 1X well, northern Western Desert, Egypt.

Figure 12. (a) Ternary plot of the Abu Tunis 1X palynofacies (Tyson, 1995). (b) Ternary plot of spores, microplankton, pollen (SMP), for samples yielding PF-1A and PF-1B in the Abu Tunis 1X well and their probable depositional environment (after Federova, 1977; Duringer and Doubinger, 1985). (c) Plot of samples yielding PF-2A, PF2-B and PF-3 in the Abu Tunis 1X well in the SMP and their probable depositional environments.

Figure 13. Depositional models showing the four regressive-transgressive sequences in the Matruh Basin.

Figure 14. Representative palynofacies. (a) PF-2B shows increased dinocyst abundances and fewer terrestrial palynomorphs and phytoclasts by comparison to PF-2A, indicating the onset of the lower Cenomanian transgressive cycle, Sample 96a/MAN-79 (5,050 ft / 1,360 m) at x250 magnification. (b) PF-3 showing dominance of dinocysts and an almost complete lack of terrestrial POM constituents, Sample 110a/MAN-82 (4,300 ft / 1,131 m) at x250 magnification.

Figure 15. (a) Palaeogeographic reconstruction at 125 Ma, showing the pre-Albian *Dicheiropollis/Afropollis* Phytogeographic Province and distribution of the most important pollen and spore species characteristic of the province. Palaeogeographic reconstruction simplified from Hay et al. (1999), and modified after Ibraim et al. (2000). Based on selected palynological studies as follows: North Africa: Egypt (Schrank, 1992; Schrank and Mahmoud, 1998, 2002, Deaf et al., 2016), Sudan (Schrank, 1992; Awad, 1994), Libya (Thusu and van der Eem, 1985; Thusu et al., 1988; Uwins and Batten, 1988), Algeria (Jardiné et al., 1974), Morocco (Gübeli et al., 1984; Bettar and Courtinat, 1987); West Africa: Gabon and Congo (Doyle et al., 1977); south Switzerland and north Italy: (Hochuli, 1981); South America: NE Brazil (Regali et al., 1974; Regali and Viana, 1989).

(b) Palaeogeographic reconstruction at 100 Ma showing the Albian-Cenomanian Elaterates Phytogeographic Province and distribution of the most important pollen and spore species characteristic of the province. Palaeogeographic reconstruction simplified from Hay et al. (1999), and modified after Ibraim et al. (2000). Based on selected palynological work as follows: North Africa: Egypt (Schrank and Ibrahim, 1995; Deaf et al., 2014), Sudan (Awad, 1994), Libya (Batten and Uwins, 1985; Uwins and Batten, 1988), Morocco (Bettar and Méon, 2001, 2006); West Africa: Ghana (Atta-Peters and Salami, 2006), Senegal and Ivory Coast (Jardiné and Magloire, 1965), Angola basin and Nigeria (Lawal and Moullade, 1986; Abubakar et al., 2006), Intertropical Africa (Salard-Cheboldaeff, 1990); south Switzerland and north Italy: (Hochuli, 1981); South America: NE Brazil (Regali et al., 1974; Herngreen, 1974; Regali, 1989; Dino et al., 1999), Colombia (Herngreen and Jimenez, 1990), Peru (Brenner, 1968; Mejia-Velasquez et al., 2018), Ecuador (Dino et al., 1999).

Figure 16. World palaeo-tectonic maps of Scotese (2014) showing the Cretaceous palaeogeographic position of Egypt, southern Tethys, and Intertropical Convergence Zone (ITCZ). (a) Hauterivian ITCZ is proposed here based on the data discussed in the paper. (b) late Aptian ITCZ after Chaboureau et al. (2012), Scotese (2014), and Carvalho et al. (2017). (c) late Albian ITCZ after Chumakov et al. (1995), Hay and Floegel (2012), and Scotese (2014). (d) Turonian. Eg = Egypt, Sd = Sudan, Mo = Morocco, Se = Senegal, Ga = Gabon, Br = Brazil, Co = Columbia, Pe = Peru.

Figure 17. (a) Quantitative and semi-quantitative vertical distributions of *Afropollis* in the Aptian–middle Cenomanian of the Abu Tunis 1X well (Modified after Deaf et al., 2016) and their relation to the relative falling and initial sea level rise and the development of humid coastal conditions.

Table caption

Table 1. Botanical affinities and suggested ecological preferences of some selected sporomorphs and freshwater algae.

Figure 1

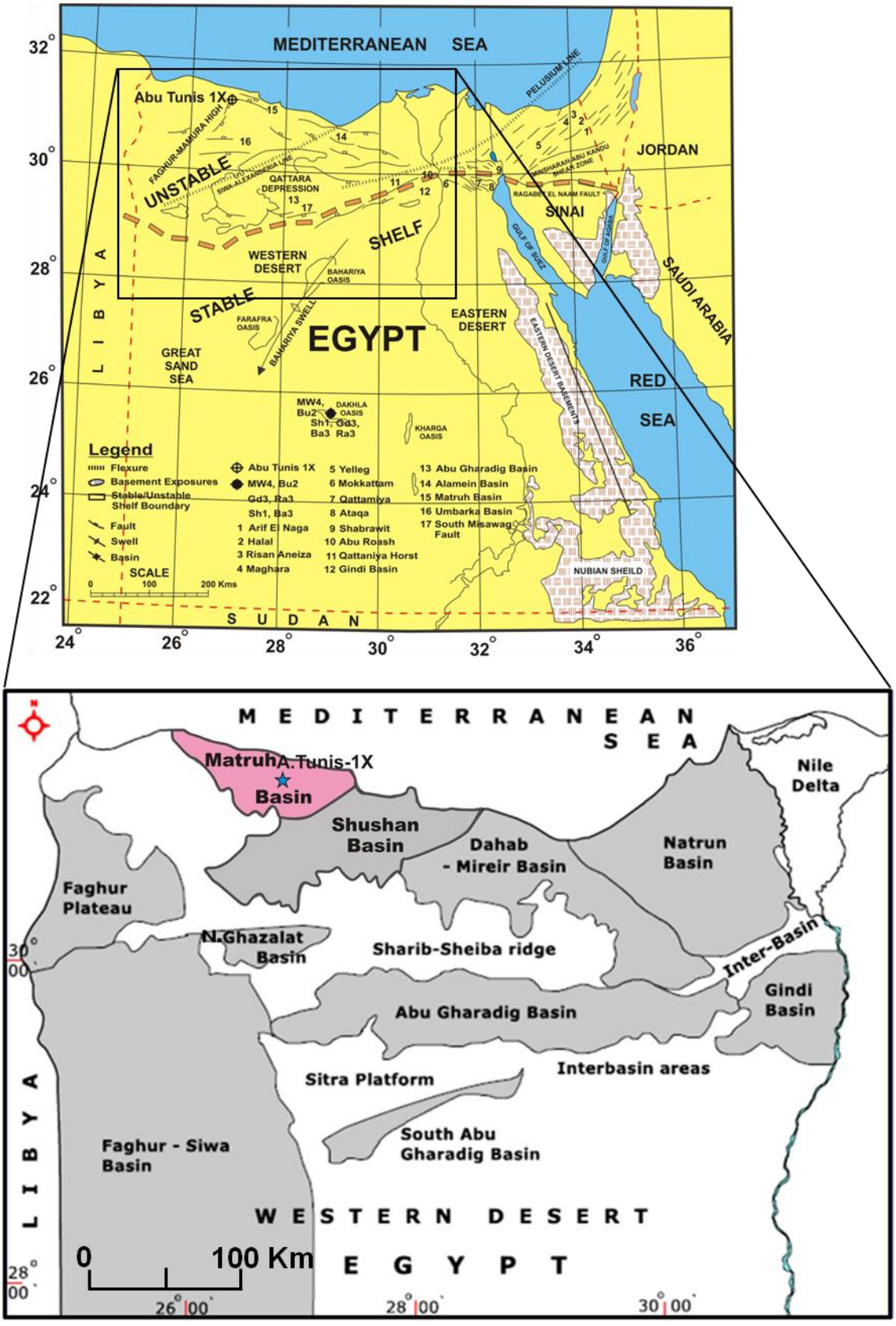

2292

2293 **Figure 2**

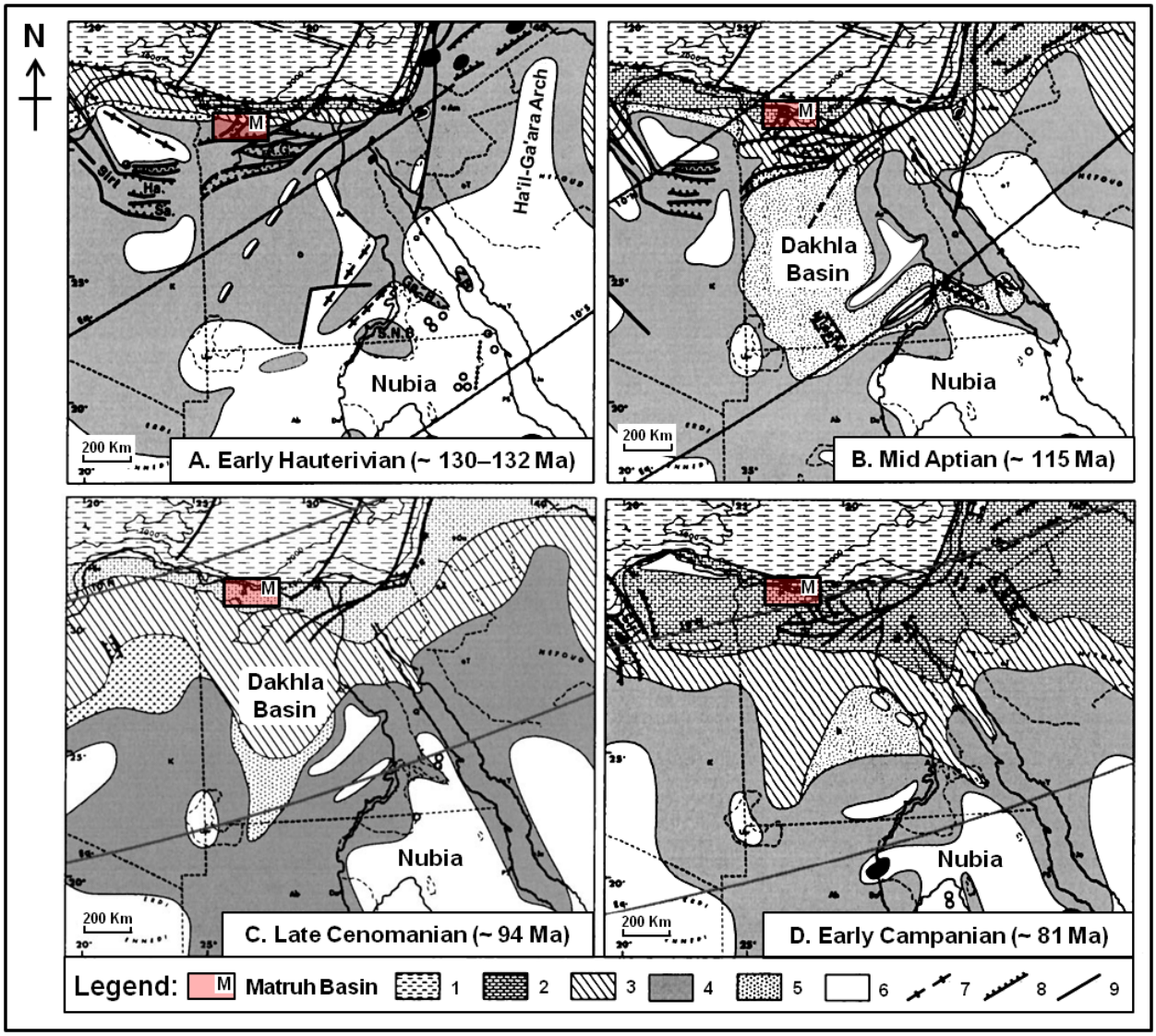

2294

2295 **Figure 3**

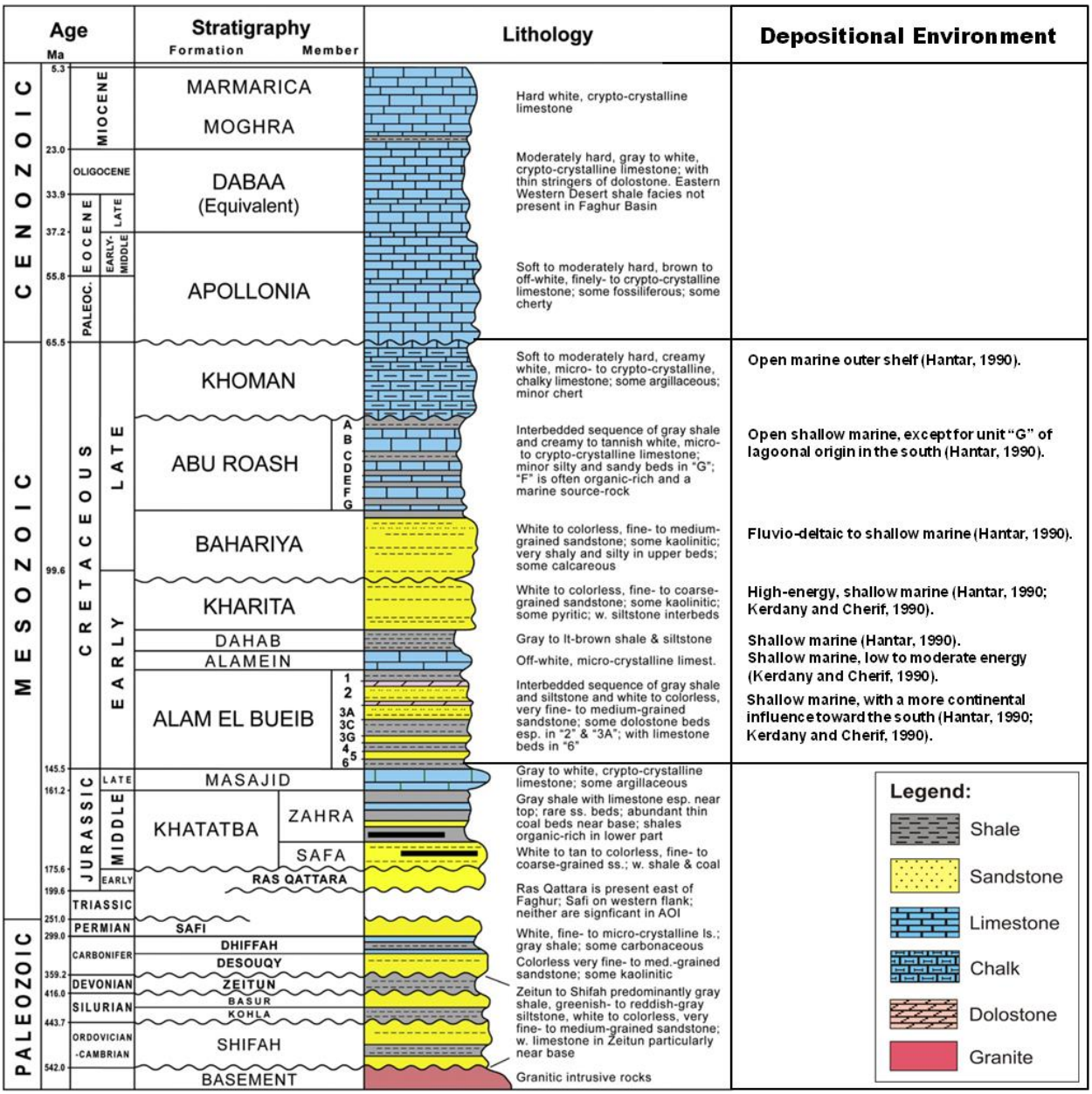

Figure 4

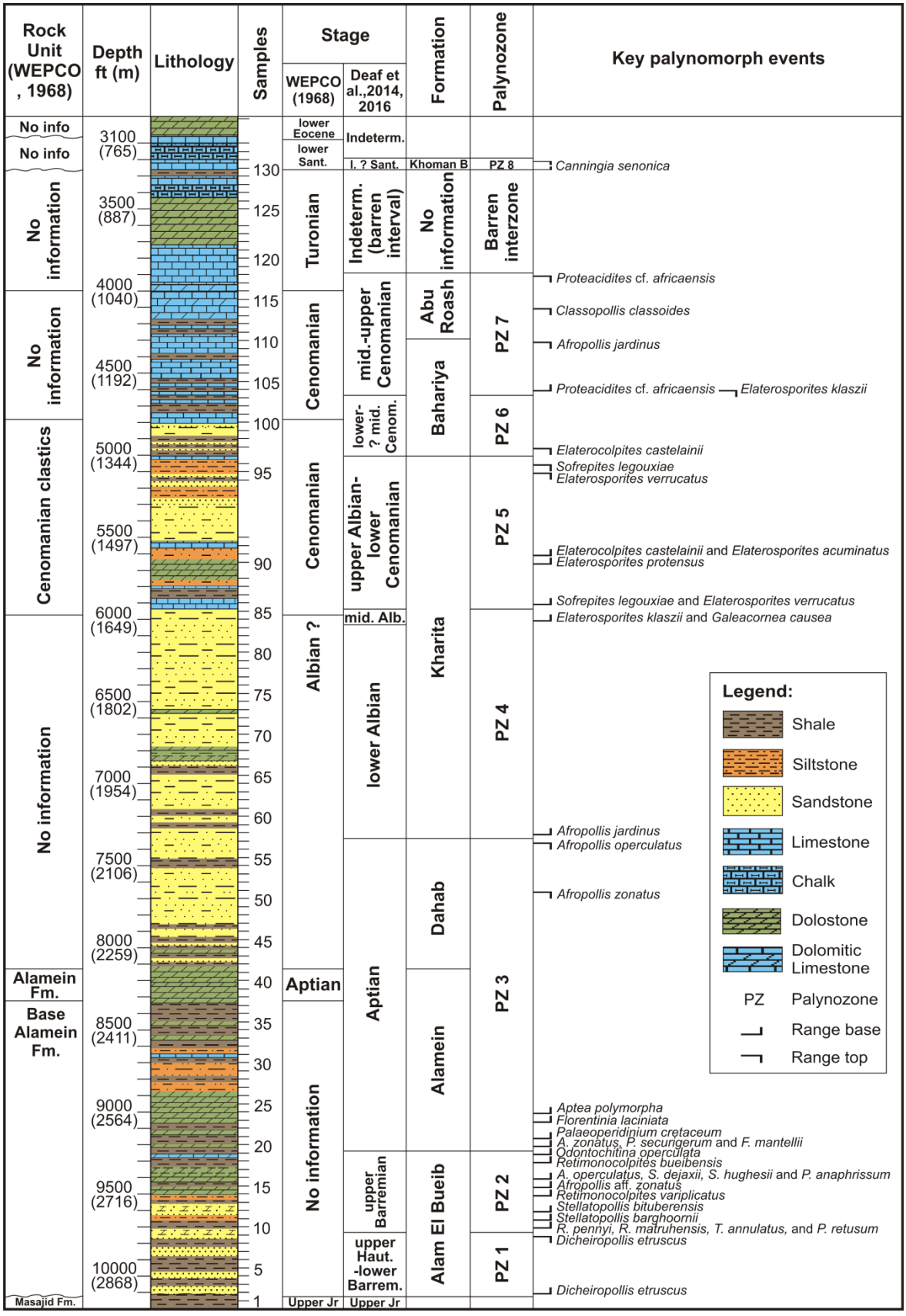
Rock Unit (WEPCO, 1968)
Depth ft (m)
Lithology
Samples
Stage
WEPCO (1968)
Deaf et al.,2014, 2016
Formation
Palynozone
Key palynomorph events
No info
No info
No information
No information
Cenomanian clastics
No information
Alamein Fm.
Base Alamein Fm.
Masajid Fm.
3100 (765)
3500 (887)
4000 (1040)
4500 (1192)
5000 (1344)
5500 (1497)
6000 (1649)
6500 (1802)
7000 (1954)
7500 (2106)
8000 (2259)
8500 (2411)
9000 (2564)
9500 (2716)
10000 (2868)
lower Eocene
lower Sant.
Turonian
Cenomanian
Cenomanian
Albian ?
Aptian
No information
Upper Jr
Indeterm.
l. ? Sant.
Indeterm. (barren interval)
mid.-upper Cenomanian
lower-? mid. Cenom.
upper Albian-lower Cenomanian
mid. Alb.
lower Albian
Aptian
upper Barremian
upper Haut. -lower Barrem.
Upper Jr
Khoman B
No information
Abu Roash
Bahariya
Kharita
Dahab
Alamein
Alam El Bueib
PZ 8
Barren interzone
PZ 7
PZ 6
PZ 5
PZ 4
PZ 3
PZ 2
PZ 1
Canningia senonica
Proteacidites cf. africaensis
Classopollis classoides
Afropollis jardinus
Proteacidites cf. africaensis
Elaterosporites klaszii
Elaterocolpites castelainii
Sofrepites legouxiae
Elaterosporites verrucatus
Elaterocolpites castelainii and Elaterosporites acuminatus
Elaterosporites protensus
Sofrepites legouxiae and Elaterosporites verrucatus
Elaterosporites klaszii and Galeacornea causea
Afropollis jardinus
Afropollis operculatus
Afropollis zonatus
Aptea polymorpha
Florentinia laciniata
Palaeoperidinium cretaceum
A. zonatus, P. securigerum and F. mantellii
Odontochitina operculata
Retimonocolpites bueibensis
A. operculatus, S. dejaxii, S. hughesii and P. anaphrissum
Afropollis aff. zonatus
Retimonocolpites variplicatus
Stellatopollis bituberensis
Stellatopollis barghoornii
R. pennyi, R. matruhensis, T. annulatus, and P. retusum
Dicheiropollis etruscus
Dicheiropollis etruscus
Legend:
Shale
Siltstone
Sandstone
Limestone
Chalk
Dolostone
Dolomitic Limestone
PZ Palynozone
Range base
Range top

2299 **Figure 5**

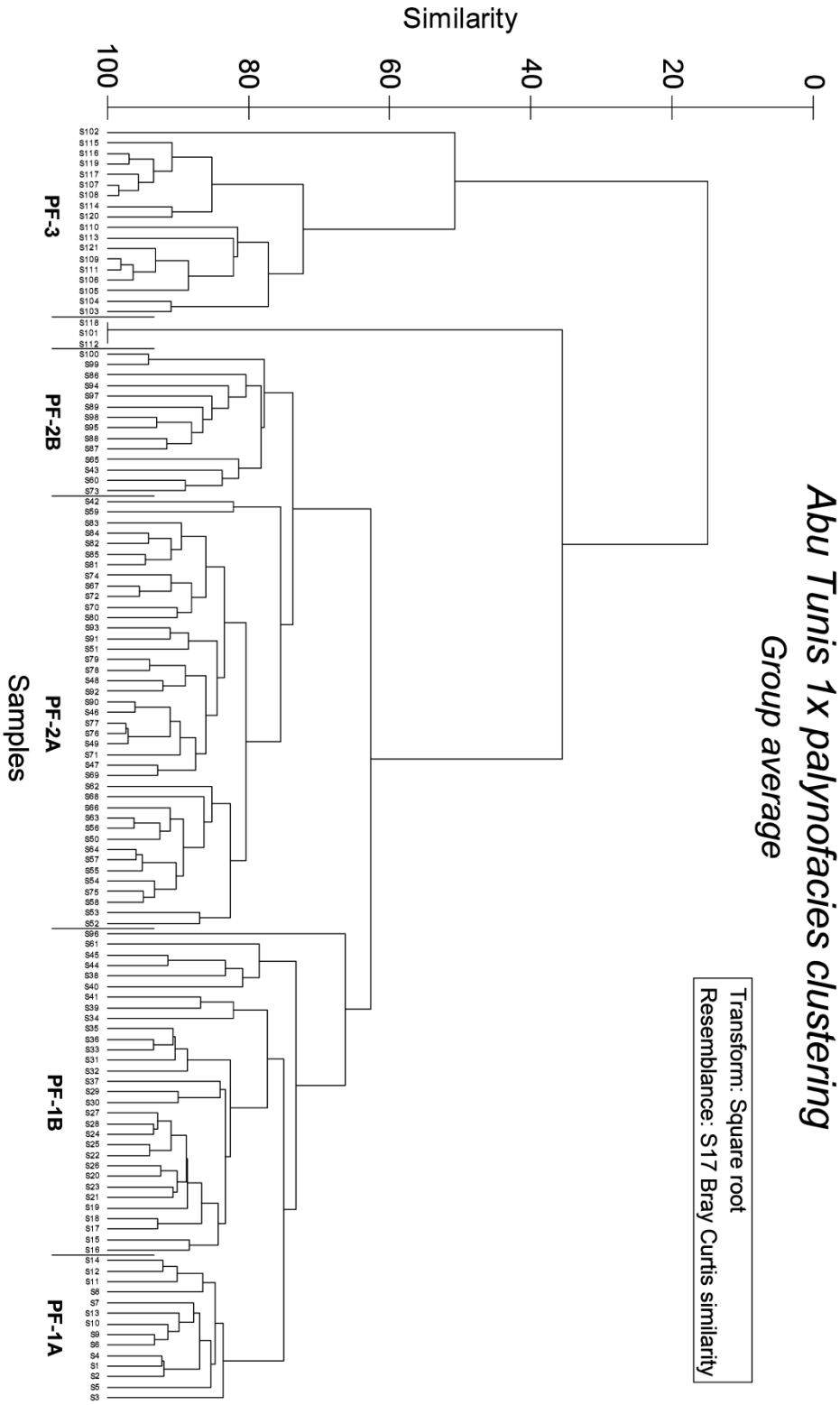

2300

2301 **Figure 6**

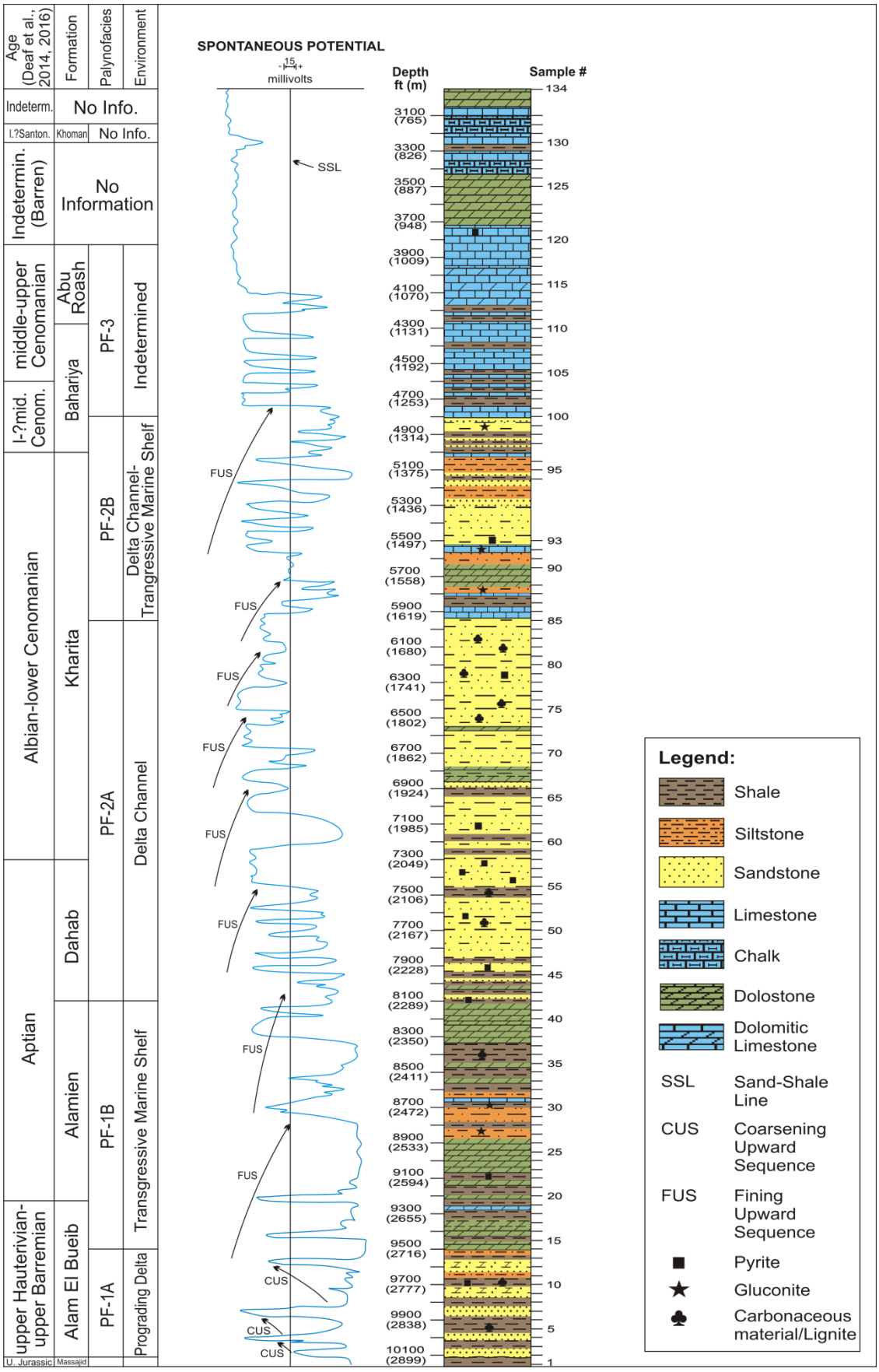

2302

2303 **Figure 7**

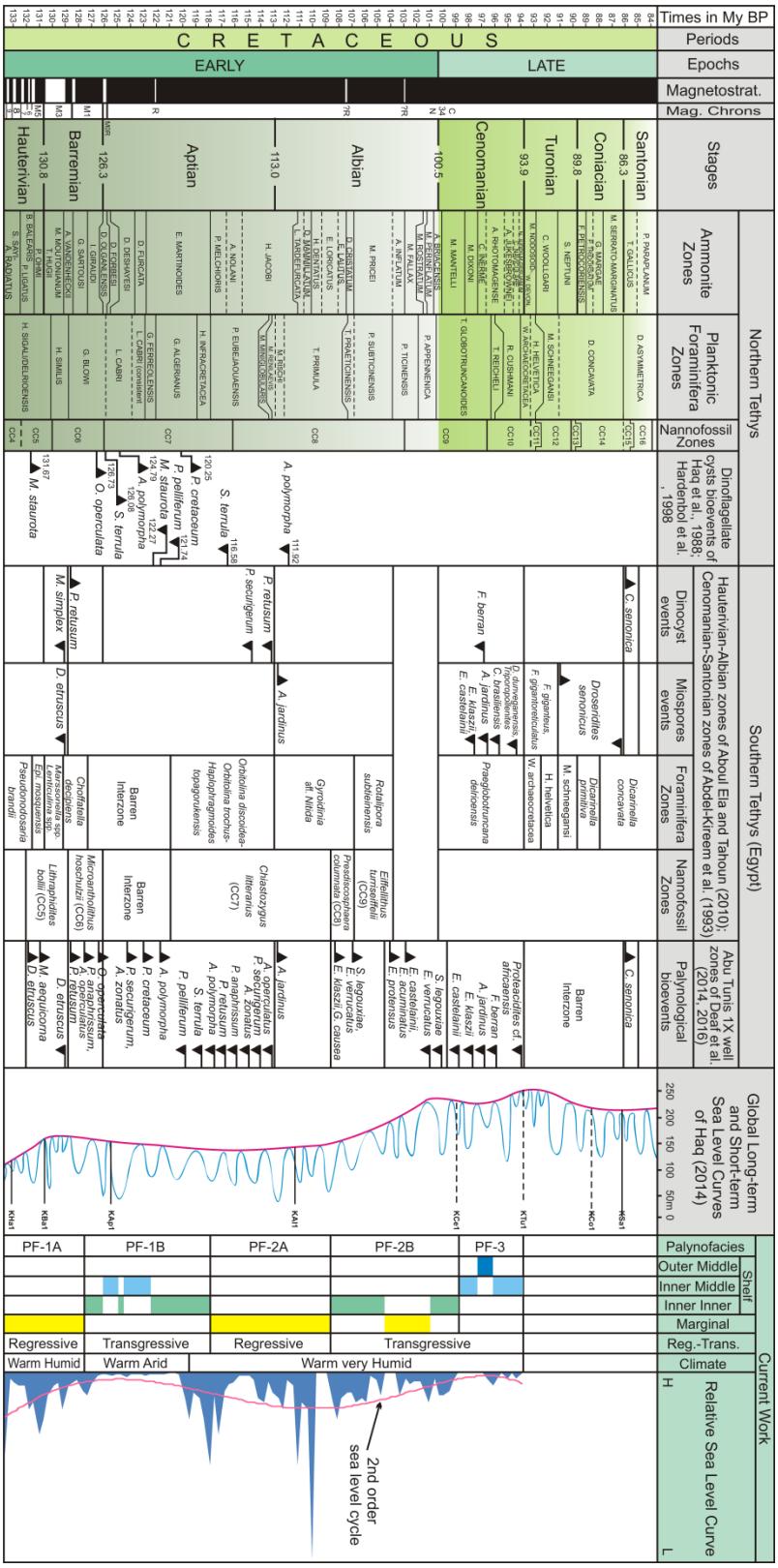

2304

2305 **Figure 8**

2306

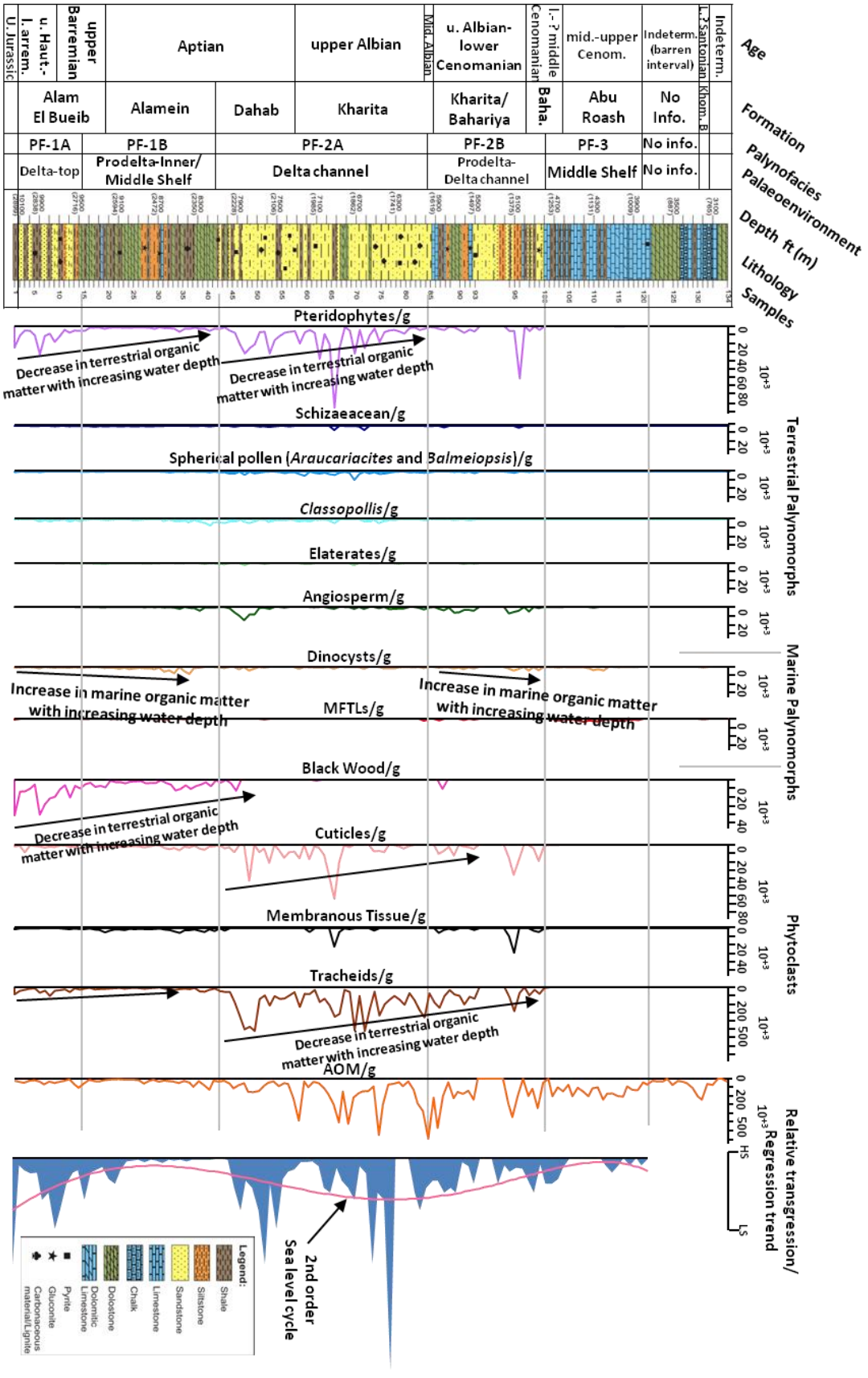

2307

2308 **Figure 9**

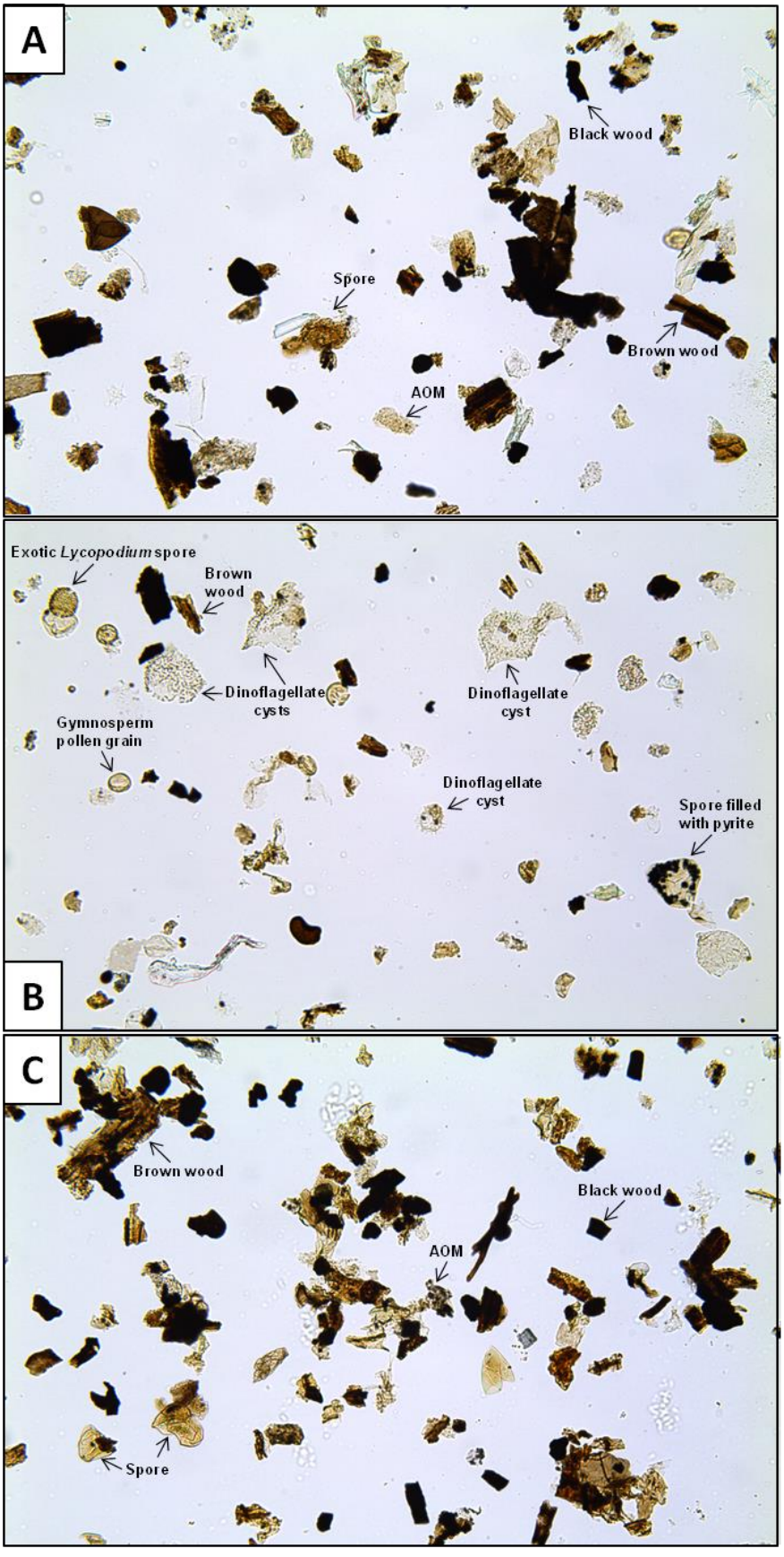

Figure 10

2311

2312 **Figure 11**

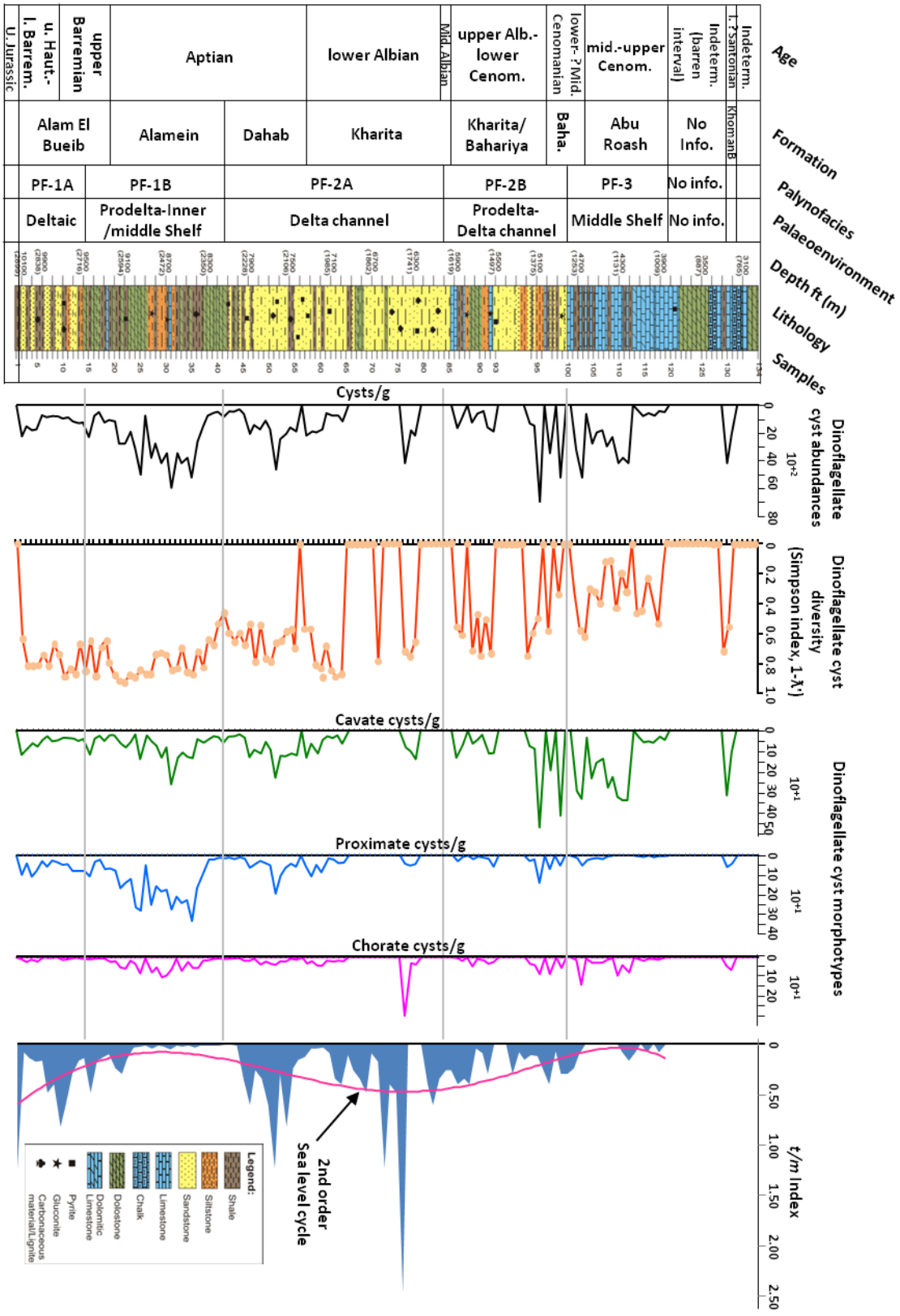

2313

2314 **Figure 12**

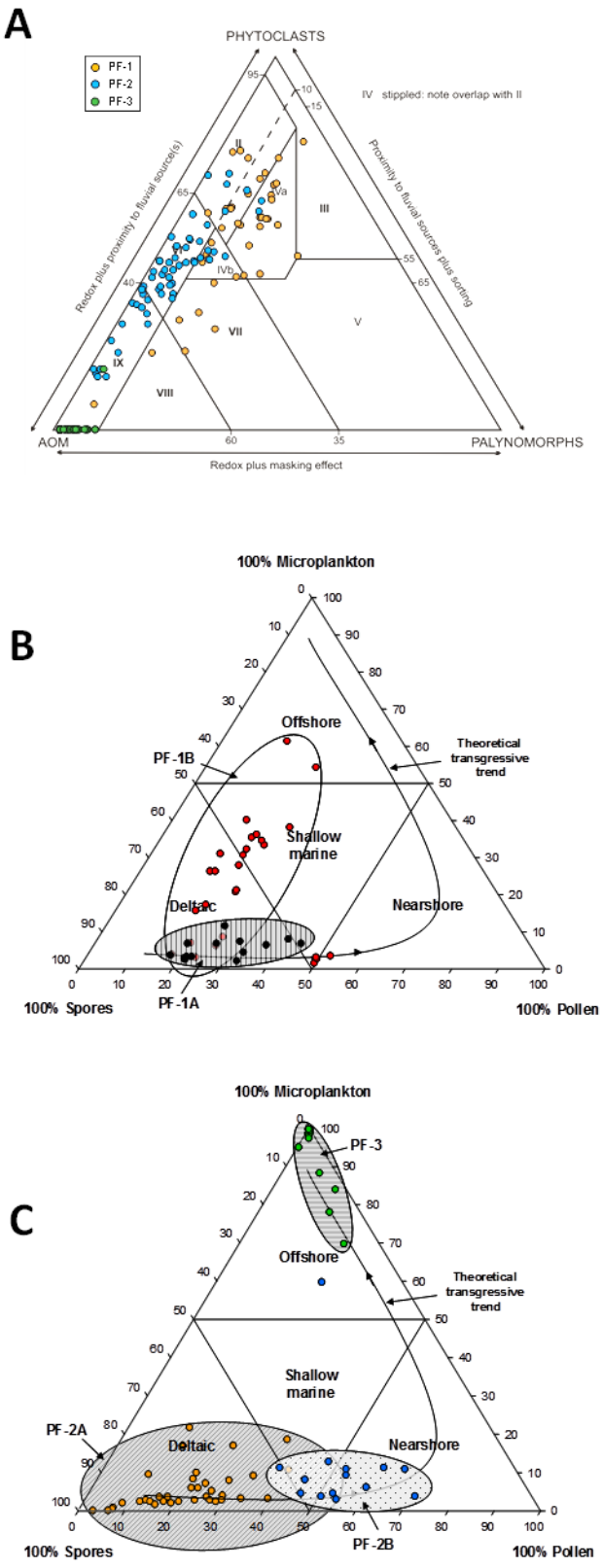

2315

2316 **Figure 13**

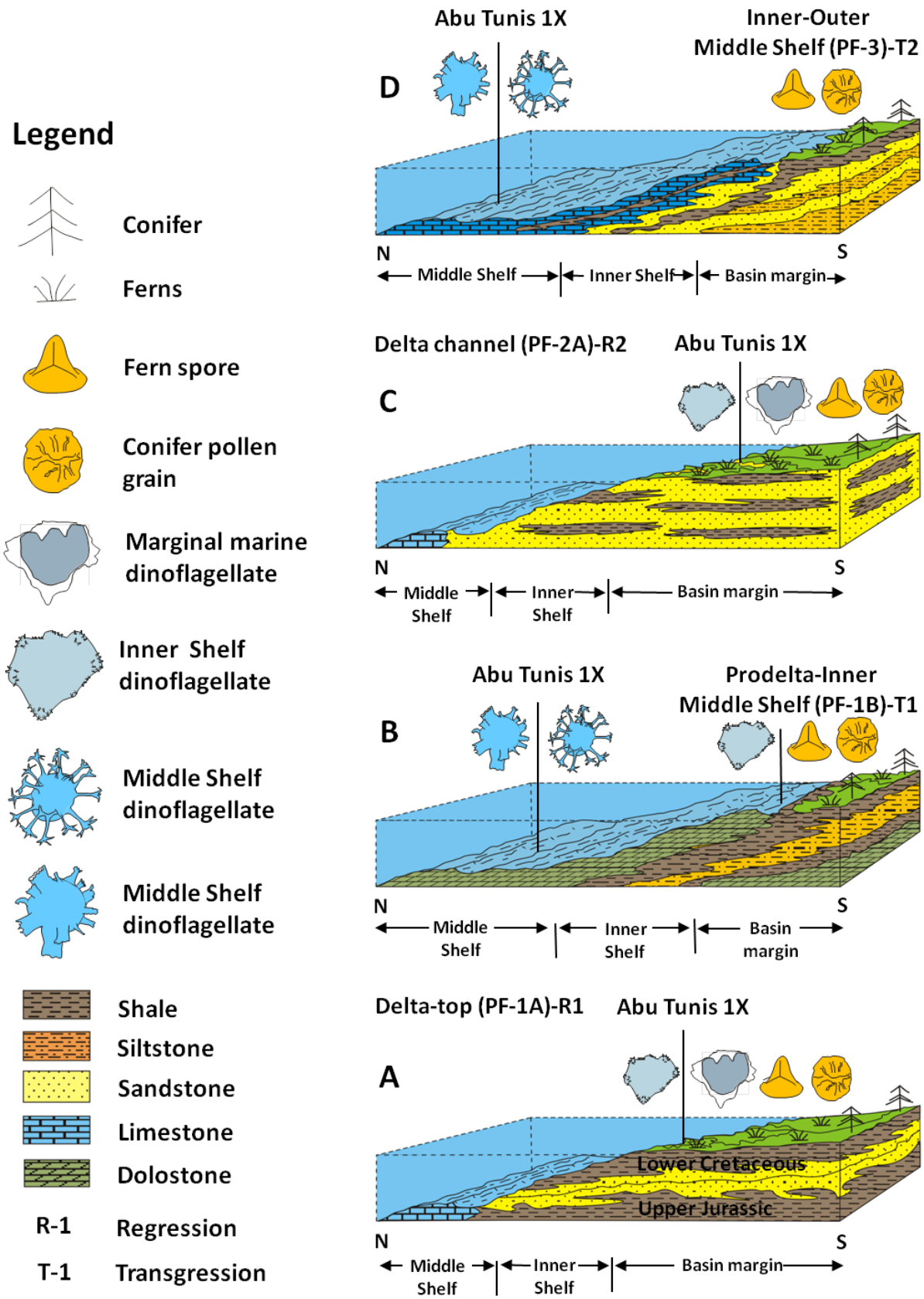

2317

2318 **Figure 14**

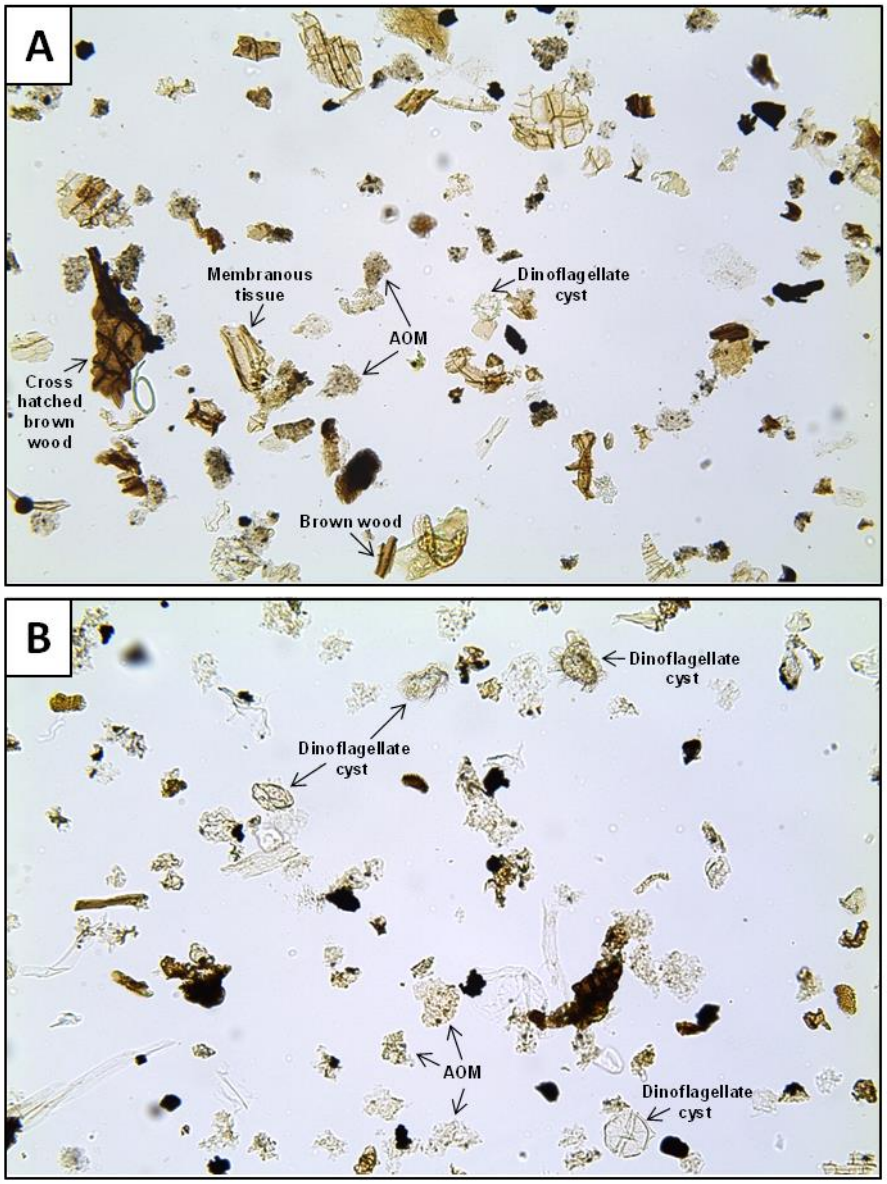

2319

2320 **Figure 15**

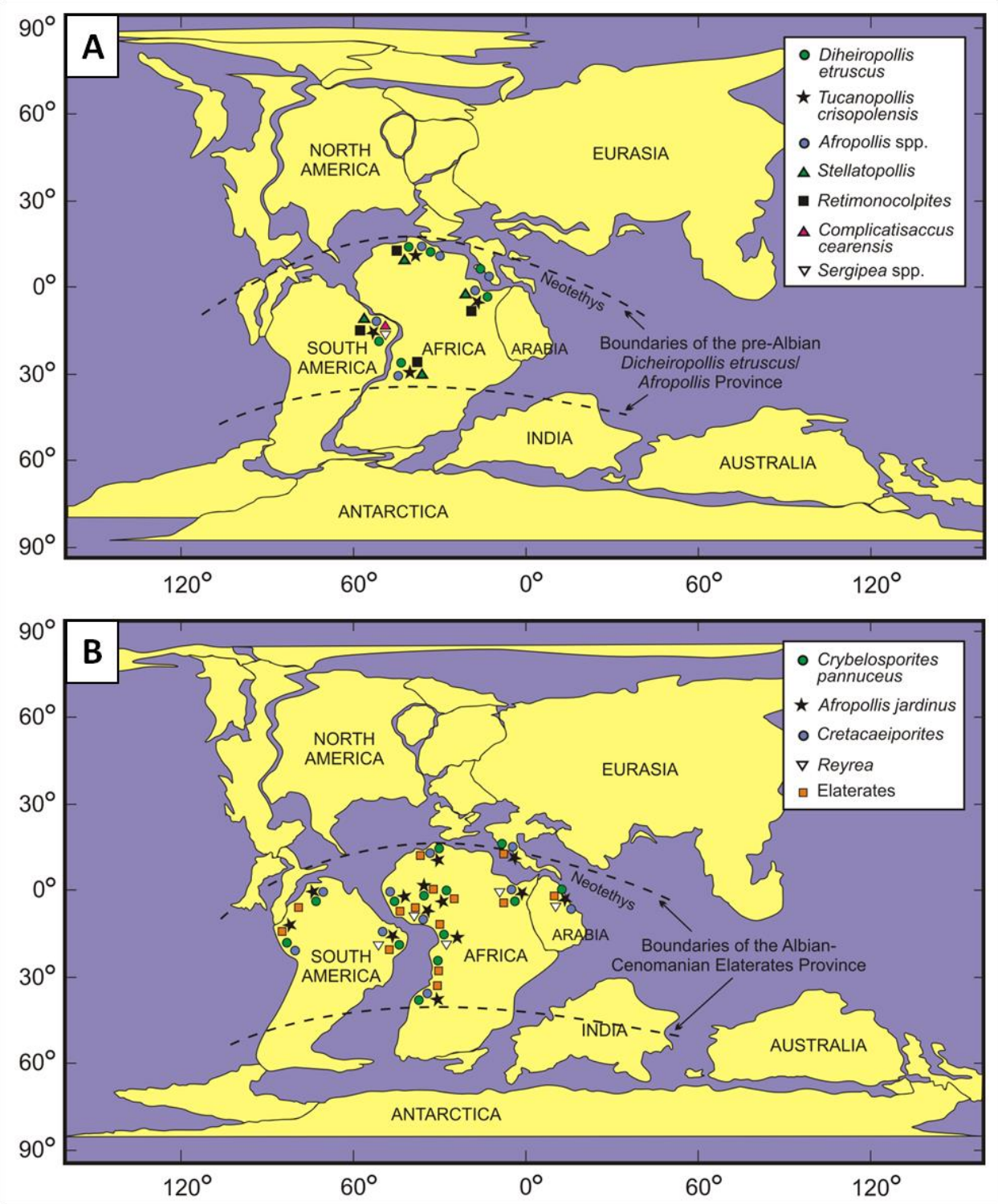

2321

2322 **Figure 16**

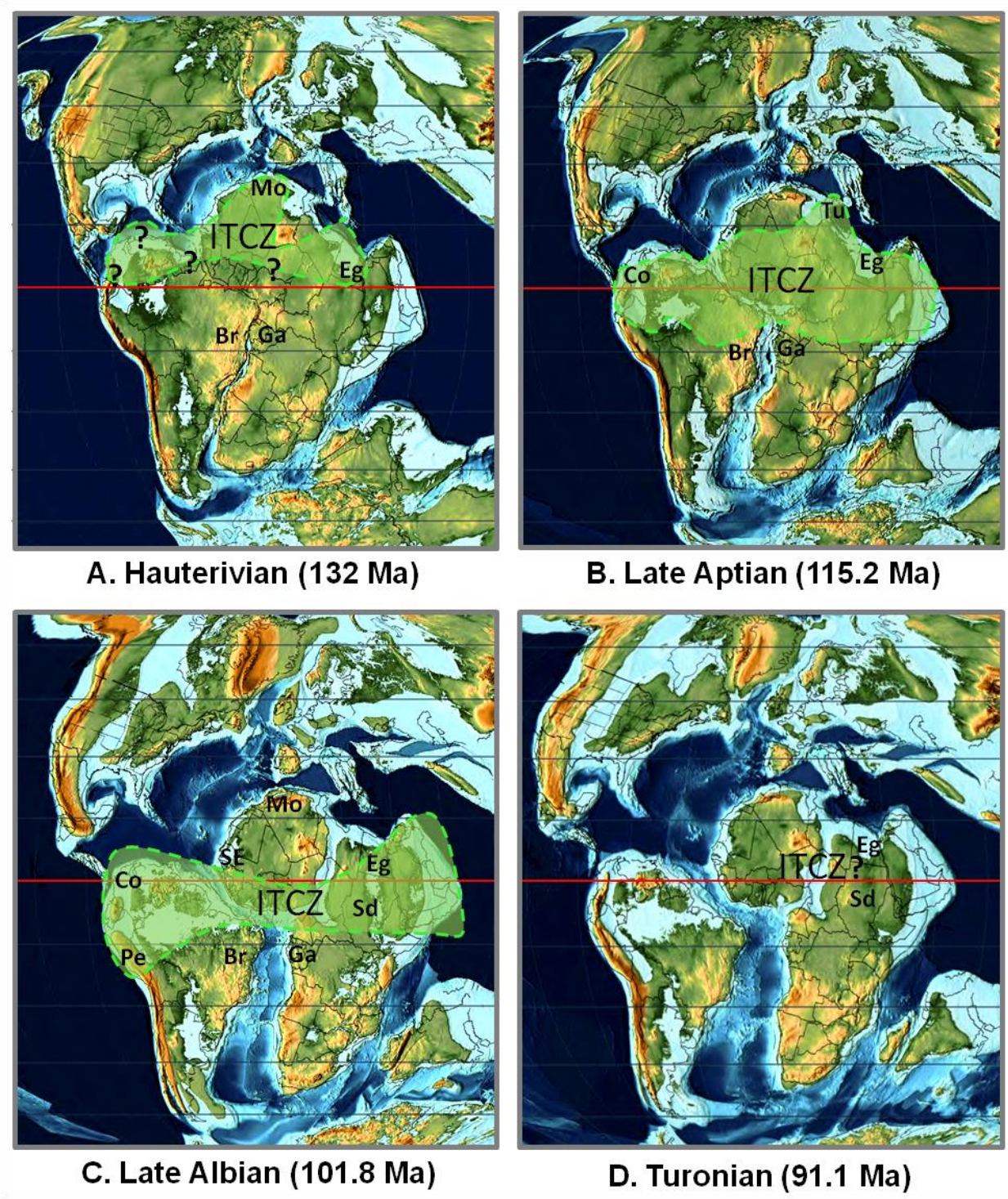

2323

2324 **Figure 17**

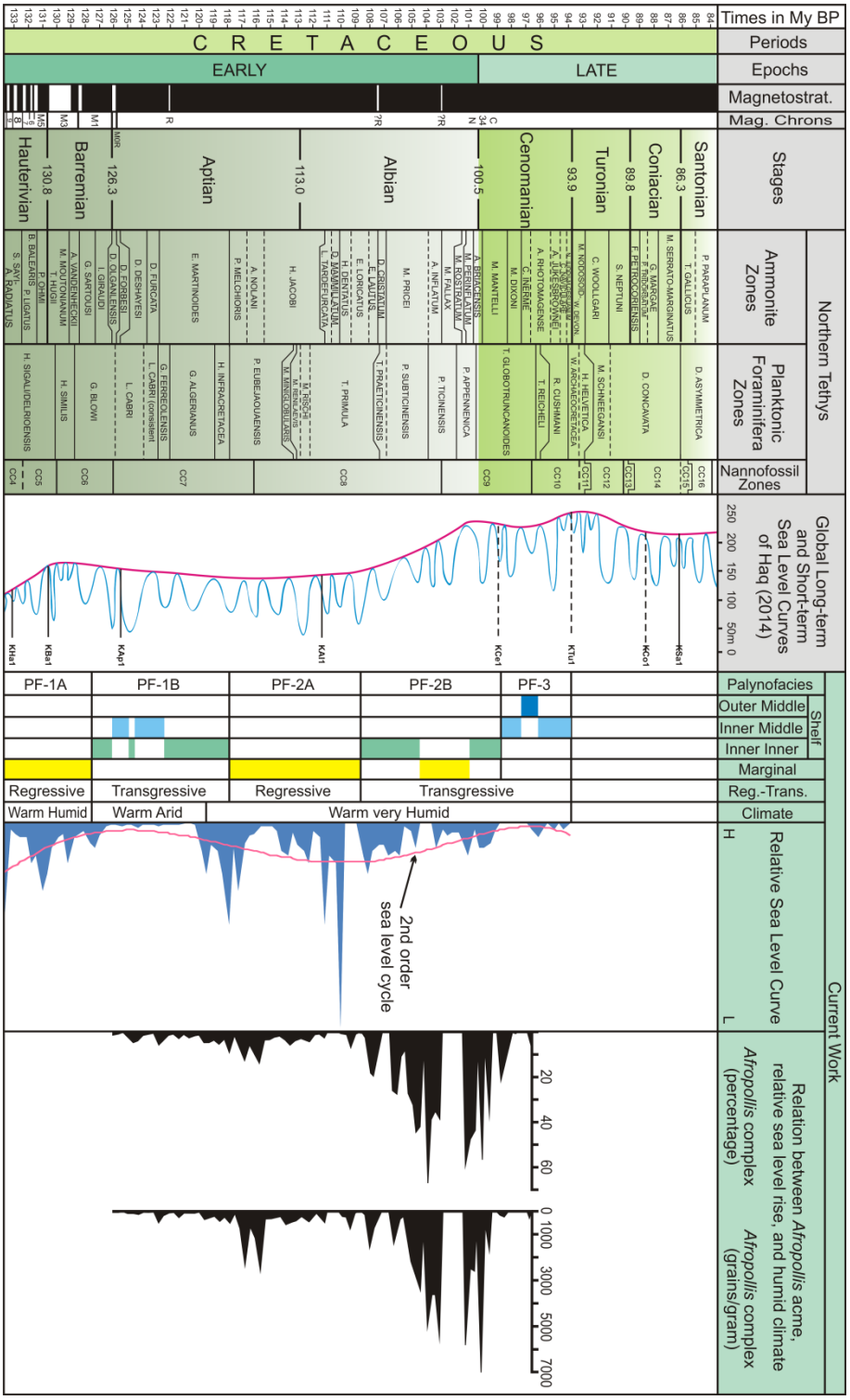

2325

2326 **Table 1**

Taxa	Botanical affinity	Palaeoclimate indication	Palaeoenvironment preference
Araucariacites	Araucariaceae (Cookson, 1947)	Local humid conditions	Relatively dry conifer vegetation
Afropollis	Winteraceae (Doyle et al., 1990)	Local costal humidity	Humid costal habitats
Aequitriradites	Liverworts	Local humid conditions	Near fluvio-lacustrine environments
Balmeiopsis	Araucariaceae (Cookson, 1947)	Local humid conditions	Relatively dry conifer vegetation
Cicatricosisporites	Schizcaeaceae (Thomson & Pflug, 1953)	Local humid conditions	Pteridophyte vegetation on wet biotopes
Classopollis	Cheirolepidiaceae	Warm dry	Costal marshes
Crybelosporites	Marsiliaceae (Dettmann, 1963); Hydropteridacean spores (Cookson & Dettmann, 1958)	Local humidity	Fresh waster environment (lakes-ponds); Swampy environment of brackish character
Deltoidospora	Matoniaceae/Cyatheaceae/Dikso niaceae (Van Erve & Mohr, 1988)	Local wet conditions	Moist habitats near rivers and freshwater lakes and lacustrine
Elaterate	Ephedroid Crane (1988)	Local costal humidity	Humid costal conditions
Ephedripites	Ephedraceae	Hot xeric climate	

2327